A SITE SPACE APPROACH TO THE MANY ELECTRON PROBLEM

This thesis is submitted in accordance with the requirements of the University of Liverpool for the degree of Doctor in Philosophy

by

JOHN ROGAN

March 1984

ACKNOWLEDGEMENTS

I would like to record my thanks to Professor T.B. Grimley for teaching me solid state physics. I could not have had a better supervisor; it has been a privilege to to work with him. I would also like to thank Dr. J.E. Inglesfield for many illuminating discussions, and Professor C. Michael for allowing me to work in DAMTP.

A special vote of thanks goes to Mrs. J.E. Powell. I am very grateful for the work she has put in to preparing a beautiful typescript.

The financial support of the S.E.R.C. is acknowledged.

I am indebted to my family and friends who have been a constant source of help and encouragement.

ABSTRACT

The excitation spectrum and one electron transition matrix elements of an inhomogeneous electron gas are determined by solving the RPAE equations in site space. There are four advantages to this approach. Firstly, the excitation energies and corresponding matrix elements are obtained from the same calculation. Secondly, the pole structure present in dielectric theory is missing, so that the site approach is mathematically attractive. Thirdly, because one electron and many electron terms are treated on the same footing, exchange interactions are easily accommodated. Finally, the key equation takes the form of a simple eigenvalue problem and so black box subroutines can be employed to deliver the excitation spectrum.

In Chapter 2 we investigate the many electron properties of a tightly bound metal, comparing the site space calculation with the standard dielectric function method. The comparison takes place on as many levels as possible. The exchange correlation energy and interaction energy of the tightly bound metal are computed. In Chapter 3 we explore the physics of a model insulator and demonstrate that a Frenkel exciton can coexist with a spectrum of Wannier excitons. Chapter 1 is of an introductory nature.

CONTENTS

CHAPTER I

COLLECTIVE EXCITATIONS OF THE INHOMOGENEOUS ELECTRON GAS.

I.1	The Excitation Spectrum	1
I.2	Charge Density Fluctuations	6
I.3	The Exchange-Correlation Energy and Interaction Energy	13
I.4	Polarisation Effects of an External Charge	16
I.5	Synopsis	22

CHAPTER II

THE RPAE EQUATIONS IN SITE SPACE - THEORY AND APPLICATION.

II.1	The Site Representation	24
	Discussion of the Eigenvalue Problem	29
	The small κ limit	35
	The large $\|\ell\|$ limit	38
	Summary	42
II.2	Plasmon Frequencies of a Simple Metal	43
	The Momentum Space Calculation	46
	The Site Space Calculation	87
II.3	A Sum Rule and Spectral Strengths	136
II.4	Results for E_{int} and E_{xc}	145

CHAPTER III

A MODEL INSULATOR - CHARGE TRANSFER STATES AND EXCITONS.

III.1	Opening Remarks	151
III.2	The Extreme Tight Binding Approximation	156
III.3	One Electron Hopping and Wannier Excitons	162
	CONCLUSION	165
	APPENDIX	

CHAPTER I

COLLECTIVE EXCITATIONS OF THE INHOMOGENEOUS ELECTRON GAS

I.1 The Excitation Spectrum.

The Born-Oppenheimer, or adiabatic, approximation is the starting point for most discussions of the collective electronic properties of a metal. It is based on the observation that the ion cores in a metal respond only slowly to changes in electron density (because of the very different masses involved) so that the lattice may be regarded as stationary.

The earliest work on the many electron problem took this approximation a stage further by smearing out the lattice of ion cores to form a uniform positive charge distribution (Pines, 1963). The lattice literally disappeared into the background so as to highlight only the electronic properties. As a consequence of this procedure, the metal could be viewed as an homogeneous electron gas, with a one electron basis set comprising simply of plane waves. A metal described in this fashion, came to be known as a 'jellium'.

It is thirty years since Bohm and Pines (1953) presented a collective description of the homogeneous electron gas. Their pioneering work centred on a linearisation rule i.e. the random phase approximation, which to this day lies at the heart of most approximate solutions to the many electron problem. We use such a linearisation procedure in this thesis to study the collective properties of two types of *inhomogeneous* electron gas: a simple metal and an insulator. The term inhomogeneous indicates that a property of the system depending on two electron co-ordinates may not simply be a function of their difference. Thus a lattice of ion cores, or the presence of a surface, causes an electron system to be inhomogeneous.

Both forms of inhomogeneity can be accommodated by working with an arbitrary one electron basis set which, for example, might comprise of Wannier functions or tight binding functions.

The many body problem posed by the inhomogeneous electron gas is the calculation of the excitation energy (ω_N) from the ground state ($|0\rangle$) to an excited state ($|N\rangle$) and the corresponding one electron transition matrix element ($\langle N|\psi^+(x)\psi(x)|0\rangle$). As we point out in this opening chapter, knowledge of these quantities establishes a route to the collective electronic properties of interest, e.g. the interaction energy per particle, the polarisation energy due to an impurity charge, and the total electrical potential at a surface or junction.

To determine the excitation energy and the one electron transition matrix elements, we employ the equation of motion method and a linearisation procedure which is commonly found in nuclear physics (Brown, 1972). [The equation of motion method as applied to the electron gas by Sawada (1957), is discussed in section 4].

Consider an interacting system of electrons described by a Hamiltonian of the form

$$H = \int dx\ \psi^+(x)h(x)\psi(x) + \frac{1}{2}\int dx \int dx'\ \psi^+(x')\psi^+(x)v(x,x')\psi(x)\psi(x') \qquad 1.1$$

where ψ^+, ψ are the electron creation and destruction operators, h denotes the kinetic energy and ionic potential of an electron, and v represents the Coulomb potential. In writing (1.1) we have used x to denote both the electron space co-ordinate (r) and the spin co-ordinate (ξ), thus $\int dx \equiv \int d^3r \int d\xi$. Also, h and v are independent of spin co-ordinate:

$$h(x) = -\frac{1}{2}\nabla_r^2 + V_{ion}(r) \quad ; \quad v(x,x') = v(r-r') \qquad 1.2$$

Having defined the Hamiltonian, we can write down the equation of motion of the density matrix operator, and form the matrix element of this operator between the Heisenberg N^{th} excited state, $|N\rangle$, and the ground state, $|O\rangle$.

$$i\frac{d}{dt}\langle N|\rho(x,x';t)|O\rangle = \langle N|[\rho(x,x';t),H]|O\rangle \qquad 1.3$$

If we express the Heisenberg density matrix operator in terms of its Schrodinger picture counterpart i.e.

$$\rho(x,x';t) = e^{iHt}\rho(x,x')\,e^{-iHt} \quad ; \quad \rho(x,x') = \psi^+(x')\psi(x) \qquad 1.4$$

then together with the definition of the stationary states:

$$H|N\rangle = E_N|N\rangle \qquad 1.5$$

we see that (1.3) becomes

$$\omega_N\langle N|\rho(x,x')|O\rangle = \langle N|[H,\rho(x,x')]|O\rangle \qquad 1.6$$

where ω_N is the excitation energy (E_N-E_o). Clearly, the left hand side of equation (1.6) provides us with the two quantities we are searching for, namely the excitation spectrum and the one electron transition matrix elements. The difficulty ofcourse, is the evaluation of the right hand side of (1.6). Let us focus our attention on the commutator. The Fermion field operators satisfy the following *anti*commutation relations

$$\{\psi(x),\psi^+(x')\} = \delta(x-x') = \delta(r-r')\delta(\xi-\xi') \quad ; \quad \{\psi(x),\psi(x')\} = 0 = \{\psi^+(x),\psi^+(x')\} \qquad 1.7$$

If we make use of the fact that both 'h' and 'v' are real, and further that v is symmetric, then it is straightforward to show that the commutator may be written (without approximation) in the following form

$$[H,\rho(x,x')] = h(x')\rho(x,x') + \rho(x,x')\int dy\ v(x',y)\rho(y,y) - h(x)\rho(x,x') - \int dy\ v(x,y)\rho(y,y)\ \rho(x,x') \qquad 1.8$$

We now come to the crucial step of linearising this equation. To do this, a four Fermion operator is factorised in accordance with the following prescription (Brown, 1972):

$$\rho(x,x')\rho(y,y') = \rho(x,x')\langle\rho(y,y')\rangle + \langle\rho(x,x')\rangle\rho(y,y') - \rho(x,y')\langle\rho(y,x')\rangle - \langle\rho(x,y')\rangle\rho(y,x') \qquad 1.9$$

where angular brackets denote expectation values taken in the Hartree-Fock ground state. To justify this linearisation rule which is valid in the high density limit, we need only comment that it reproduces the time dependent Hartree-Fock equation (Thouless, 1961). Note also that by dropping the terms with negative sign in (1.9) we obtain the time dependent Hartree equation. Because of this, the terms with positive sign are known as direct terms, and those going with negative sign as exchange terms. The exchange terms are required for a complete description of semi-conductors and insulators. However, they must be dropped from (1.9) if we wish to describe a metal accurately. Such interactions in a metal produce an unstable ground state and infinite Fermi velocity (Seitz, 1940). Thus, since Chapters I and II are primarily concerned with metal

physics, we at this stage drop the exchange terms, and in consequence equation (1.6) becomes

$$\omega_N \langle N|\rho(x,x')|O\rangle = (H_o(x')-H_o(x))\langle N|\rho(x,x')|O\rangle + \langle\rho(x,x')\rangle\int dy\ (v(x',y)-v(x,y))\langle N|\rho(y,y)|O\rangle \qquad 1.10$$

where H_o is the Hartree Hamiltonian i.e.

$$H_o(x) = h(x) + \int dy\ v(x,y)\langle\rho(y,y)\rangle \qquad 1.11$$

It is worth stating again that (1.10) is an approximate result, and the reason why we have to resort to an approximation is that the exact expression for ω_N (namely 1.6) relates a two Fermion matrix element to a four Fermion matrix element. If we look at the equation of motion of the four Fermion term, we find a six Fermion term, and so on. An intractable situation. To make progress we linearised the four Fermion term. The approximation is commonly referred to as the *random phase approximation* (RPA). See Ehrenreich and Cohen, 1959.

With the aid of the following identity we can derive an integral equation for the one electron transition matrix element of the charge density operator

$$\langle N|\rho(x,x')|O\rangle = \frac{1}{\{\omega_N-(H_o(x')-H_o(x))\}}\{\omega_N-(H_o(x')-H_o(x))\}\langle N|\rho(x,x')|O\rangle \qquad 1.12$$

This identity is verified by going to a momentum space representation for the density matrix operator, and using the fact that H_o is the Hartree Hamiltonian.

We are therefore able to deduce that:

$$\langle N|\rho(x,x')|O\rangle = \frac{1}{\{\omega_N-(H_o(x')-H_o(x))\}} \langle\rho(x,x')\rangle \int dy\ \{v(x',y)-v(x,y)\}\langle N|\rho(y,y)|O\rangle \qquad 1.13$$

and in particular

$$\langle N|\rho(x,x)|O\rangle = \int dy\ \Lambda(x,y;\omega_N)\langle N|\rho(y,y)|O\rangle \qquad 1.14$$

where the kernel, Λ, is given by

$$\Lambda(x,y;\omega_N) = \lim_{x'\to x} \frac{1}{\{\omega_N-(H_o(x')-H_o(x))\}} \langle\rho(x,x')\rangle\{v(x',y)-v(x,y)\} \qquad 1.15$$

The linearised equation of motion (1.10) and the integral equation (1.14) are the main results of this section. We will use (1.10) expressed in a site representation, to calculate the excitation spectrum and electron hole matrix elements of a simple metal-see Chapter II. Equation (1.14) however, establishes an important connection with the charge density fluctuations of the system. It is this connection which we go on to explore in Section 2.

I.2 The Self-Sustaining Nature of Charge Density Fluctuations.

The self-sustaining modes of the system i.e. the elementary excitations, are formed from the charge density fluctuations ($\delta\rho$) induced in the inhomogeneous electron gas by the presence of a small external charge (ρ_{ext}) oscillating with frequency ω say:

$$\delta\rho(x;\omega) = \int dx'\ \Lambda(x,x';\omega)\{\delta\rho(x';\omega) + \rho_{ext}(x';\omega)\} \qquad 2.1$$

where the polarisation kernel (Λ) is given by

$$\Lambda(x,x';\omega) = \sum_{\mu,\nu} \frac{(n_\nu-n_\mu)}{[\omega-(\varepsilon_\mu-\varepsilon_\nu)]} \Phi_\nu(x)\Phi^*_\mu(x) \int dx''\ v(x',x'')\Phi^*_\nu(x'')\Phi_\mu(x'') \qquad 2.2$$

To obtain this result, we neglect product terms of the effective potential with the charge density fluctuation, in the equation of motion of the density matrix. The key reference here is Hedin and Lundquist (1969). Let us investigate the relationship of this approach to the equation of motion method adopted in Section I.1.

The basis states in (2.2) are taken to satisfy the restricted Hartree equation, so that the one electron wavefunction ($\Phi_\mu(x)$) factorises into a space orbital ($\phi_k(r)$) and spin orbital ($\theta_\sigma(\xi)$). Thus μ is a composite index representing both momentum and spin eigenvalues. The corresponding single particle energy is denoted by ε_μ, and the occupation number by n_μ.

The self-sustaining modes are obtained from (2.1) by allowing the external charge density to vanish, so producing an eigenvalue problem (Inglesfield and Wikborg, 1974):

$$\lambda_N(\omega)\ \delta\rho_N(x;\omega) = \int dx'\ \Lambda(x,x';\omega)\,\delta\rho_N(x';\omega) \qquad 2.3$$

subject to the constraint

$$\lambda_N(\omega) = 1 \qquad 2.4$$

This constraint determines the frequencies (ω_N) of the elementary excitations of the system: $\delta\rho_N(x;\omega_N)$

$$\delta\rho_N(x;\omega_N) = \int dx'\ \Lambda(x,x';\omega_N)\,\delta\rho_N(x';\omega_N) \qquad 2.5$$

We now show that the above polarisation kernel is in fact the same as the kernel defined by (1.15) of the opening section and hence deduce that

$$\langle N|\psi^+(x)\psi(x)|O\rangle = C_N\ \delta\rho_N(x;\omega_N) \qquad 2.6$$

where, for the moment, C_N may be regarded as a proportionality constant. Consider then equation (2.2)

$$\Lambda(x,x';\omega_N) = \lim_{y\to x} \frac{1}{[\omega_N-(H_o(y)-H_o(x))]} \sum_{\mu,\nu} (n_\nu-n_\mu)\phi_\nu(x)\phi^*_\mu(y)\int dx'' \; v(x',x'')\phi^*_\nu(x'')\phi_\mu(x'') \tag{2.7}$$

$$= \lim_{y\to x} \frac{1}{[\omega_N-(H_o(y)-H_o(x))]}\{v(x',y)\sum_\nu n_\nu\phi_\nu(x)\phi^*_\nu(y) - v(x',x)\sum_\mu n_\mu\phi^*_\mu(y)\phi_\mu(x)\} \tag{2.8}$$

which is in perfect agreement with (1.15), thereby establishing the validity of (2.6). Since the polarisation kernel is not Hermitian it possesses left eigenfunctions (δV_M) defined by

$$\lambda^*_M(\omega)\,\delta V_M(x;\omega) = \int dx' \; \delta V_M(x';\omega)\Lambda(x',x;\omega) \tag{2.9}$$

The left eigenfunctions can be expressed in terms of the right eigenfunctions by realising that the polarisation kernel can be written in the form (see 2.2):

$$\Lambda(x,x';\omega) = \int dx'' \; \Pi(x,x'';\omega)v(x'',x') \tag{2.10}$$

where Π is an Hermitian kernel (known as the susceptibility). It is then straightforward to show that

$$\delta V_M(x;\omega) = \int dx' \; v(x,x')\,\delta\rho^*_M(x';\omega) \tag{2.11}$$

and further that the left and right eigenfunctions are orthogonal, Feibelman et al, 1972.

$$\int dx \; \delta V_M(x;\omega)\,\delta\rho_N(x;\omega) = \delta_{M,N} \tag{2.12}$$

We can investigate the self-sustaining nature of the elementary

excitations by observing from (2.6) that:

$$\delta\rho_N(x;\omega_N) \quad \propto \quad \sum_{\mu,\nu} \Phi^*_\mu(x)\Phi_\nu(x)\langle N|a^+_\mu a_\nu|O\rangle \qquad 2.13$$

where 'a^+' and 'a' are the momentum space Fermion creation and destruction operators. The charge density fluctuation, $\delta\rho_N(x;\omega_N)$, is thus made up of a superposition of electron hole excitations i.e. $\langle N|a^+_\mu a_\nu|O\rangle$. We now show how $\delta\rho_N(x;\omega_N)$ in turn excites the electron hole pairs so that a *self-sustaining* cycle is set up. To do this, we write down the linearised equation of motion (1.10) in momentum space

$$[\omega_N-(\varepsilon_\mu-\varepsilon_\nu)]\langle N|a^+_\mu a_\nu|O\rangle = (n_\nu-n_\mu)\sum_{\alpha,\beta} V_{\nu\alpha,\beta\mu}\langle N|a^+_\alpha a_\beta|O\rangle \qquad 2.14$$

where

$$V_{\nu\alpha,\beta\mu} = \int dx \int dx' \; \Phi^*_\nu(x)\Phi^*_\alpha(x')v(x,x')\Phi_\beta(x')\Phi_\mu(x) \qquad 2.15$$

and express the above integral as a sum over self-sustaining modes. This is facilitated by means of the decomposition:

$$\Phi^*_\mu(x)\Phi_\nu(x) = \sum_M A^M_{\mu\nu}(\omega)\,\delta\rho_M(x;\omega) \qquad 2.16$$

To determine the coefficients, $A^M_{\mu\nu}(\omega)$, we multiply this equation by the left eigenfunction, $\delta V_N(x;\omega)$, and integrate over all space.

$$A^N_{\mu\nu}(\omega) = \int dx \; \Phi^*_\mu(x)\,\delta V_N(x;\omega)\,\Phi_\nu(x) \qquad 2.17$$

Substituting (2.16) into (2.15) we readily obtain the desired sum over modes

$$V_{\nu\alpha,\beta\mu} = \sum_N A^{N*}_{\mu\nu}(\omega) A^N_{\alpha\beta}(\omega) \qquad 2.18$$

Physically, it is useful to express the Coulomb integral as a sum over modes because of the screening properties of the plasmon excitations. Mathematically, this decomposition results in a decoupling of the matrix elements giving an explicit solution. To see this we substitute (2.18) into (2.14):

$$\langle N|a^+_\mu a_\nu|O\rangle = \frac{(n_\nu - n_\mu)}{[\omega_N - (\varepsilon_\mu - \varepsilon_\nu)]} \sum_M A^{M*}_{\mu\nu}(\omega) \sum_{\alpha,\beta} A^M_{\alpha\beta}(\omega) \langle N|a^+_\alpha a_\beta|O\rangle \qquad 2.19$$

and look for a solution satisfying

$$\sum_{\alpha,\beta} A^M_{\alpha\beta}(\omega) \langle N|a^+_\alpha a_\beta|O\rangle = C_N \delta_{N,M} \qquad 2.20$$

This condition implies that

$$\langle N|a^+_\mu a_\nu|O\rangle = \frac{(n_\nu - n_\mu)}{[\omega_N - (\varepsilon_\mu - \varepsilon_\nu)]} A^{N*}_{\mu\nu}(\omega) \; C_N \qquad 2.21$$

By reference to (2.17) and (2.6) we find that (2.20) is indeed satisfied provided $\omega = \omega_N$. In consequence our solution for the electron hole matrix element is:

$$\langle N|a^+_\mu a_\nu|O\rangle = \frac{(n_\nu - n_\mu)}{[\omega_N - (\varepsilon_\mu - \varepsilon_\nu)]} C_N \{\int dx \; \Phi^*_\mu(x) \delta V_N(x;\omega_N) \Phi_\nu(x)\}^* \qquad 2.22$$

which shows explicitly how $\delta\rho_N(x;\omega_N)$ excites the electron hole pairs.

Finally in this section, we determine the constant of proportionality C_N. Define a function F, such that

$$F(x,x';\omega) = \Lambda(x,x';\omega) + \int dx'' \; \Lambda(x,x'';\omega) F(x'',x';\omega) \qquad 2.23$$

then (2.1) yields

$$\delta\rho(x;\omega) = \int dx'\ F(x,x';\omega)\,\rho_{ext}(x';\omega) \qquad 2.24$$

showing that the change in charge density is linearly related to the external charge. The function (F) which accommodates this relationship characterises properties of both the unperturbed and perturbed system and is known as the *response function*. Since the response function is defined solely in terms of the polarisation kernel, it is clear that Λ and F have simultaneous eigenfunctions $\delta\rho_N(x;\omega)$. The eigenvalue equation for the response function is:

$$\frac{\lambda_N(\omega)}{[1-\lambda_N(\omega)]}\,\delta\rho_N(x;\omega) = \int dx'\ F(x,x';\omega)\,\delta\rho_N(x';\omega) \qquad 2.25$$

from which we observe that the eigenvalues of F, subject to the constraint (2.4), are infinite, i.e. plasmons (and all other elementary excitations) occur at frequencies which correspond to the poles of the response function. To proceed further we note that there are two equivalent expressions for the response function namely

$$F(x,x';\omega) = \sum_N \frac{\lambda_N(\omega)}{[1-\lambda_N(\omega)]}\,\delta\rho_N(x;\omega)\,\delta V_N(x';\omega) \qquad 2.26$$

and

$$F(x,x';\omega) = \sum_N \left\{\frac{\langle N|\rho(x,x)|0\rangle\langle 0|V(x',x')|N\rangle}{(\omega-\omega_N)} - \frac{\langle N|\rho(x,x)|0\rangle^*\langle 0|V(x',x')|N\rangle^*}{(\omega+\omega_N)}\right\} \qquad 2.27$$

where

$$V(x,x) = \int dx'\ v(x,x')\ \rho(x',x') \qquad 2.28$$

Whilst the first expression can be deduced from our discussion of the eigenfunctions of the response function, the second one cannot. It results from the Kubo formulation of the many body problem (Kubo, 1957). Let us equate the residues at the pole: $\omega = \omega_N$, of these representations

$$\langle N|\rho(x,x)|0\rangle\langle 0|V(x',x')|N\rangle = \lim_{\omega\to\omega_N} (\omega-\omega_N)\frac{\lambda_N(\omega)}{[1-\lambda_N(\omega)]}\,\delta\rho_N(x;\omega)\delta V_N(x';\omega) \qquad 2.29$$

To first order in $(\omega-\omega_N)$ we have that

$$1-\lambda_N(\omega) = 1-\{\lambda_N(\omega_N) + (\omega-\omega_N)\left.\frac{\partial\lambda_N}{\partial\omega}\right|_{\omega=\omega_N}\} = -(\omega-\omega_N)\left.\frac{\partial\lambda_N}{\partial\omega}\right|_{\omega=\omega_N} \qquad 2.30$$

This enables us to evaluate the limit in (2.29) to obtain

$$\langle N|\rho(x,x)|0\rangle\langle 0|V(x',x')|N\rangle = -\frac{\delta\rho_N(x;\omega_N)\;\delta V_N(x';\omega_N)}{\left.\frac{\partial\lambda_N}{\partial\omega}\right|_{\omega=\omega_N}} \qquad 2.31$$

and by referring to (2.6) we conclude that:

$$|C_N|^2 = -1/\left.\frac{\partial\lambda_N}{\partial\omega}\right|_{\omega=\omega_N} \qquad 2.32$$

As we shall soon discover (Sections 3 and 4), physically meaningful quantities are related only to $|C_N|^2$ and not to C_N, so that expression (2.32) is sufficient. In fact C_N which started out simply as a proportionality constant, provides a route to the spectral strength of the response function.

I.3 The Exchange-Correlation Energy and Interaction Energy.

A quantity of some interest in the study of the electron gas is the exchange-correlation energy, E_{xc}. Whilst this energy has no physical significance in itself, it is nonetheless very important. For example, the van der Waals interaction energy of two metal films, a distance d apart, is defined by:

$$E_{xc}(d) - E_{xc}(\infty).$$

Harris and Griffen have calculated this van der Waals energy by expressing E_{xc} in terms of the zero point energy of the normal modes. They adopted a semi-classical approach and represented the metal surfaces by infinite plane barriers. The separation, d, was chosen to be large enough so that electron tunnelling between the films was effectively zero, an important consideration. This guarenteed that the coupling came only from the electromagnetic fluctuations occurring in each film.

The conclusion they reached was that the van der Waals energy is dominated by the surface plasmons. The work of Harris and Griffen (1975) gives an indication of the importance of the exchange-correlation energy. This point is also exemplified by the work of Wikborg and Inglesfield (1977). Historically, the exchange-correlation energy was calculated from the interaction energy i.e. the ground state expectation value of the term in the Hamiltonian describing the electron electron interaction. In a private communication to Weisskopf, Pauli demonstrated the now ubiquitous technique of integrating over the coupling constant, thereby providing a route to the exchange-correlation energy from the interaction energy (E_{int}):

$$E_{xc} = \int_0^1 d(e^2)\ \frac{1}{e^2}\ E_{int}(e^2) \qquad 3.1$$

This result can be established by switching on the electron electron interaction adiabatically and requiring that the system follow the ground state (Pines, 1963). It also forms the basis of the Sawada method for calculating the exchange-correlation energy of the jellium model (Sawada, 1957).

We too, will use the Pauli formula to verify the well known result that the Sawada expression for the exchange-correlation energy is valid for the inhomogeneous electron gas (Harris and Griffen, 1975). However, the primary aim of this section is to show how the interaction energy may be written as a sum (over all modes) of the quantity: $|C_N|^2$. This <u>modal</u> sum will enable us to evaluate the relative contributions to E_{int} and E_{xc} of the single particle and plasmon excitations in a simple tightly bound metal, thereby gaining insight into the physical make-up of the exchange correlation energy and interaction energy.

Our first task is to determine the ground state expectation value of the potential energy operator, P. By definition:

$$P = \frac{1}{2} \int dx \int dx'\ \psi^+(x')\psi^+(x)v(x,x')\psi(x)\psi(x') \qquad 3.2$$

This operator may equivalently be expressed in the form

$$P = \frac{1}{2} \int dx \int dx'\ v(x,x')\rho(x,x)\rho(x',x') - \frac{v(0)}{2} \int dx\ \rho(x,x) \qquad 3.3$$

The potential energy of the ground state is therefore

$$\langle O|P|O\rangle = \frac{1}{2}\int dx \int dx'\ v(x,x')\langle O|\rho(x,x)\rho(x',x')|O\rangle - \frac{N}{2}v(0) \qquad 3.4$$

The final term in (3.4) represents the self interaction of the electrons, and since this is constant for fixed particle number we drop it. Inserting a complete set of states between the charge density operators we obtain:

$$\langle O|P|O\rangle = \frac{1}{2}\sum_M \int dx \int dx'\ v(x,x')\langle M|\rho(x,x)|O\rangle^*\langle M|\rho(x',x')|O\rangle \qquad 3.5$$

and so equation (2.6) gives

$$\langle O|P|O\rangle = \frac{1}{2}\sum_M |C_M|^2 \int dx \int dx'\ v(x,x')\delta\rho_M^*(x;\omega_M)\delta\rho_M(x';\omega_M) \qquad 3.6$$

Using the definition of the left eigenfunction $\delta V_M(x;\omega_M)$, and the biorthogonality relation, yields the interaction energy per particle

$$E_{int} = \frac{1}{2}\frac{1}{N}\sum_M |C_M|^2 \qquad 3.7$$

In order to determine the exchange-correlation energy we note that in the frequency domain of the elementary excitations

$$\frac{\partial\lambda_M}{\partial e^2} + \frac{\partial\lambda_M}{\partial\omega}\frac{\partial\omega}{\partial e^2} = 0 \qquad 3.8$$

and since the eigenvalue λ_M is directly proportional to the coupling constant, e^2, we conclude that

$$\lambda_M(\omega) + \frac{\partial\lambda_M}{\partial\omega}e^2\frac{\partial\omega}{\partial e^2} = 0 \quad , \text{ at } \omega = \omega_M \qquad 3.9$$

Equation (3.9) together with (2.32) gives the value of $|C_M|^2$

$$|C_M|^2 = e^2 \frac{\partial \omega_M}{\partial e^2} \qquad 3.10$$

This is precisely the result we need in order to use the Pauli formula. Performing the integration over the coupling constant, we establish the generalised Sawada expression for the exchange correlation energy:

$$E_{xc} = \frac{1}{2N} \sum_M \{\omega_M(e^2=1) - \omega_M(e^2=0)\} \qquad 3.11$$

with the understanding that the excitation energies $\omega_M(e^2=0)$ are to be assigned Hartree values. Thus, E_{xc} is the change in zero point energy of the system, in going from the Hartree self consistent field approximation to the random phase approximation (Schmit and Lucas, 1972 ; Wikborg and Inglesfield, 1977).

This derivation completes our present discussion of the interaction energy and exchange-correlation energy of the inhomogeneous electron gas. In Chapter II we employ the modal sums (3.7) and (3.11) to calculate the percentage contribution of the plasmon excitation in a simple metal, to E_{int} and E_{xc}.

I.4 Polarisation Effects of an External Charge.

In 1957 a Japanese scientist, Katuro Sawada, searched for a transformation which would redescribe the interacting homogeneous electron gas as a system of approximately non interacting Bosons. Sawada found a clue to the nature of the transformation in a paper written by Gell-Mann and Brueckner (1957), who had

used a diagrammatic approach to determine the correlation energy per particle for the electron gas. In this calculation a particle and hole travelled (between interactions) as if they were a single particle. The propogator for this system was thus evaluated by summing an infinite set of ring diagrams.

Observing this fact, Sawada noticed a similarity to the well known and exactly solved problem of the interaction of an infinitely heavy particle with a neutral scalar meson field (Wentzel, 1942). Since the Hamiltonian for such a system is in bilinear form, there exists a normal co-ordinate transformation to non interacting modes. Sawada set out to replace the exact Hamiltonian for the homogeneous electron gas by an approximate Hamiltonian in bilinear form. The criterion for this procedure was that the Hamiltonian should accommodate all the diagrams retained by Gell-Mann and Brueckner. This was succesfully accomplished by adopting Boson commutation relations for the electron hole operator $a^{+}_{\mu}a_{\nu}$ (Sawada et al, 1957).

In order to simplify our discussion of the polarisation effects of impurity charges, we will Bosonise the <u>inhomogeneous</u> electron gas, i.e. we diagonalise the equation of motion of the density matrix operator (2.14) thereby defining a transformation to quasi Boson modes. The merit of this approach (in contrast to the Sawada method) is that there is no need to simplify the Hamiltonian from the outset. To be completely general, let us reinstate the exchange term into (2.14):

$$\omega_N \langle N|a^{+}_{\mu}a_{\nu}|0\rangle = (\varepsilon_{\mu}-\varepsilon_{\nu})\langle N|a^{+}_{\mu}a_{\nu}|0\rangle + (n_{\mu}-n_{\nu}) \sum_{\alpha,\beta} (V_{\alpha\nu,\beta\mu}-V_{\nu\alpha,\beta\mu})\langle N|a^{+}_{\alpha}a_{\beta}|0\rangle \quad 4.1$$

The exchange interaction of the electron hole pairs (α,β) and (μ,ν) is characterised by $V_{\alpha\nu,\beta\mu}$, whilst $V_{\nu\alpha,\beta\mu}$ characterises the direct interaction. It is unnecessary to define separate operators for the creation of electrons and holes with respect to the Fermi level. Such canonical transformations are favoured in nuclear physics; for example the Tamm Dancoff approximation utilises the concept of particles and holes to determine the frequency of the giant dipole resonance (Fetter and Walecka, 1971).

Let us look for an operator such that †

$$[H, O_M^+] = \omega_M O_M^+ \qquad 4.2$$

By expressing the operator in terms of the electron creation and destruction operators

$$O_M^+ = \sum_{\mu,\nu} O_{\mu\nu}^{M^+} a_\mu^+ a_\nu \qquad 4.3$$

and by equating coefficients of the electron hole operator in the equation of motion of O_M^+ (viz 4.2) we find that

$$[\omega_M - (\varepsilon_\mu - \varepsilon_\nu)] O_{\mu\nu}^{M^+} = \sum_{\alpha,\beta} (n_\beta - n_\alpha)(V_{\beta\mu,\nu\alpha} - V_{\mu\beta,\nu\alpha}) O_{\alpha\beta}^{M^+} \qquad 4.4$$

Comparing this equation with the linear equation for the one electron transition matrix elements (4.1) we obtain the coefficients $O_{\mu\nu}^{M^+}$ explicitly

† If such an operator exists it is clear that it will act on the ground state to give an eigenstate of the Hamiltonian going with energy E_M. In consequence O_M^+ is a raising operator providing a route to excited states from the ground state.

$$O^{M+}_{\mu\nu} = \frac{\langle M|a^{+}_{\mu}a_{\nu}|O\rangle^{*}}{(n_{\nu}-n_{\mu})} \qquad 4.5$$

It would appear that in writing (4.5) we are missing out a constant of proportionality. However, without loss of generality this may be taken as unity. To determine the lowering operator, which we write as

$$O^{-}_{M} = \sum_{\mu,\nu} O^{M-}_{\mu\nu}\, a^{+}_{\mu}a_{\nu} \qquad 4.6$$

we simply require that it is the Hermitian conjugate of the raising operator, satisfying the appropriate Harmonic equation. This gives

$$O^{M-}_{\mu\nu} = \frac{\langle M|a^{+}_{\nu}a_{\mu}|O\rangle}{(n_{\mu}-n_{\nu})} \qquad 4.7$$

In order to investigate the commutation relations of the raising and lowering (*ladder*) operators, we first establish the following identity

$$\langle N|O^{+}_{M}|O\rangle = \delta_{N,M} \qquad 4.8$$

This is achieved by

(i) multiplying (4.1) by $O^{M+}_{\mu\nu}$, summing over μ,ν

(ii) multiplying (4.4) by $\langle N|a^{+}_{\mu}a_{\nu}|O\rangle$, summing over μ,ν

and subtracting the resulting two equations:

$$(\omega_{N}-\omega_{M})\ \langle N|O^{+}_{M}|O\rangle = O \qquad 4.9$$

so that with suitable normalisation (4.8) holds. As a consequence of this:

$$\langle O|[O_N^-, O_M^+]|O\rangle = \delta_{N,M} \quad \Rightarrow \quad \sum_{\alpha,\beta} \frac{\langle N|a_\alpha^+ a_\beta|O\rangle\langle M|a_\alpha^+ a_\beta|O\rangle^*}{(n_\beta - n_\alpha)} = \delta_{N,M} \qquad 4.10$$

It can similarly be shown that

$$\langle O|[O_N^+, O_M^+]|O\rangle = O = \langle O|[O_N^-, O_M^-]|O\rangle \qquad 4.11$$

We therefore conclude that the ladder operators have Boson commutation relations under the ground state expectation value. For this reason we refer to the operators as *quasi* Bosons. It is clear that the Hamiltonian describing our inhomogeneous interacting Fermion system can be approximately constructed from non interacting quasi Boson operators, which is obviously a simplification.

$$H = E_O + \sum_M \omega_M O_M^+ O_M^- \qquad 4.12$$

This result is valid provided the linearisation rule holds (i.e. in the high density limit) and has been obtained without dropping the exchange term in the equation of motion of the density matrix operator. We have therefore Bosonised the inhomogeneous electron gas within the random phase approximation with exchange (RPAE). This is put to good use in the following discussion of the polarisation effects of impurity charges.

Consider the response of the inhomogeneous electron gas to an external potential - in the form of a static impurity. The interaction term to be added to the Hamiltonian is

$$H_{int} = \int dx\, V_{ext}(x)\,\rho(x,x) \qquad 4.13$$

Let us express the charge density operator, $\rho(x,x)$, in terms of the ladder operators.

$$\rho(x,x) = \sum_M \{\, F_M(x) O_M^+ + G_M(x) O_M^- \,\} \qquad 4.14$$

Taking a scalar product between an excited state and the ground state, and using the definition of the ladder operators, gives the value of the coefficients $F_M(x)$ and $G_M(x)$.

$$\rho(x,x) = \sum_M \{\, \langle M|\rho(x,x)|O\rangle O_M^+ + \langle M|\rho(x,x)|O\rangle^* O_M^- \,\} \qquad 4.15$$

The total Hamiltonian is therefore of the form

$$H = E_o + \sum_M \omega_M O_M^+ O_M^- + \sum_M (\gamma_M O_M^+ + \gamma_M^* O_M^-) \quad ; \quad \gamma_M = \int dx\, V_{ext}(x)\langle M|\rho(x,x)|O\rangle \qquad 4.16$$

We can diagonalise the Hamiltonian by use of the transformation $O_M^+ \rightarrow O_M^+ + \alpha_M^* \quad ; \quad O_M^- \rightarrow O_M^- + \alpha_M$, where α_M is a scalar quantity to be determined. Under this transformation the Hamiltonian becomes

$$H = E_o + \sum_M \omega_M O_M^+ O_M^- + \sum_M \{\, (\omega_M\alpha_M + \gamma_M) O_M^+ + (\omega_M\alpha_M^* + \gamma_M^*) O_M^- + \gamma_M\alpha_M^* + \gamma_M^*\alpha_M + \omega_M|\alpha_M|^2 \,\}$$

Choosing α_M to be $(-\gamma_M/\omega_M)$ removes the terms linear in the ladder operators.

$$H = (E_o - E_{pol}) + \sum_M \omega_M O_M^+ O_M^- \quad ; \quad E_{pol} = \sum_M \frac{|\gamma_M|^2}{\omega_M} \qquad 4.17$$

E_{pol} is the polarisation energy. We note that $\gamma_M \propto C_M$.

I.5 Synopsis.

The collective properties we have considered in this opening chapter, are (within the random phase approximation) modal sums of the form

$$\sum_{M} \text{function } (\omega_M, |C_M|^2)$$

where $|C_M|^2$ is itself a function of ω_M. An efficient determination of the excitation spectrum is therefore a crucial factor in calculating such properties. Although the sums are wave vector summations, the excitation energies can be determined in any suitable representation.

The early papers on the many electron problem, treat a metal as a plasma - a homogeneous system, so that momentum space is a convenient form of representation. However, if a lattice of ion cores is introduced, the momentum representation might not be the most appropriate choice, because although the system is periodic, it is not translationally invariant. Thus in order to obtain an accurate description of the response of a 'real' metal to an external perturbation, momentum transfers involving Umklapp processes need to be included.

In the next chapter we show that the site representation is ideally suited to the calculation of the excitation spectrum of an inhomogeneous electron gas. The transformation of the real space RPAE equations to site space, presents no difficulty since the RPAE is an operator approximation.

Hanke (1978) has used the site representation to calculate the dielectric function of covalent crystals, and in this way he

has investigated the optical properties of semiconductors. The difficulty with the response function approach is that exchange interactions are not easily accommodated (Hubbard, 1957). However the equation of motion method developed in this chapter, allows us to deal with exchange interactions in a straightforward way. Because of this, charge transfer states, excitons, plasmons and single particle modes, are all contained in the formalism.

The equation of motion technique, coupled with the site representation, therefore provides a unified treatment of many electron excitations.

CHAPTER II

THE RPAE EQUATIONS IN SITE SPACE - THEORY AND APPLICATION.

II.1 The Site Representation.

It is apparent from our discussion of charge density fluctuations, that if a test charge weakly interacts with an electron gas then (within the RPA) the resulting effective potential is linearly related to the external potential:

$$' V_{eff} = (1-\Lambda)^{-1} V_{ext} ' \qquad 1.1$$

This equation (which is strictly an integral equation) serves to define the *dielectric function* (ε)

$$\varepsilon = 1 - \Lambda \qquad 1.2$$

We see that for a homogeneous electron gas, the self sustaining modes occur when the dielectric function vanishes

$$\varepsilon(\kappa,\omega) = 0 \qquad 1.3$$

Equation (1.3) provides the traditional route to the excitation spectrum of such a solid. For a periodic system, Saslow and Reiter (1973) have shown that this equation is replaced by a determinantal relation

$$\det[\varepsilon(\kappa+G,\kappa+G';\omega)] = 0 \qquad 1.4$$

where κ is a 1^{st} Brillouin zone wave vector and G is a reciprocal lattice vector. We can therefore calculate the energy spectrum by searching out the zeros of the dielectric function (or the associated determinant). In practise, scanning a frequency range at a given wave vector is inconvenient and an iterative technique is normally employed to deliver the excitation energies to a

predetermined accuracy. However, as we will presently discover this is by no means straightforward.

It is the purpose of this section to demonstrate how the excitation spectrum of a solid can be determined (in the RPAE) from a simple eigenvalue problem of the form:

$$\omega X_{\ell} = \sum_{\ell'} a_{\ell,\ell'} X_{\ell'} \quad , \quad \ell = \text{lattice vector} \qquad 1.5$$

i.e. without resort to (1.4). There are three distinct advantages to this approach

(i) There is no need to determine the dielectric function

(ii) One electron terms and many body terms are treated on one and the same footing

(iii) Both the excitation energy and the corresponding matrix element (X_{ℓ}) are obtained from the same calculation.

To derive (1.5) consider a solid in which both direct and exchange interactions are present. For simplicity, let us deal with a *single* band. The derivation can be easily generalised to accommodate many bands (Chapter III). Our starting point is the equation of motion of the density matrix operator

$$\begin{aligned}
\omega_M \langle M|\rho(x,x')|0\rangle = \\
\{h(x') + \int dy\, v(x',y)\langle\rho(y,y)\rangle\}\langle M|\rho(x,x')|0\rangle - \int dy\, v(x',y)\langle\rho(y,x')\rangle\langle M|\rho(x,y)|0\rangle \\
- \{h(x) + \int dy\, v(x,y)\langle\rho(y,y)\rangle\}\langle M|\rho(x,x')|0\rangle + \int dy\, v(x,y)\langle\rho(x,y)\rangle\langle M|\rho(y,x')|0\rangle \\
+ \int dy\, v(x',y)\{\langle\rho(x,x')\rangle\langle M|\rho(y,y)|0\rangle - \langle\rho(x,y)\rangle\langle M|\rho(y,x')|0\rangle\} \\
- \int dy\, v(x,y)\{\langle\rho(x,x')\rangle\langle M|\rho(y,y)|0\rangle - \langle\rho(y,x')\rangle\langle M|\rho(x,y)|0\rangle\}
\end{aligned} \qquad 1.6$$

Hidden in the first four terms of this expression are two Hartree-Fock Hamiltonians, whilst the remaining terms describe the many body effects. Note that integrals involving the charge density operator: $\psi^+(y)\psi(y)$, represent direct Coulomb interactions.

Let us write equation (1.6) in site space. To do this, we define site creation and destruction operators as follows

$$a^+_{\ell,\sigma} = \int dx'\ \theta_\sigma(\xi')w(r'-\ell)\psi^+(x')$$
$$a_{\ell',\sigma'} = \int dx\ \theta^*_{\sigma'}(\xi)w^*(r-\ell')\psi(x) \qquad 1.7$$

where w is a Wannier function. We also define site integrals

$$H_{\ell',\ell} = \int d^3r\ w^*(r-\ell')h(r)w(r-\ell) \qquad 1.8$$

$$V_{\ell'L',L\ \ell} = \int d^3r \int d^3r'\ w^*(r-\ell')w^*(r'-L')v(r-r')w(r'-L)w(r-\ell)$$

In general, a matrix element in site space looks like: $\langle M|a^+_{\ell,\sigma}a_{\ell',\sigma'}|0\rangle$. However, we need only consider matrix elements of the form $\langle M|a^+_{\ell,\sigma}a_{0,\sigma'}|0\rangle$ because of the Bloch property of a many body wavefunction, which implies that

$$\langle M|a^+_{(\ell+\ell'),\sigma}a_{\ell',\sigma'}|0\rangle = e^{-i\kappa.\ell'}\ \langle M|a^+_{\ell,\sigma}a_{0,\sigma'}|0\rangle \qquad 1.9$$

The letter M which we have used to label the exact eigenstates of the system is of course a composite symbol. It denotes mode type (e.g. single particle, plasmon, exciton) and a wave vector. The wave vector going with the state $|M\rangle$ will <u>always</u> be denoted by κ. It is with this understanding that we have written (1.9). Having established the Bloch property of the matrix elements, we return to equation (1.6), multiply thro' by $\theta^*_{\sigma'}(\xi)\theta_\sigma(\xi')w^*(r)w(r'-\ell)$ and integrate over x and x'.

$$\omega_M \langle M|a^+_{\ell,\sigma} a_{0,\sigma'}|0\rangle =$$

$$\sum_{\ell'} \{H_{\ell',\ell} + \sum_{L,L'} V_{\ell'L',L\ell} \sum_{\gamma} \langle a^+_{L',\gamma} a_{L,\gamma}\rangle\}[1 - e^{-i\kappa.(\ell-\ell')}]\langle M|a^+_{\ell',\sigma} a_{0,\sigma'}|0\rangle$$

$$+ \sum_{\ell',L,L'} V_{\ell'L',\ell L} \sum_{\gamma} \langle a^+_{L',\gamma} a_{L,\sigma'}\rangle e^{-i\kappa.(\ell-\ell')} \langle M|a^+_{\ell',\sigma} a_{0,\gamma}|0\rangle$$

$$- \sum_{\ell',L,L'} V_{\ell'L',\ell L} \sum_{\gamma} \langle a^+_{L',\sigma} a_{L,\gamma}\rangle \langle M|a^+_{\ell',\gamma} a_{0,\sigma'}|0\rangle$$

$$+ \sum_{\ell'} \{ \sum_{L,L'} V_{L(\ell'+L'),L'\ell} e^{-i\kappa.L'} \langle a^+_{L,\sigma} a_{0,\sigma'}\rangle\} \sum_{\gamma} \langle M|a^+_{\ell',\gamma} a_{0,\gamma}|0\rangle$$

$$- \sum_{\ell',L,L'} V_{(\ell'+L')L,L'\ell} e^{-i\kappa.L'} \sum_{\gamma} \langle a^+_{L,\gamma} a_{0,\sigma'}\rangle \langle M|a^+_{\ell',\sigma} a_{0,\gamma}|0\rangle$$

$$- \sum_{\ell'} \{ \sum_{L,L'} V_{(\ell'+L')0,L\,L'} e^{-i\kappa.L'} \langle a^+_{\ell,\sigma} a_{L,\sigma'}\rangle\} \sum_{\gamma} \langle M|a^+_{\ell',\gamma} a_{0,\gamma}|0\rangle$$

$$+ \sum_{\ell',L,L'} V_{(\ell'+L')0,L'L} e^{-i\kappa.L'} \sum_{\gamma} \langle a^+_{\ell,\sigma} a_{L,\gamma}\rangle \langle M|a^+_{\ell',\gamma} a_{0,\sigma'}|0\rangle$$

1.10

This equation has precisely the same structure as (1.5), with the matrix element $\langle M|a^+_{\ell,\sigma} a_{0,\sigma'}|0\rangle$ playing the role of $\hat{X}_\ell$, and because of the presence of the exchange terms it can be used to study the properties of semi-conductors and insulators.

The next part of this section deals with an application of (1.10). Let us focus our attention on metal physics. We take as our model of a simple metal, a cubic lattice of N atoms with one electron per lattice site located in a 1s hydrogen like orbital (χ). The band structure of the metal will be described with the aid of a well known approximation, the tight binding approximation. The TBA has won much favour with theoreticians in the realms of both solid state and surface physics because of its mathematical simplicity. In contrast to the jellium model of a metal, the TBA deals with the case in which the overlap of

atomic orbitals is sufficiently small so that in the vicinity of a lattice point, an atomic description is appropriate. In consequence, the Bloch states may be constructed from atomic orbitals instead of Wannier functions

$$\phi_k(r) = \frac{1}{\sqrt{N}} \sum_{\ell} \chi(r-\ell) e^{ik.\ell} \qquad 1.11$$

This approximation has been particularly successful in describing transition metal d bands, and it was for this reason that early chemisorption studies courted the TBA (Grimley, 1958). Working within the TBA much simplifies equation (1.10) because the Coulomb integrals $V_{\ell'L',L\ell}$ i.e. integrals of the form

$$\int d^3r \int d^3r' \; \chi^*(r-\ell')\chi^*(r'-L')v(r-r')\chi(r'-L)\chi(r-\ell)$$

are zero unless $\ell' = \ell$ and $L' = L$. To see this we need only express $v(r-r')$ as a Fourier series and neglect the overlap of atomic orbitals on different lattice sites in the resulting integrals.

$$V_{\ell'L',L\ell} = 0 \qquad \text{unless} \quad \ell' = \ell \quad \text{and} \quad L' = L \qquad 1.12$$

Under these circumstances, the excitation spectrum of the metal is determined by solving the eigenvalue problem generated by the following linear equation

$$\omega_M \langle M|a^+_{\ell,\sigma}a_{0,\sigma'}|0\rangle = \sum_{\ell'} H_{\ell',\ell}\left[1 - e^{-i\kappa.(\ell-\ell')}\right] \langle M|a^+_{\ell',\sigma}a_{0,\sigma'}|0\rangle$$
$$+ \langle a^+_{\ell,\sigma}a_{0,\sigma'}\rangle \sum_{\ell'} (V_{\ell\ell',\ell'\ell} - V_{\ell'0,0\ell'}) e^{-i\kappa.\ell'} \sum_{\gamma} \langle M|a^+_{0,\gamma}a_{0,\gamma}|0\rangle$$

1.13

In writing (1.13) we have dropped exchange terms from (1.10).

Discussion of the Eigenvalue Problem.

Let us consider the nature of the coefficients of the one electron transition matrix elements in equation (1.13). Firstly, there are one electron terms:

$$H_{\ell',\ell} = \int d^3r\ \chi^*(r-\ell')\{-\tfrac{1}{2}\nabla_r^2 + V_{ion}(r)\}\chi(r-\ell) \qquad 1.14$$

We can express these coefficients as a function of a 'hopping' parameter by defining a potential, V, as follows

$$V(r-\ell) = V_{ion}(r) - V_a(r-\ell) \qquad 1.15$$

where $V_a(r-\ell)$ is the potential that an electron at position r would experience if there were only a single atom present, namely that at site ℓ. Thus $V(r-\ell)$ is the potential energy of an electron at r resulting from all the ion cores in the crystal except the one at site ℓ. Therefore

$$H_{\ell',\ell} = \int d^3r\ \chi^*(r-\ell')\{-\tfrac{1}{2}\nabla_r^2 + V_a(r-\ell)\}\chi(r-\ell) + \int d^3r\ \chi^*(r-\ell')V(r-\ell)\chi(r-\ell) \qquad 1.16$$

and so if ε_a is the energy of atomic orbital χ, then

$$H_{\ell',\ell} = \varepsilon_a\delta_{\ell,\ell'} + \int d^3r\ \chi^*(r-\ell')V(r-\ell)\chi(r-\ell) \qquad 1.17$$

At this point we can again invoke the TBA which implies that the above overlap integral is only non zero for neighbouring lattice sites ℓ and ℓ'. Thus

$$H_{\ell',\ell} = \varepsilon_a\delta_{\ell,\ell'} + u\,\tilde{\delta}_{\ell,\ell'} \qquad 1.18$$

where the tilde over the Kronecker delta function indicates that ℓ and ℓ' refer to neighbouring ion cores. Note also that u, the hopping parameter, is independent of our choice of neighbouring sites. This is a consequence of the simple cubic structure of the lattice and the spherical symmetry of the atomic orbital χ.

The second type of coefficient appearing in (1.13) is a many body term:

$$\langle a^{+}_{\ell,\sigma} a_{O,\sigma'} \rangle \sum_{\ell'} (V_{\ell\ell',\ell'\ell} - V_{\ell' O, O\ell'}) \, e^{-i\kappa.\ell'}$$

An important factor in this term is the expectation value of the site operators.

$$\langle a^{+}_{\ell,\sigma} a_{O,\sigma'} \rangle = \langle O | a^{+}_{\ell,\sigma} a_{O,\sigma'} | O \rangle_{Har} = \delta_{\sigma,\sigma'} \frac{1}{N} \sum_{k} n_{k,\sigma} \, e^{ik.\ell} \qquad 1.19$$

Unfortunately, the wave vector summation cannot be carried out analytically because of the presence of the occupation number. However, recalling that for a jellium model

$$\frac{1}{N} \sum_{k} n_k \, e^{ik.\ell} \propto \frac{\sin k_f \ell - k_f \ell \cos k_f \ell}{k_f^3 \, \ell^3} \qquad 1.20$$

one expects the expectation value to rapidly decrease as $|\ell|$ increases. It only remains to deal with the direct lattice summation over the so called dipolar integrals: $\sum_{\ell'} V_{\ell\ell',\ell'\ell} \, e^{-i\kappa.\ell'}$ (The dipolar terms are discussed in Chapter III. They in fact correspond to an electron being tightly bound to a hole). In particular we require the functional dependence of this sum on the lattice vector ℓ. This can be obtained as follows

$$\sum_{\ell'} V_{\ell\ell',\ell'\ell}\, e^{-i\kappa.\ell'} = \sum_{\ell'} \int d^3r \int d^3r'\ |\chi(r-\ell)|^2 v(r-r') |\chi(r'-\ell')|^2\ e^{i\kappa.\ell'} \qquad 1.21$$

so that writing the Coulomb potential as a Fourier series

$$v(r-r') = \sum_{k} v(k) e^{-ik.(r-r')} \quad ; \quad v(k) = \frac{4\pi\, e^2}{(\text{vol of crystal})\, k^2} \qquad 1.22$$

we are able to separate the real space integration over r and r', leaving the summation over ℓ' trivial

$$\sum_{\ell'} V_{\ell\ell',\ell'\ell}\, e^{-i\kappa.\ell'} = \sum_{k} v(k) |F(k)|^2\, e^{-ik.\ell} \sum_{\ell'} e^{i(k-\kappa).\ell'} \qquad 1.23$$

where F(k) is the Fourier transform of the atomic orbital density

$$F(k) = \int d^3r\ |\chi(r)|^2\ e^{ik.r} \qquad 1.24$$

The right hand side of (1.23) is therefore $N \sum_{G} v(\kappa+G) |F(\kappa+G)|^2\, e^{-i\kappa.\ell}$. It is useful to have a symbol for the sum over reciprocal lattice vectors, and so we define

$$\Omega(\kappa) = N \sum_{G} v(\kappa+G) |F(\kappa+G)|^2 \qquad 1.25$$

Thus

$$\sum_{\ell'} V_{\ell\ell',\ell'\ell}\, e^{-i\kappa.\ell'} = \Omega(\kappa)\ e^{-i\kappa.\ell} \qquad 1.26$$

which clearly displays the dependence of the sum on ℓ. Also, since $V_{\ell\ell',\ell'\ell} = V_{\ell'\ell,\ell\ell'}$, then we deduce from (1.26) that

$$\sum_{\ell'} V_{\ell' 0, 0\ell'}\, e^{-i\kappa.\ell'} = \Omega(\kappa) \qquad 1.27$$

It is now apparent that the linear equation for the electron hole

matrix element (1.13) can be written in the form:

$$\omega_M \langle M|a^+_{\ell,\sigma}a_{O,\sigma'}|O\rangle = u \sum_{\ell'} [1 - e^{-i\kappa.(\ell-\ell')}]\, \tilde{\delta}_{\ell',\ell}\, \langle M|a^+_{\ell',\sigma}a_{O,\sigma'}|O\rangle$$

$$+ \langle a^+_{\ell,\sigma}a_{O,\sigma'}\rangle\, \Omega(\kappa)\, [e^{-i\kappa.\ell} - 1] \sum_{\gamma} \langle M|a^+_{O,\gamma}a_{O,\gamma}|O\rangle \qquad 1.28$$

We observe from (1.19) that $\langle a^+_{\ell,\sigma}a_{O,\sigma'}\rangle \propto \delta_{\sigma,\sigma'}$, and so only amplitudes with parallel spin eigenvalue need concern us (amplitudes with $\sigma \neq \sigma'$ satisfy the equation for non interacting particles). Also, since there are no spin operators in the Hamiltonian, the excitations can be classified as singlet or triplet states (Oddershede, 1978)

$$\langle M|a^+_{\ell,\uparrow}a_{O,\uparrow}|O\rangle = + \langle M|a^+_{\ell,\downarrow}a_{O,\downarrow}|O\rangle \quad \text{for a singlet state} \qquad 1.29$$

$$\langle M|a^+_{\ell,\uparrow}a_{O,\uparrow}|O\rangle = - \langle M|a^+_{\ell,\downarrow}a_{O,\downarrow}|O\rangle \quad \text{for a triplet state}$$

Because of this, the summation over γ in (1.28) vanishes for triplet states. These states are therefore physically uninteresting in a many body context. However, the singlet states satisfy

$$\omega_M \langle M|a^+_{\ell,\uparrow}a_{O,\uparrow}|O\rangle = u \sum_{\ell'} [1 - e^{-i\kappa.(\ell-\ell')}]\, \tilde{\delta}_{\ell',\ell}\, \langle M|a^+_{\ell',\uparrow}a_{O,\uparrow}|O\rangle$$

$$+ 2\, \Omega(\kappa)\, \langle a^+_{\ell,\uparrow}a_{O,\uparrow}\rangle\, [e^{-i\kappa.\ell} - 1]\, \langle M|a^+_{O,\uparrow}a_{O,\uparrow}|O\rangle \qquad 1.30$$

This is the key equation for our investigation of the excitation spectrum of the simple metal detailed on page 27. By writing this equation down for all possible values of ℓ (there are N of them)

we generate an eigenvalue problem of order N x N. It takes the form

$$\omega \underline{X} = \underline{a}\,\underline{X} \qquad 1.31$$

where $\underline{X}$ is the column vector: $(\langle M|a^{+}_{\ell,\uparrow}a_{0,\uparrow}|0\rangle)$

and the square matrix $\underline{a}$ has elements:

$$a_{\ell,\ell'} = u\,[1 - e^{-i\kappa.(\ell-\ell')}]\tilde{\delta}_{\ell',\ell} + 2\Omega(\kappa)\langle a^{+}_{\ell,\uparrow}a_{0,\uparrow}\rangle[e^{-i\kappa.\ell} - 1]\,\delta_{\ell',0} \qquad 1.32$$

one electron coefficients *many body coefficients*

The eigenvalues ω_M are obtained by solving the characteristic equation

$$\det\,(\omega\underline{1} - \underline{a}) = 0 \qquad 1.33$$

For ease of reference, let us agree to call the matrix: $(\omega\underline{1} - \underline{a})$, the 'characteristic matrix'. The presence of nearest neighbour interactions in (1.32) means that the rows of the characteristic matrix are linearly independent, because of this the elements of the eigenvector $\underline{X}$ (the electron hole amplitudes) define a linearly dependent set in which all the amplitudes can be expressed in terms of any given amplitude. Let us single out the amplitude at the origin and write

$$\langle M|a^{+}_{\ell,\uparrow}a_{0,\uparrow}|0\rangle \propto \langle M|a^{+}_{0,\uparrow}a_{0,\uparrow}|0\rangle \quad \text{for all } \ell \qquad 1.34$$

The absolute value of $\langle M|a^{+}_{\ell,\uparrow}a_{0,\uparrow}|0\rangle$ is determined from the following normalisation condition (see I.2.12).

$$\int dx\ \delta V_M(x;\omega_M)\,\delta\rho_M(x;\omega_M) = 1 \qquad 1.35$$

This identity can be written in the form (see I.2.6 and I.2.11)

$$\int dx \int dx'\ v(r-r')\langle M|\psi^+(x')\psi(x')|O\rangle^*\langle M|\psi^+(x)\psi(x)|O\rangle = |C_M|^2 \qquad 1.36$$

or in site space (for singlet states) as

$$4 \sum_{\ell,\ell'} \sum_{L,L'} V_{\ell(L'+L),L'(\ell+\ell')} e^{i\kappa.(\ell-L')}\langle M|a^+_{\ell',\uparrow}a_{O,\uparrow}|O\rangle^*\langle M|a^+_{L,\uparrow}a_{O,\uparrow}|O\rangle = |C_M|^2 \qquad 1.37$$

Equation (1.37) is model independent. For our tightly bound metal however, we only retain those terms which have $\ell' = 0$ and $L = 0$. In consequence, the normalisation condition becomes

$$|C_M|^2 = 4\ |\langle M|a^+_{O,\uparrow}a_{O,\uparrow}|O\rangle|^2 \sum_{\ell} e^{i\kappa.\ell} \{\sum_{\ell'} V_{\ell\ell',\ell'\ell} e^{-i\kappa.\ell'}\} \qquad 1.38$$

and reference to (1.26) shows that

$$|C_M|^2 = 4N\ \Omega(\kappa)\,|\langle M|a^+_{O,\uparrow}a_{O,\uparrow}|O\rangle|^2 \qquad 1.39$$

The above relation determines the absolute value of the amplitude at the origin (once the value of the eigenvalue ω_M is known †), and therefore the absolute value of $\langle M|a^+_{\ell,\uparrow}a_{O,\uparrow}|O\rangle$.

The eigenvalue problem (1.31) is now completely defined. What type of solutions do we anticipate ? It is clear that the one electron coefficients in (1.32) vanish as $\kappa \to 0$ and that the many body coefficients are small at large ℓ (since $\langle a^+_{\ell,\uparrow}a_{O,\uparrow}\rangle$ is a rapidly decreasing function of ℓ). In view of this, let us consider the long wavelength and asymptotic behaviour of the electron hole matrix elements.

† $|C_M|^2 = e^2 \dfrac{\partial \omega_M}{\partial e^2}$ (I.3.10)

The small κ limit.

In the absence of the electron electron interaction, the characteristic equation (1.33) takes the trivial form: $\det(\omega\underline{1})=0$ at small κ, giving N zero values of ω_M. The effect of the Coulomb interaction between electrons is to give the possibility of non zero frequencies at $\kappa = 0$, for although the one electron terms in (1.32) go to zero as $O(\kappa)$, the Coulomb interaction terms diverge as $O(1/\kappa)$. If non zero values of ω_M do exist at long wavelengths, they will be obtained from an iterative procedure - because the many body coefficients in the characteristic matrix dominate in this limit.

The appropriate iterative solution is shown below.

$$\omega_M^2 \langle M|a^+_{\ell,\uparrow}a_{0,\uparrow}|0\rangle =$$

$$2\,\omega_M\,\Omega(\kappa)\langle a^+_{\ell,\uparrow}a_{0,\uparrow}\rangle[e^{-i\kappa.\ell} - 1]\langle M|a^+_{0,\uparrow}a_{0,\uparrow}|0\rangle$$

$$+ 2\,\Omega(\kappa)\{\,u\sum_{\ell'}[1 - e^{-i\kappa.(\ell-\ell')}]\langle a^+_{\ell',\uparrow}a_{0,\uparrow}\rangle[e^{-i\kappa.\ell'} - 1]\tilde{\delta}_{\ell',\ell}\}\,\langle M|a^+_{0,\uparrow}a_{0,\uparrow}|0\rangle$$

$$+ \ldots \qquad 1.40$$

By setting $\ell=0$, the eigenvalue is obtained explicitly for small κ.

$$\omega_M^2 = 2\,\Omega(\kappa)\,\frac{1}{N}\sum_k n_k\,u\sum_{\ell'}[1 - e^{i\kappa.\ell'}][e^{-i\kappa.\ell'} - 1]\,e^{ik.\ell'}\,\tilde{\delta}_{\ell',0} \qquad 1.41$$

We can simplify this equation by introducing the tight binding expression for the one electron energy (ε)

$$\varepsilon(k) = \varepsilon_a + u\sum_{\ell} e^{ik.\ell}\,\tilde{\delta}_{\ell,0} \qquad 1.42$$

For a simple cubic lattice, ε is an even function of k:

$$\varepsilon(k) = \varepsilon_a + 2u(\cos k_x a + \cos k_y a + \cos k_z a) \qquad 1.43$$

and so (1.41) becomes

$$\omega_M^2 = 4\Omega(\kappa)\ \frac{1}{N} \sum_k n_k [\varepsilon(k+\kappa) - \varepsilon(k)] \qquad 1.44$$

Is ω_M non zero as $\kappa \to 0$? To answer this question we need to look at the definition of the energy: $\Omega(\kappa)$. For convenience we reproduce it again here

$$\Omega(\kappa) = N \sum_G v(\kappa+G)\,|F(\kappa+G)|^2$$

where v and F are the Fourier transforms of the Coulomb potential and atomic orbital density $|\chi(r)|^2$, respectively. The reciprocal lattice vector $G = 0$ is included in the summation so that for small values of κ

$$\Omega(\kappa) = N\ v(\kappa)\,|F(\kappa)|^2$$

and since $F(0)=1$, then

$$\Omega(\kappa) \to N\ v(\kappa) \qquad \text{as} \quad \kappa \to 0$$

We need also to look at the Brillouin zone summation in (1.44). Let us fix the Fermi level at the atomic orbital energy (ε_a). The occupation numbers are therefore step functions

$$n_k = \Theta(\cos k_x a + \cos k_y a + \cos k_z a) \quad ; \quad \Theta(x) = \begin{matrix} 1 & \text{if } x > 0 \\ 0 & \text{otherwise} \end{matrix} \qquad 1.45$$

We see that the Fermi function (n) is an even function of each of the components of the wave vector k, and further that it is invariant under the interchange of the components. Because of this, the Brillouin zone summation can be expressed as follows

$$\frac{1}{N}\sum_k n_k[\varepsilon(k+\kappa)-\varepsilon(k)] = 2u(\cos\kappa_x a + \cos\kappa_y a + \cos\kappa_z a - 3)\frac{1}{N}\sum_k n_k \cos k_x a \qquad 1.46$$

We conclude that

$$\omega_M^2(\kappa=0) = \lim_{\kappa\to 0} 4N\, v(\kappa)\, 2u(-\frac{\kappa^2 a^2}{2})\frac{1}{N}\sum_k n_k \cos k_x a \qquad 1.47$$

and substituting expression (1.22) for $v(\kappa)$, we finally obtain the eigenvalue in units of Hartree

$$\omega_M^2(\kappa=0) = -16\pi u(\frac{a}{a_o})\frac{1}{N}\sum_k n_k \cos k_x a \qquad (\text{N.B. } u<0) \qquad 1.48$$

The above equation shows that the long range nature of the Coulomb interaction gives rise to a non zero eigenvalue at $\kappa = 0$. The corresponding eigenmode is the *plasmon* excitation. The existence of such an excitation can be understood qualitatively by considering a more obvious manifestation of the electron electron interaction in a metal; screening. Any imbalance in the charge distribution of an electron gas will quickly be screened. This is the short range effect of the Coulomb potential. The long range effect is to <u>sustain</u> the polarisation wave accompanying such screening processes thereby establishing a collective oscillation of the electron density: the plasmon mode.

The electron hole amplitudes for the plasmon excitation are determined (at small κ) from (1.40)

$$\langle M|a^+_{\ell,\uparrow}a_{O,\uparrow}|O\rangle = \frac{2\Omega(\kappa)}{\omega_M}\langle a^+_{\ell,\uparrow}a_{O,\uparrow}\rangle[e^{-i\kappa.\ell} - 1]\langle M|a^+_{O,\uparrow}a_{O,\uparrow}|O\rangle \qquad 1.49$$

The plasmon amplitude is therefore localised in site space, and as such, only a relatively small portion of the lattice may be required to give accurate values of the plasmon energy.

The magnitude of the plasmon amplitude at the origin is easily obtained with the aid of the normalisation relation (1.39)

$$e^2 \frac{\partial \omega_M}{\partial e^2} = 4N\ \Omega(\kappa) \left| \langle M | a^+_{O,\uparrow} a_{O,\uparrow} | O \rangle \right|^2 \qquad 1.50$$

Since the eigenvalue is known at small κ, the differentiation with respect to the coupling constant e^2 can be carried out explicitly. The result is that the left hand side of (1.50) is equal to half the plasmon energy, and so

$$\left| \langle M | a^+_{O,\uparrow} a_{O,\uparrow} | O \rangle \right|^2 = \frac{\omega_M}{8N\ \Omega(\kappa)} \qquad 1.51$$

Without loss of generality, we take $\langle M | a^+_{O,\uparrow} a_{O,\uparrow} | O \rangle$ to be real. The normalised plasmon amplitude at an arbitrary lattice site is thus

$$\langle M | a^+_{\ell,\uparrow} a_{O,\uparrow} | O \rangle = \sqrt{\frac{\Omega(\kappa)}{2N\omega_M}}\ \langle a^+_{\ell,\uparrow} a_{O,\uparrow} \rangle [e^{-i\kappa.\ell} - 1] \quad \text{for small } \kappa \qquad 1.52$$

We have learned from studying the long wavelength limit that

(i) There exists a mode with non zero frequency at $\kappa = 0$.

(ii) The mode is localised in site space.

The large $|\ell|$ limit.

The many body interaction term in (1.30) is small at large values of $|\ell|$ so that the electron hole amplitudes asymptotically satisfy the following equation

$$\omega_M \langle M | a^+_{\ell,\uparrow} a_{O,\uparrow} | O \rangle = u \sum_{\ell'} [1 - e^{-i\kappa.(\ell-\ell')}] \tilde{\delta}_{\ell',\ell} \langle M | a^+_{\ell',\uparrow} a_{O,\uparrow} | O \rangle \qquad 1.53$$

which admits a solution of the form

$$\langle M|a^{+}_{\ell,\uparrow}a_{0,\uparrow}|0\rangle \quad \propto \quad e^{-i(k+\kappa).\ell} \qquad \text{provided} \qquad \omega_M = \varepsilon(k+\kappa) - \varepsilon(k) \qquad 1.54$$

This solution set clearly contains the Hartree values of the electron hole amplitudes and excitation energies.

$$\langle M|a^{+}_{\ell,\uparrow}a_{0,\uparrow}|0\rangle_{Har} = \frac{1}{\sqrt{2}}\frac{1}{N}\, e^{-i(k+\kappa).\ell} \qquad 1.55$$

$$\omega_{Har} = 2u\,[\cos(k_x+\kappa_x)a - \cos k_x a + \cos(k_y+\kappa_y)a - \cos k_y a + \cos(k_z+\kappa_z)a - \cos k_z a\,]$$

The first Brillouin zone wave vectors k and κ in (1.55) satisfy

$$n_k(1-n_{k+\kappa}) = 1 \qquad 1.56$$

This restriction on the occupation numbers ensures that the frequency of an elementary excitation $(E_M - E_o)$ does not take on negative values. (Allowing k and κ to be wave vectors outside the 1^{st} B.Z. only produces values already in the Hartree solution set).

It is worth discussing the Hartree spectrum in some detail. The lower bound of the spectrum for a given value of κ is zero, whilst the upper bound is determined in the usual way: we search for those values of k_x, k_y and k_z which render $\frac{\partial\omega}{\partial k_i}$ zero (i = x,y,z). By symmetry it is sufficient to consider i = x. We find that the requirement on k_x is

$$\tan k_x a = \frac{\sin\kappa_x a}{1 - \cos\kappa_x a} \qquad 1.57$$

It is easy to see without resorting to higher derivatives, that the maximum single particle excitation energy, for fixed κ, is

$$\omega^{max}_{Har} = -4u\,(|\sin\tfrac{1}{2}\kappa_x a| + |\sin\tfrac{1}{2}\kappa_y a| + |\sin\tfrac{1}{2}\kappa_z a|\,) \qquad 1.58$$

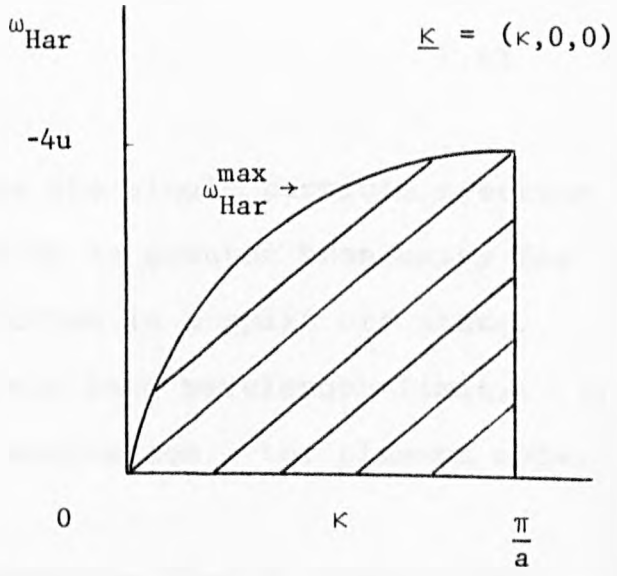

Figure 1: The Hartree Spectrum.

The shading indicates that the spectrum is continuous to the order of $\frac{1}{N}$.

$$\omega^{min}_{Har} = 0$$

$$\omega^{max}_{Har} = -4u \sin \tfrac{1}{2}\kappa_x a$$

In addition to the Hartree solutions, there are exponentially decaying solutions to (1.53). They correspond to complex values of k in (1.54). Let $k \to k - ij$, for real k and j. The amplitudes then take the form

$$\langle M | a^{+}_{\ell,\uparrow} a_{O,\uparrow} | O \rangle \propto e^{-i(k+\kappa).\ell} e^{-j.\ell} \qquad 1.59$$

subject to the constraint $\omega_M = \varepsilon(k+ij+\kappa) - \varepsilon(k+ij)$.

To explore this further, take κ to be in the (100) direction, so that the constraint on k and j becomes

$$\frac{\omega_M}{2u} = [\cos(k_x+\kappa_x)a - \cos k_x a]\cosh j_x a \;\; ; \;\; [\sin k_x a - \sin(k_x+\kappa_x)a]\sinh j_x a = 0$$

We disregard the possibility of $\sinh j_x a$ being zero, since this reproduces the Hartree spectrum. In consequence k_x must satisfy

$$\sin k_x a - \sin (k_x+\kappa_x)a = 0 \quad \Rightarrow \quad \tan k_x a = \frac{\sin \kappa_x a}{1 - \cos \kappa_x a} \qquad 1.60$$

and referring to (1.57) we find that

$$\omega_M = \omega_{Har}^{max} \cosh j_x a \qquad 1.61$$

This solution always lies above the single particle spectrum for $j_x a \neq 0$, since the hyperbolic cosine is greater than unity for non vanishing argument, i.e. the solution is a split off state. We have met such a state before. In the long wavelength limit, $\kappa \to 0$, there is only one non zero frequency excitation - the plasmon mode. This is our split off state.

The above analysis does not guarentee that a plasmon mode exists for all values of the wave vector κ. The prerequisite for the existence of a plasmon is that the asymptotic solution is compatible with the full eigenvalue problem i.e. that solutions at large $|\ell|$ can be joined smoothly to those at small $|\ell|$. It is this 'matching' criterion which determines the values of $j_x a$.

We conclude from our investigation of the long wavelength and asymptotic limits, that in general there are both *extended* and *localised* solutions to the RPA equations in site space. The extended solutions (to the order of $\frac{1}{N}$) are simply the Hartree excitations of the model, whilst the localised solution is the plasmon mode.

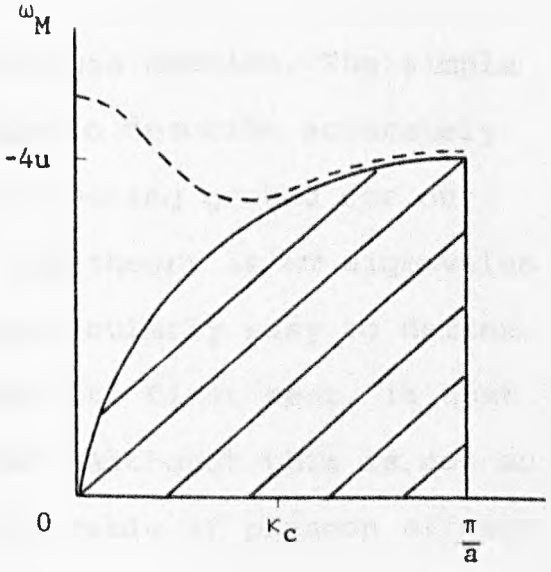

Figure 2: The RPA Spectrum.

The broken line shows the plasmon mode split off from the continuum for $\kappa < \kappa_c$. Above this cut off wave vector the plasmon mode is no longer well defined.

It is convenient at this stage to consider the number of modes in the metal. We see from the spectral representation of the response function, that if ω is a solution to the characteristic equation (1.33), then so too is $-\omega$. This can also be deduced from the linear equation (1.30), and is a consequence of the electron hole symmetry incorporated in the linearisation procedure. The negative frequencies are disregarded, so that for each value of κ, ω_M takes only $\frac{N}{2}$ values (not necessarily distinct). This is true whether or not the electron electron interaction is taken into account. Therefore, in order to accommodate the plasmon mode in our metal, we must lose one excitation from the Hartree spectrum. Which excitation is lost ?

Clearly, the plasmon mode returns to the single particle continuum in the absence of the electron electron interaction. The only way this can happen is for $j_x a \to 0$ as $e^2 \to 0$ (see 1.61) in which case $\omega_{plasmon} \to \omega_{Har}^{max}$. Thus the effect of the electron electron interaction is to lift the single particle excitation with *maximum* frequency from the Hartree spectrum.

Summary.

Let us reflect on the contents of this section. The simple model we have considered, makes no claim to describe accurately a real physical system, rather, it is a testing ground for our site space method. The focal point of the theory is an eigenvalue equation, and as we have seen, it is particularly easy to define. The site space approach therefore passes its first test, in that the key equations are readily formulated. Although this is not an essential requirement, it is highly desireable if plasmon effects

are to be calculated for more complicated tight binding systems e.g. transition metal surfaces.

Another test of the method, is whether the key equation can be solved for simple cases, or at appropriate limits. If this is possible it can provide insight into the physics of a model at an early stage. We found for example that the excitation spectrum of a tightly bound metal consists of a plasmon and a continuum of one electron transitions - without solving the eigenvalue problem first (Pt 4 Rogan and Inglesfield, 1981). A study of simple cases can also indicate whether the method in general, is likely to be a good one. This consideration is especially relevant to the site space approach. We showed that the plasmon is localised in site space, so that solving the eigenvalue equation for the plasmon mode is a sensible and direct way to proceed.

The final and important test, is the amount of computing effort required by the method. This merits a section to itself.

II.2 Plasmon Frequencies of a Simple Metal.

The existence of organised electronic excitations in a metal was first demonstrated theoretically by Bohm and Pines (1953). They showed that the collective co-ordinate of the homogeneous electron gas, exhibits oscillatory behaviour in the long wavelength limit.

$$\ddot{\rho}_k + \omega^2 \rho_k = 0 \quad ; \quad \rho_k = \sum_i e^{-ik.r_i} \qquad 2.1$$

To obtain this result, Pines had neglected terms of *randomly* varying phases in the equation of motion of ρ_k, and in doing so established the random phase approximation in its simplest form. The frequency of the simple harmonic motion described by (2.1) -

the plasma frequency, is easily written in terms of the electron density n, $\omega^2 = 4\pi n$. This can be deduced from equation (II.1.44). The plasma frequencies of the alkali metals are tabulated below.

Table 1 Classical Plasma Frequencies (Kunz, 1965).

	Experiment	Theory (RPA)
Potassium	0.14	0.16
Sodium	0.21	0.22
Lithium	0.26	0.30

The values quoted are in Hartrees (1 a.u.$\sim$ 27eV). We note that the theoretical values of the plasma frequency are about 10% too high.

Table 1 helps us to assign the two parameters of our model namely the lattice parameter and hopping parameter. We have seen that the long wavelength plasmon frequency of the tightly bound metal is given by (II.1.48). The Brillouin zone summation in this formula is trivial to compute, the answer is 0.1671. Therefore

$$\omega_M^2(\kappa=0) = - 8.344u \left(\frac{a}{a}o\right) \qquad 2.2$$

Take the crystal to be a cube of side La so that the total number of electrons (N) is simply L^3, and the volume per electron is a^3. Thus the lattice parameter is a measure of electron density, and in keeping with convention we introduce the r_s value: $\frac{4}{3}\pi r_s^3 = \left(\frac{a}{a_o}\right)^3$.

The range of metallic densities is $1.8 < r_s < 5.5$, and a typical value is $r_s=4$. For a simple cubic lattice this means that $a = 6.5a_o$ (there is only one metal in the periodic table with a simple cubic lattice - polonium, this has $a = 6.33a_o$). If we now set $u = -0.01, -0.03, -0.05$ then the plasmon frequencies at $\kappa=0$ are 0.11, 0.20, and 0.25 a.u. which are close to the experimental

values of the alkali metals. Choosing $a = 6.5a_o$ (r_s=4) is taking the validity of the RPA beyond its limit, it is strictly valid for $r_s < 1$. Because of this, let us also take $a = 2.5a_o$ (r_s=0.9) and an intermediate value of $a = 2.5a_o$ (r_s=1.5).

Table 2 Plasmon Frequencies at $\kappa = 0$ of the T.B. Metal

	$a = 1.5a_o$	$a = 2.5a_o$	$a = 6.5a_o$
u = -0.01	0.2366	0.1833	0.1137
u = -0.03	0.4098	0.3175	0.1969
u = -0.05	0.5291	0.4098	0.2542

The trends in the plasmon frequency are readily interpreted. For a given value of u, as we increase the lattice spacing the volume per electron is increased, thus the electron density, and therefore the plasmon frequency, decreases. As we increase the hopping parameter, 'a' fixed, the electron system becomes more free electron like i.e. more responsive to changes in electron density - $\omega_{plasmon}$ increases.

The maximum values of the one electron transition frequencies produced by this choice of parameters are shown below.

Table 3 Maximum One Electron Transition Frequencies ω_{Har}^{max}

	$\underline{\kappa} = \frac{\pi}{a}(100)$	$\underline{\kappa} = \frac{\pi}{a}(110)$	$\underline{\kappa} = \frac{\pi}{a}(111)$
u = -0.01	0.04	0.08	0.12
u = -0.03	0.12	0.24	0.36
u = -0.05	0.20	0.40	0.60

This table demonstrates that the excitation energies of the single particle modes can become comparable to plasmon energies.

By selecting three values of the lattice parameter, and three values of the hopping parameter, we are in effect going to explore the many body properties of nine different physical models. The reasons for choosing this number of pairings of the parameters u and a (in addition to those already given) are outlined below.

(i) The position of the plasmon mode with respect to the single particle continuum, is parameter dependent. Certain choices of u and a might give rise to a plasmon excitation which lies well above the continuum over the entire Brillouin zone. In this case the eigenvalue of maximum modulus will be well separated from the others and one expects that there would be little difficulty in calculating it. For other choices of u and a, the plasmon mode will merge with the single particle continuum along some directions in the Brillouin zone - this is a more realistic situation. How easily would the site space technique deliver the eigenvalue of maximum modulus if it lay close to the continuum? This question is particularly important if the plasmon mode merges with the continuum at small $|\kappa|$. By varying the parameters we can control the way in which the plasmon mode merges with the continuum and look for any situations where the site space technique would in inapplicable.

(ii) Quantities of physical interest such as the interaction energy, can be expressed as Brillouin zone summations over functions of the frequencies and spectral strengths of the elementary excitations of the many body system.

It is of value therefore to ask during our investigations, if the site space method is capable of delivering the excitation spectrum (and the related spectral strengths) at an arbitrary wave vector in an efficient manner, so that modal sums such as the interaction energy can be determined without further approximation (Baldereschi, 1978). The answer to this question is parameter dependent, for the computing effort required to obtain plasmon energies well above the single particle continuum will be much less than that required to obtain plasmon energies close to the continuum. Furthermore, variation of the lattice parameter allows us to examine the dependence of the interaction energy and exchange correlation energy on the electron density of the metal.

(iii) In a later section we determine the spectral strength of a single particle mode. This involves the use of a Lippman-Schwinger scattering theory approach coupled with the plasmon pole approximation. As a test of the reliability of the resulting expression for the spectral strength, we look to a sum rule. How well the sum rule is satisfied depends on the status of the plasmon pole approximation - this is parameter dependent since at high electron density and small $|\kappa|$, the plasmon excitation will screen the single particle modes more efficiently (for a given value of hopping parameter) than at lower densities.

It is for these reasons that we have chosen a wide range of parameters. Having set the range of parameters,

we compare the site space calculation of the excitation spectrum and spectral strengths, with that of the dielectric method. The comparison will take place on as many levels as possible e.g. we will look at the work involved in setting up the computer programs and the computer time required by the methods. All computations in this thesis were carried out on the IBM 4341 machine at Liverpool University (this machine sets double precision by default). The range of the computer is approximately 10^{-77} to 10^{+75}.

A quantity common to both methods is the energy term $\Omega(\kappa)$

$$\Omega(\kappa) = N \sum_{G} v(\kappa+G) |F(\kappa+G)|^2; \quad F(\kappa) = \int d^3r |\chi(r)|^2 e^{i\kappa.r}$$

The Fourier transform, F, is easy to evaluate for the 1s hydrogen-like orbital.

$$\chi(r) = \sqrt{\frac{1}{\pi}} \left(\frac{z}{a_o}\right)^3 e^{-(z/a_o)r}; \quad F(\kappa) = \frac{16\, z^4}{(4z^2+a_o^2\kappa^2)^2}$$

Although we have displayed explicitly the nuclear charge z, we take z = 1 in the final calculations. We see that Ω is an even function of each of the components of κ, and that it is invariant under the interchange of the components. This statement holds true for n and ε, and consequently also for the plasmon energy itself. Because of this, knowledge of the plasmon energy in one sixth of the positive octant of the first Brillouin zone enables us to write down the plasmon energy for <u>any</u> value of wave vector in the zone.

We therefore only calculate plasmon energies in the wedge shaped region of the positive octant, shown in Figure 3.

FIGURE 3

Diagrams (2), (3), and (4) in this figure demonstrate how the invariance of the plasmon energy under the interchange of κ_x with κ_y, κ_x with κ_z, and finally κ_y with κ_z means that we need calculate plasmon frequencies in a wedge shaped volume of the positive octant shown in diagram (1).

$$\text{Volume of the wedge} = \int_0^{\pi/a} d\kappa_x \int_0^{\kappa_x} d\kappa_y \int_0^{\kappa_y} d\kappa_z = \frac{1}{6}\left(\frac{\pi}{a}\right)^3$$

which is one fortyeighth of the volume of the first Brillouin zone.

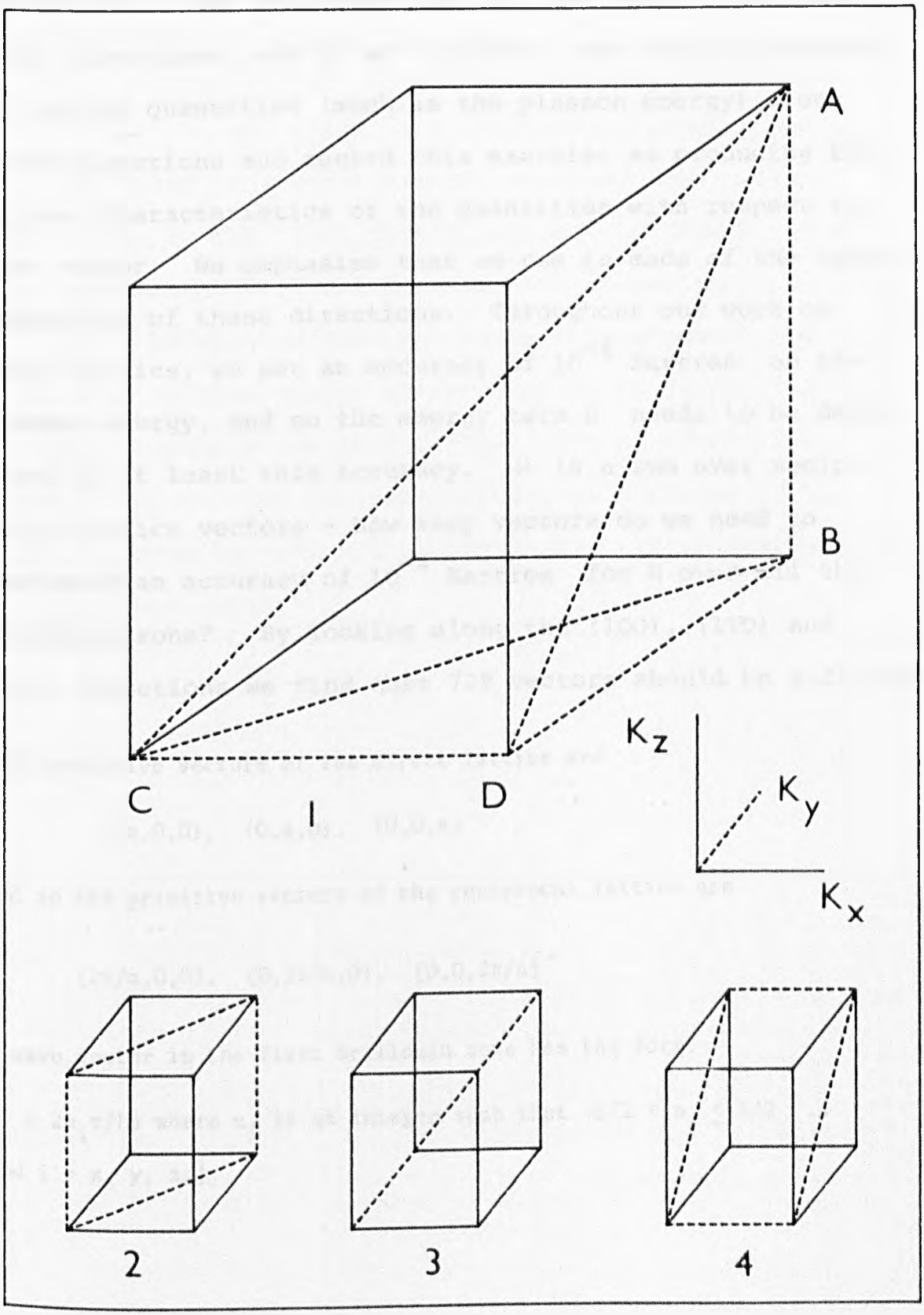
A
B
C
D
1
K_z
K_y
K_x
2
3
4

It is clear from Figure 3 that three important directions in the Brillouin zone are the (100), (110) and (111) directions, and so we initially look at the behaviour of various quantities (such as the plasmon energy) along these directions and regard this exercise as producing the salient characteristics of the quantities with respect to wave vector. We emphasise that no use is made of the special symmetries of these directions. Throughout our work on metal physics, we set an accuracy of 10^{-4} Hartree on the plasmon energy, and so the energy term Ω needs to be determined to at least this accuracy. Ω is a sum over reciprocal lattice vectors - how many vectors do we need to guarantee an accuracy of 10^{-4} Hartree for Ω over all the Brillouin zone? By looking along the (100), (110) and (111) directions we find that 729 vectors should be sufficient.

[The primitive vectors of the direct lattice are

$$(a,0,0), \quad (0,a,0), \quad (0,0,a)$$

and so the primitive vectors of the reciprocal lattice are

$$(2\pi/a,0,0), \quad (0,2\pi/a,0), \quad (0,0,2\pi/a)$$

A wave vector in the first Brillouin zone has the form:

$k_i = 2n_i\pi/La$ where n_i is an integer such that $-L/2 < n_i \leq L/2$

and $i = x, y, z$.]

TABLE 4

'OM n' is the value of Ω obtained by summing over the n shortest reciprocal lattice vectors. The table refers only to the (111) direction i.e. κ = (K,K,K), and K is incremented from 0.1 π/a to π/a in steps of 0.1 π/a. We observe from the table that although one reciprocal lattice vector gives a reasonable approximation at small K (namely the zero vector), 729 G vectors are needed to obtain the desired accuracy at the edge of the Brillouin zone for a = 6.5 atomic units. (Ω is independent of hopping parameter).

KAPPA = (K,K,K)

A	K	OM 1	OM 7	OM 19	OM 343	OM 729
1.5	0.21	24.8580	24.8597	24.8598	24.8598	24.8598
1.5	0.42	4.3139	4.3159	4.3161	4.3161	4.3161
1.5	0.63	1.1141	1.1166	1.1168	1.1168	1.1168
1.5	0.84	0.3258	0.3289	0.3291	0.3292	0.3292
1.5	1.05	0.1026	0.1062	0.1066	0.1067	0.1067
1.5	1.26	0.0345	0.0385	0.0391	0.0392	0.0392
1.5	1.47	0.0124	0.0164	0.0173	0.0175	0.0175
1.5	1.68	0.0048	0.0085	0.0098	0.0100	0.0100
1.5	1.88	0.0019	0.0051	0.0070	0.0074	0.0074
1.5	2.09	0.0008	0.0033	0.0059	0.0068	0.0068
2.5	0.13	16.1955	16.2136	16.2162	16.2168	16.2168
2.5	0.25	3.5268	3.5471	3.5500	3.5506	3.5506
2.5	0.38	1.2579	1.2815	1.2850	1.2857	1.2857
2.5	0.50	0.5300	0.5573	0.5617	0.5625	0.5625
2.5	0.63	0.2406	0.2713	0.2769	0.2779	0.2779
2.5	0.75	0.1139	0.1465	0.1542	0.1555	0.1555
2.5	0.88	0.0555	0.0883	0.0986	0.1005	0.1005
2.5	1.01	0.0278	0.0585	0.0724	0.0754	0.0754
2.5	1.13	0.0142	0.0413	0.0594	0.0643	0.0643
2.5	1.26	0.0075	0.0300	0.0527	0.0612	0.0612
6.5	0.05	6.4839	6.6117	6.6757	6.7191	6.7196
6.5	0.10	1.5874	1.7180	1.7835	1.8278	1.8284
6.5	0.14	0.6815	0.8159	0.8840	0.9301	0.9306
6.5	0.19	0.3654	0.5036	0.5756	0.6241	0.6246
6.5	0.24	0.2200	0.3608	0.4380	0.4898	0.4904
6.5	0.29	0.1420	0.2830	0.3668	0.4230	0.4236
6.5	0.34	0.0959	0.2339	0.3255	0.3874	0.3880
6.5	0.39	0.0667	0.1982	0.2987	0.3681	0.3688
6.5	0.43	0.0474	0.1693	0.2792	0.3584	0.3591
6.5	0.48	0.0342	0.1443	0.2632	0.3554	0.3561

The Momentum Space Calculation.

The standard dielectric function approach, requires us to determine the excitation spectrum of the tightly bound metal by use of the determinantal relation (II.1.4). We therefore need to look at the equation:

$$\det[\delta_{G,G'} - \Lambda(\kappa+G,\kappa+G';\omega)] = 0 \qquad 2.3$$

The Fourier transform of the kernel Λ, is by definition

$$\Lambda(\kappa+G,\kappa+G';\omega) = \int d^3r \int d^3r' \; \Lambda(r,r';\omega) \; e^{i(\kappa+G).r} \; e^{-i(\kappa+G').r'} \qquad 2.4$$

$$\Lambda(r,r';\omega) = 2 \sum_{k,q} \frac{(n_k - n_q)}{[\omega-(\varepsilon(q)-\varepsilon(k))]} \phi_q^*(r)\phi_k(r) \int d^3\mathcal{r} \; v(r'-\mathcal{r})\phi_q(\mathcal{r})\phi_k^*(\mathcal{r})$$

The three real space integrals implicit in the Fourier transform are separated by the translation $r' \to r' + \mathcal{r}$, as shown below.

$$\Lambda(\kappa+G,\kappa+G';\omega) =$$

$$2v(\kappa+G') \sum_{k,q} \frac{(n_k - n_q)}{[\omega-(\varepsilon(q)-\varepsilon(k))]} \int d^3r \; \phi_q^*(r)\phi_k(r) e^{i(\kappa+G).r} \int d^3\mathcal{r} \; \phi_q(\mathcal{r})\phi_k^*(\mathcal{r}) e^{-i(\kappa+G').\mathcal{r}}$$

It is at this stage in the dielectric theory that we make the tight binding approximation. Consider the following integral.

$$\int d^3r \; \phi_q^*(r)\phi_k(r) \; e^{i(\kappa+G).r} = \frac{1}{N} \sum_{\ell,\ell'} e^{-iq.\ell'} e^{ik.\ell} \int d^3r \; \chi^*(r-\ell')\chi(r-\ell) \; e^{i(\kappa+G).r}$$

By neglecting the overlap of atomic orbitals on different sites, we conclude that

$$\int d^3r \; \phi_q^*(r)\phi_k(r) \; e^{i(\kappa+G).r} = F(\kappa+G) \; \delta_{q,k+\kappa+G(k+\kappa)} \qquad 2.5$$

where F is the Fourier transform of the orbital density, $|\chi(r)|^2$, and the wave vector q, belongs to the first Brillouin zone. The reciprocal lattice vector: $G(k+\kappa)$, ensures that this is so. For convenience however, we never display $G(k+\kappa)$ explicitly. The Fourier transform of the polarisation kernel is thus

$$\Lambda(\kappa+G,\kappa+G';\omega) = 2N\, v(\kappa+G')F(\kappa+G)F^{*}(\kappa+G')\,\frac{1}{N}\sum_{k}\frac{(n_k-n_{k+\kappa})}{[\omega-(\varepsilon(k+\kappa)-\varepsilon(k))]} \qquad 2.6$$

Note that because Λ is a separable function of G and G', then

$$\det[\delta_{G,G'} - \Lambda(\kappa+G,\kappa+G';\omega)] = 1 - \text{Trace}\,\Lambda(\kappa+G,\kappa+G';\omega) \qquad 2.7$$

The frequency of an elementary excitation therefore satisfies

$$\sum_{G}\Lambda(\kappa+G,\kappa+G;\omega) = 1 \qquad 2.8$$

Substituting our expression for the polarisation kernel into this equation, and making use of the definition of $\Omega(\kappa)$, gives *the dispersion relation*

$$2\Omega(\kappa)\,\frac{1}{N}\sum_{k}\frac{(n_k-n_{k+\kappa})}{[\omega_M-(\varepsilon(k+\kappa)-\varepsilon(k))]} = 1 \qquad 2.9$$

The omission of $G(k+\kappa)$ from this relation presents no difficulty since it is clear that the domain of the functions n and ε (the occupation number and tight binding energy) is the first Brillouin zone. Returning to the key equation in the site space approach (II.1.30), we can establish a more general result than (2.9), by means of Fourier lattice transforms.

$$\langle M|a^{+}_{\ell,\uparrow}a_{0,\uparrow}|0\rangle = 2\Omega(\kappa)\,\frac{1}{N}\sum_{k}\frac{(n_k-n_{k+\kappa})}{[\omega_M-(\varepsilon(k+\kappa)-\varepsilon(k))]}\,e^{-i(k+\kappa).\ell}\,\langle M|a^{+}_{0,\uparrow}a_{0,\uparrow}|0\rangle \qquad 2.10$$

The usefulness of this explicit expression for the plasmon amplitude is rather limited - for it only provides a means of attaching a number to the plasmon amplitude (via a Brillouin zone summation) once the plasmon energy is known, and whilst it is possible to employ the expression to explore the symmetry properties of the plasmon amplitudes, such properties can be established directly from the eigenvalue equation. To proceed with the momentum space calculation of the plasmon energy, we need to select a frequency interval in which to look for the excitation. We can obtain successive approximations to the plasmon energy by casting the dispersion relation in the form:

$$4\Omega(\kappa)\ \frac{1}{N}\sum_{k}\frac{n_k\,(\varepsilon(k+\kappa)\ -\ \varepsilon(k))}{[\omega_M^2\ -\ (\varepsilon(k+\kappa)\ -\ \varepsilon(k))^2]}\ =\ 1 \qquad 2.11$$

We have made use of the fact that n and ε are even functions. The plasmon excitation is only well defined above the single particle continuum, so that for the plasmon mode

$$\omega_M\ >\ (\varepsilon(k+\kappa)\ -\ \varepsilon(k))\quad \text{for all } k,\ \kappa \qquad 2.12$$

It is clear from this inequality that the plasmon energy satisfies

$$\omega_M^2\ =\ 4\Omega(\kappa)\ \{S_1\ +\ \frac{S_3}{\omega_M^2}\ +\ \frac{S_5}{\omega_M^4}\ +\ \frac{S_7}{\omega_M^6}\ +\ \ldots.\} \qquad 2.13$$

where

$$S_m = \frac{1}{N} \sum_k n_k (\varepsilon(k+\kappa) - \varepsilon(k))^m \quad \text{for } m = 1, 3, 5, \ldots \qquad 2.14$$

The jth order approximation to the plasmon energy is obtained by terminating the series on the RHS of (2.13) at the jth term, and solving a jth degree polynomial in ω_M^2. The first, second, third and fourth order approximations to the plasmon energy can be written down explicitly and since the sums S_1, S_3, S_5 and S_7 can be evaluated by the same do loop, it is worth looking at all four approximations - the better the approximation to the plasmon energy at this stage, the less computing effort will be required later. For ease of writing we define:

$$\alpha = 4\Omega S_1, \quad \beta = 4\Omega S_3, \quad \gamma = 4\Omega S_5, \quad \varepsilon = 4\Omega S_7$$

The first and second order approximations are trivially determined.

$$\omega_1^2 = \alpha \quad \text{and} \quad \omega_2^2 = \frac{\alpha \pm \sqrt{(\alpha^2 - 4\beta)}}{2} \qquad 2.15$$

The '+' sign gives the appropriate second order approximation to the plasmon energy for this ensures that $\omega_2 \to \omega_1$ as $\beta \to 0$ i.e. as $\kappa \to 0$ (N.B. $\alpha \neq 0$ as $\kappa \to 0$; β, γ, $\varepsilon \to 0$ as $\kappa \to 0$). The square of the third order approximation satisfies a cubic equation and by writing $y = \omega_3^2 - \frac{1}{3}\alpha$ we put the cubic equation in standard form

$$p = -(\frac{1}{3}\alpha^2 + \beta)$$

$$y^3 + py + q = 0 \qquad q = -(\frac{2}{27}\alpha^3 + \frac{1}{3}\alpha\beta + \gamma)$$

$$D^2 = \frac{q^2}{4} + \frac{p^3}{27}$$

The discriminant, D^2, is positive for $\kappa \neq 0$ and so the solution for the third order approximation is

$$\omega_3^2 = (D - \frac{q}{2})^{1/3} - \frac{p}{3(D - \frac{q}{2})^{1/3}} + \frac{\alpha}{3} \qquad 2.16$$

The square of the fourth order approximation satisfies a quartic equation. We solve the quartic by writing it in biquadratic form

$$(\omega_4^4 - \frac{\alpha}{2}\omega_4^2 + h)^2 - (a\omega_4^2 + b)^2 = 0 \quad \begin{cases} (\alpha^2 + 8h + 4\beta)(h^2 + \varepsilon) = (\gamma - \alpha h)^2 \\ a^2 = \frac{\alpha^2}{4} + \beta + 2h \\ b^2 = \varepsilon + h^2 \end{cases}$$

The four solutions of the original quartic are thus

$$\omega_4^4 + (-\frac{\alpha}{2} - a)\omega_4^2 + h - b = 0 \qquad 2.17$$

$$\omega_4^4 + (-\frac{\alpha}{2} + a)\omega_4^2 + h + b = 0 \qquad 2.18$$

Equation (2.17) is the correct choice for the plasmon energy since ω_4 coincides with ω_2 when $\gamma = \varepsilon = 0$ (take the '+' for the discriminant when solving the biquadratic). Here then, are the first four approximations to the plasmon energy. It was very clear and straightforward as to how one would

obtain them. However, if we try to compute the sums S_m (m = 1,3,5,7) and thence the four approximations, we find that for certain values of wave vector the program fails. This is the first indication that the dielectric function approach is not without computational difficulties. The reason why the program fails is due to underflow problems i.e. the computer is attempting to evaluate a number smaller than 10^{-77}.

Suppose we compute the first four approximations to the plasmon energy along the (100) direction with u = 0.01 and a = 1.5. We take $(30)^3$ vectors in the Brillouin zone in order to evaluate the sums S_m. At $\kappa = 0.4\pi/a$ there is a program interrupt - there are underflow problems, the computer attempts a standard fix up and eventually the program fails. We trace the problem to lie with S_5 and S_7. For $(30)^3$ wave vectors in the first Brillouin zone, the smallest value of $|\varepsilon(k+\kappa) - \varepsilon(k)|$ (zero excepted) is of the order of 10^{-4} Hartree , so there should be no difficulty in computing S_5 or S_7. However, if we put a write statement in the program for this energy difference, we find values of the order of 10^{-16} present. Thus in evaluating S_5 and S_7 the computer generates numbers of the order of 10^{-80} and 10^{-112}. As we have indicated, the components of $\underline{k}$ take the following values in units of π/a

$$\frac{-14}{15}, \frac{-13}{15}, \ldots, 0, \ldots, \frac{14}{15}, 1$$

The values of the energy difference $\varepsilon(k+\kappa) - \varepsilon(k)$ which are assigned magnitudes of 10^{-16} correspond to $k_x = 12\pi/15a$ and $k_x = -3\pi/15a$, for all k_y, k_z. Recalling that $\underline{\kappa} = (0.4\pi/a,0,0)$ we can show that such numbers should be identically zero. The program will run if we assign the energy difference its precise zero:

$$\text{If} \quad |\varepsilon(k+\kappa) - \varepsilon(k)| < 10^{-10}, \quad \varepsilon(k+\kappa) - \varepsilon(k) = 0$$

We have mentioned that $(30)^3$ vectors were used in the initial evaluation of the sums S_m, in fact $(18)^3$ vectors ensure that the sums are sufficiently convergent. For this number of vectors there are no underflow problems in the (100) direction - they occur in the (111) direction. We therefore note the existence in our model of a typical computational difficulty associated with the dielectric function approach, during the first stage of the calculation.

For the second stage of the calculation, we return to the dispersion relation and continue the expansion of the trace of the polarisation kernel to higher orders. The resulting polynomial equation is solved numerically by testing for the sign (-, 0, +) of the product of the values of the polynomial function at the ends of a frequency interval determined by ω_4. The interval is appropriately reduced by a factor of one half and the process repeated until the zero of the polynomial function is delivered to the required accuracy. The smallest value of $|\varepsilon(k+\kappa) - \varepsilon(k)|$ (taking $(18)^3$ k vectors in the Brillouin zone) for the

nine choices of u/a, is of the order of 10^{-5} Hartree (zero excepted). Because of this, the trace of the polarisation kernel can only be expanded to ninth order without incurring genuine underflow/overflow problems, and even then the energy difference $\varepsilon(k+\kappa) - \varepsilon(k)$ needs to be rescaled by a factor of 10^{+4}. However, although we are able to determine the ninth order approximation to the plasmon energy, it is clear that this will be a poor approximation for values near the single particle continuum. In such circumstances we go on to a third stage of calculation - the evaluation of the complete dielectric function.

We can calculate the plasmon energy to any degree of precision by looking for the zeros of the dielectric function. Because the dielectric function is not a simple polynomial the best way to proceed is to use Newton's method, this minimises the number of iterations. We begin with a trail value of the plasmon energy (ω_9 say, the ninth order approximation) and evaluate the trace of the polarisation kernel and its derivative with respect to frequency, at ω_{Trail}. We thereby obtain a better approximation to the plasmon energy, ω_{Shift}

$$\omega_{Shift} = \omega_{Trail} + \frac{(1 - \text{Trace } \Lambda)}{\text{Derivative Trace } \Lambda}$$

The differentiation can be carried out explicitly and the derivative evaluated by the same do loop as the trace. We then set ω_{Trail} equal to ω_{Shift} and repeat the process

until the determinant of the dielectric function is smaller than 10^{-4}. (N.B. at points in the Brillouin zone where the plasmon mode lies close to the continuum, it is possible that ω_9 might be smaller than ω_{Har}^{max}. In this situation ω_{Trail} is initially assigned a value which is slightly greater than the maximum single particle excitation energy). The main features of the dielectric function method are brought together in the form of a flow chart shown over the page.

THE DIELECTRIC FUNCTION METHOD

Compute the sums S_m (m = 1,3,...,17) and ω_4 (STAGE 1)

Using ω_4 to set a frequency range, compute ω_9 (STAGE 2)

Is $|\omega_9-\omega_4| < 10^{-4}$? ——yes——> plasmon energy = ω_9

no ↓

(STAGE 3)

Is ω_9 > Maximum single particle excitation energy ?

yes ↙ ↘ no

$\omega_{Trail} = \omega_9$ $\qquad$ $\omega_{Trail} = 1.01\ \omega_{Har}^{max}$

Compute the trace (and the derivative of the trace) of Λ at ω_{Trail}, to obtain a better approximation : ω_{Shift}

Is $\omega_{Shift} > \omega_{Har}^{max}$? ——no——> single particle modes only

yes ↓

Is |Dielectric Function(ω_{Shift})| $< 10^{-4}$ ——no——> $\omega_{Trail} = \omega_{Shift}$

yes ↓

plasmon energy = ω_{Shift}

At first sight, the calculation of ω_9 seems unnecessary; however, there are good reasons for supposing that this stage of the calculation might improve the overall efficiency and effectiveness of the dielectric function method. The calculation of ω_9 alters the efficiency of the method in three ways. Firstly, on the debit side, we need to determine the sums $S_9, S_{11}, \ldots, S_{17}$ (five in all) in addition to the four required for stage one of the calculation, but since the sums S_m ($m = 1,3,\ldots,17$) can all be determined by the same do loop, this should not bring about a significant increase in computer time. Secondly, it is possible that for small and intermediate values of κ, stages one and two of the calculation would be sufficient to guarantee an accuracy of 10^{-4} Hartree on the plasmon energy, so that the computation of the dielectric function is not required. This clearly represents a saving in computer time, as does our third point. By definition, ω_9 is a better approximation to the plasmon energy than ω_4, and so fewer iterations are required in the third stage of the calculation if ω_9 is used as trail value in preference to ω_4.

The way in which the calculation of ω_9 alters the effectiveness of the dielectric function method is linked to the pole structure of the trace of the polarisation kernel, for in order to pick up plasmon energies close to the single particle continuum we need a very good initial guess, and the best approximation is ω_9.

One final general point about the efficiency of dielectric function method concerns the convergence of Brillouin zone summations. It was eventually found that $(18)^3$ points in the Brillouin zone, coupled with an accuracy of 10^{-4} on the dielectric function, guaranteed that plasmon energies were correct to 10^{-4} Hartree (we looked along the three directions discussed earlier i.e. (100), (110) and (111) directions, for our nine choices of u/a). If one requires an appreciable number of plasmon energies (>100 say) for use in further calculations, then there is one more step we can take to reduce the computer time. Having decided that a sufficient number of wave vectors in the Brillouin zone is $(18)^3$, then for each of these wave vectors we test to see if the corresponding one electron state is occupied. In this way, we generate a set of wave vectors going with occupied states, so that Brillouin zone summations which incorporate a factor n_k (and they all do) are carried out only over this predetermined set i.e. only over occupied states.

We now present the results of the dielectric function method in the form of a series of graphs and tables together with appropriate comments.

Graphical Representation of the Excitation Spectra of the Tightly Bound Metal

The next three pages show excitation spectra in the (100), (110), and (111) directions. For each direction we look at the plasmon mode and the electron hole continuum associated with the nine tightly bound metals defined by our nine choices of u / a. Rather than give nine separate graphs per direction, we superimpose the three spectra corresponding to a given value of u and three choices of a onto one figure.

The first page shows three figures labelled by u = -0.01, u = -0.03, and u = -0.05. On each figure there are three plasmon modes and three electron hole continua associated with a = 1.5, a = 2.5, and a = 6.5. However, since the electron hole continua depend only on u, they are coincident. The plasmon modes are distinguished by solid and dashed lines as described below.

upper solid line — represents a plasmon mode with a = 1.5

---------- — represents a plasmon mode with a = 2.5

— — — — — — — represents a plasmon mode with a = 6.5

lower solid line — represents the continuum edge.

The ordinate axis (energy) is marked off in steps of 0.1 Hartree and the abscissa (K) is marked in steps of 0.2 π/a.

κ = (K,0,0) for the (100) direction

κ = (K,K,0) for the (110) direction

and κ = (K,K,K) for the (111) direction.

(1 0 0)

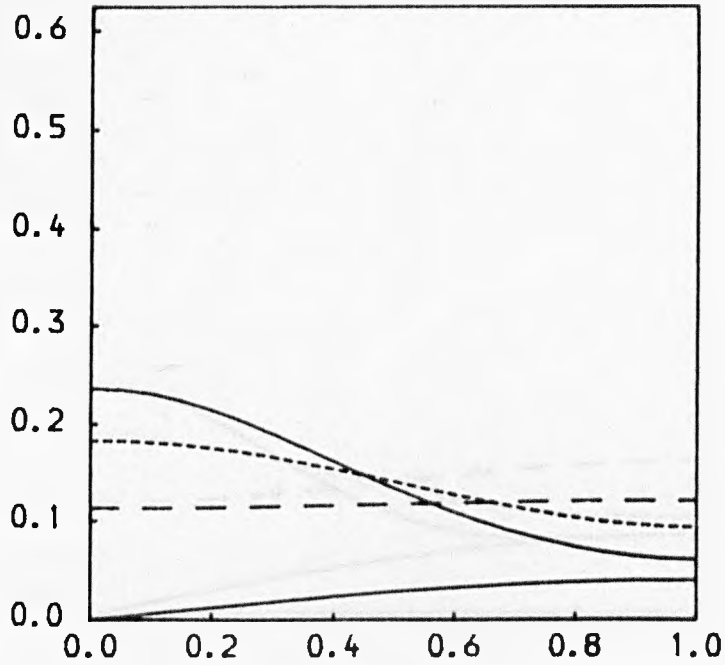

u = - 0,01

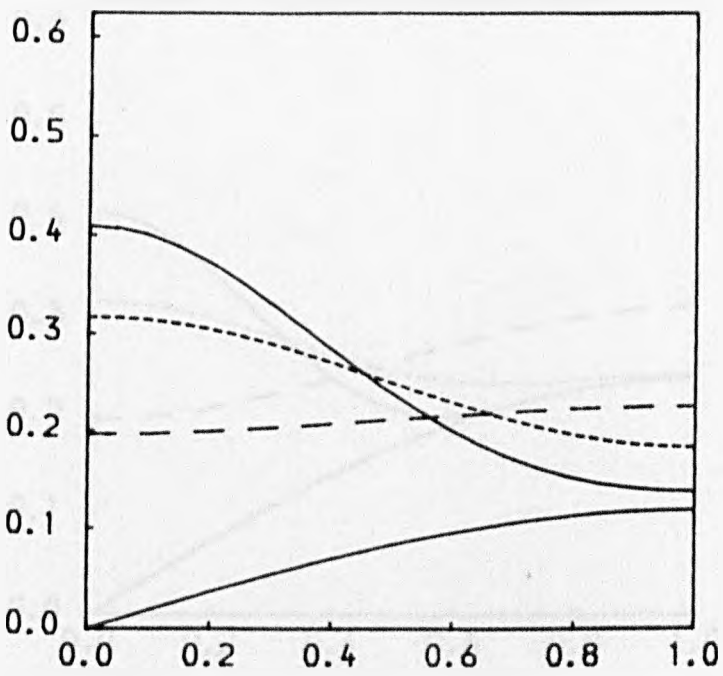

u = - 0,03

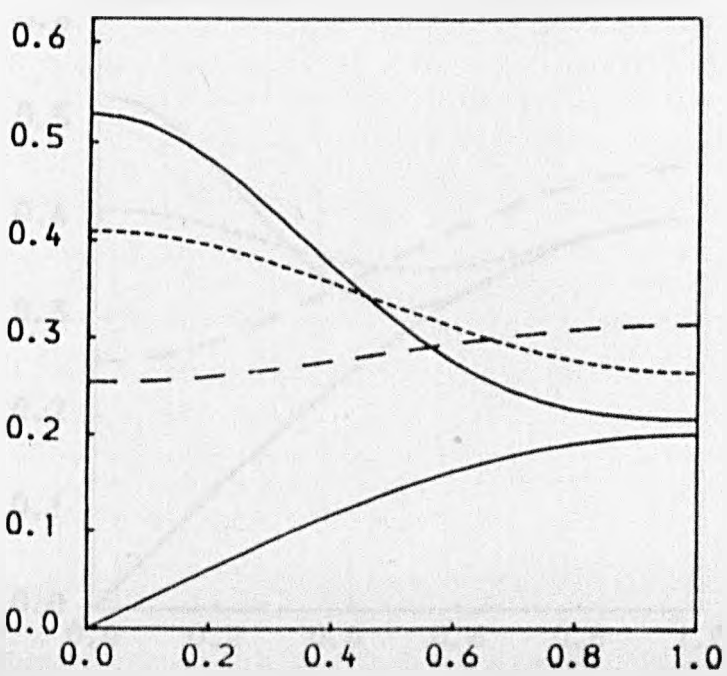

u = - 0,05

(110)

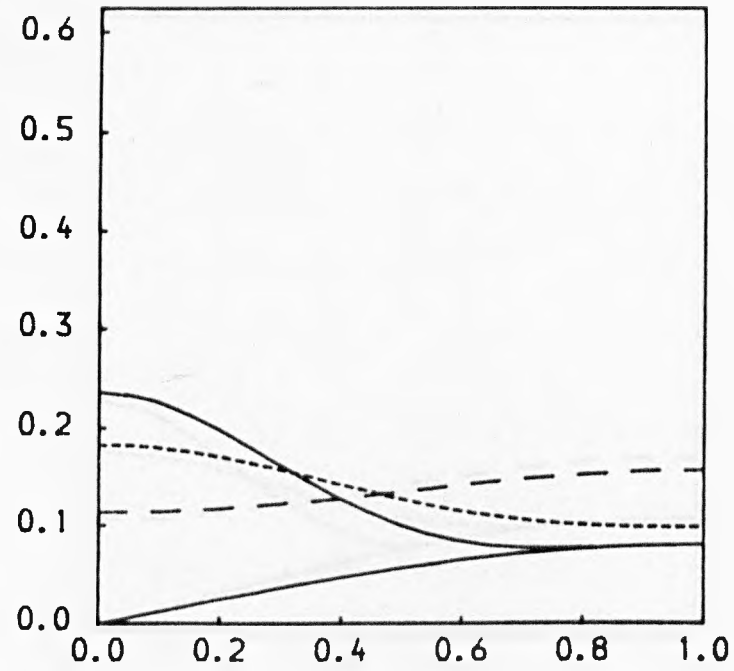

u = - 0.01

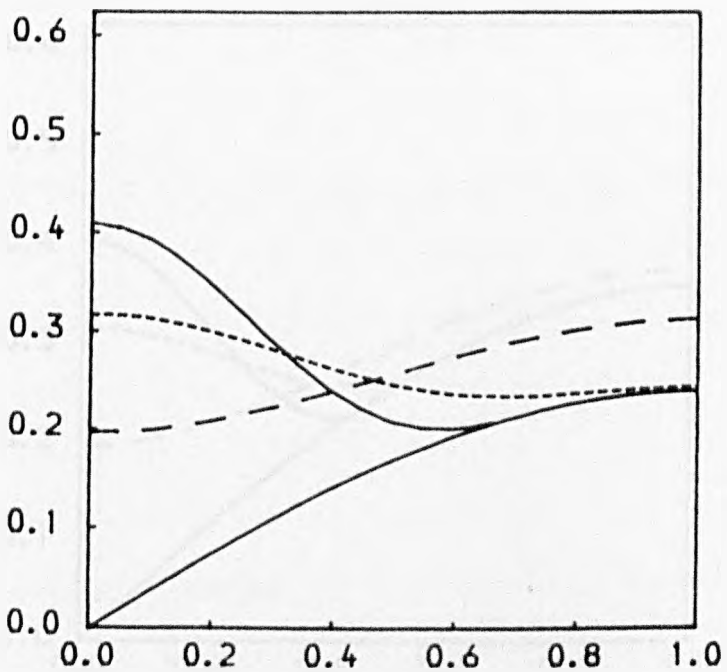

u = - 0,03

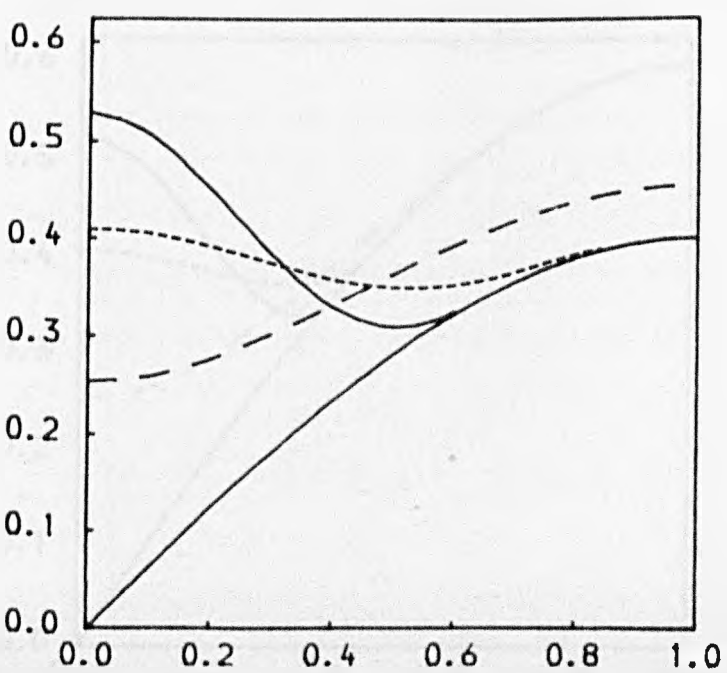

u = - 0,05

(1 1 1)

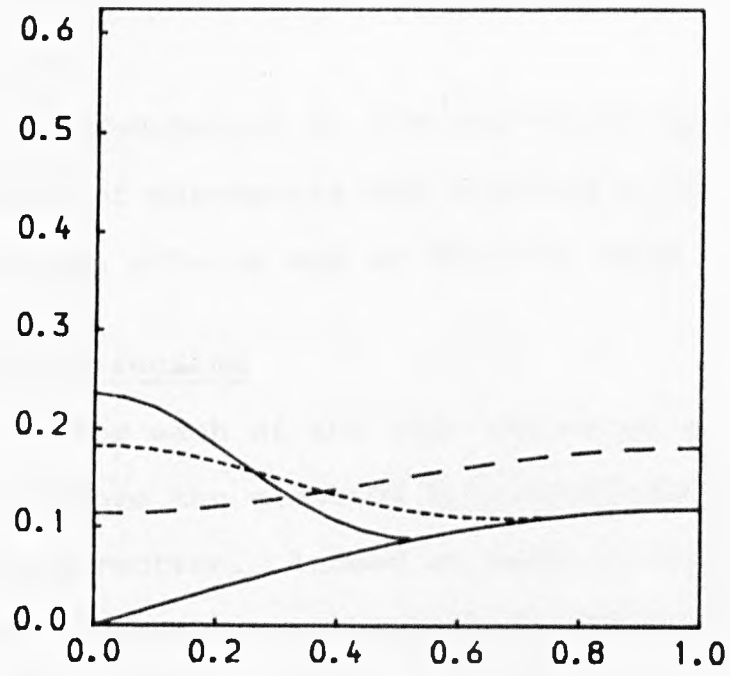

u = -0,01

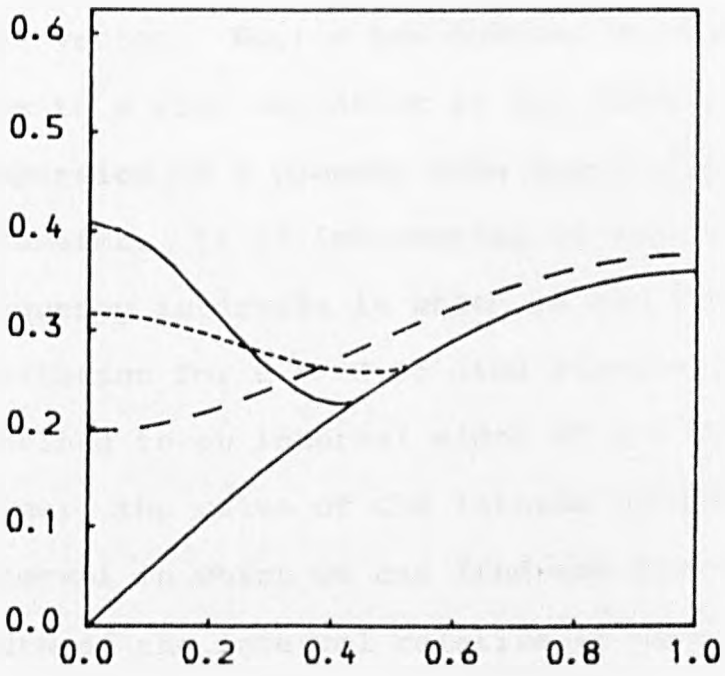

u = -0,03

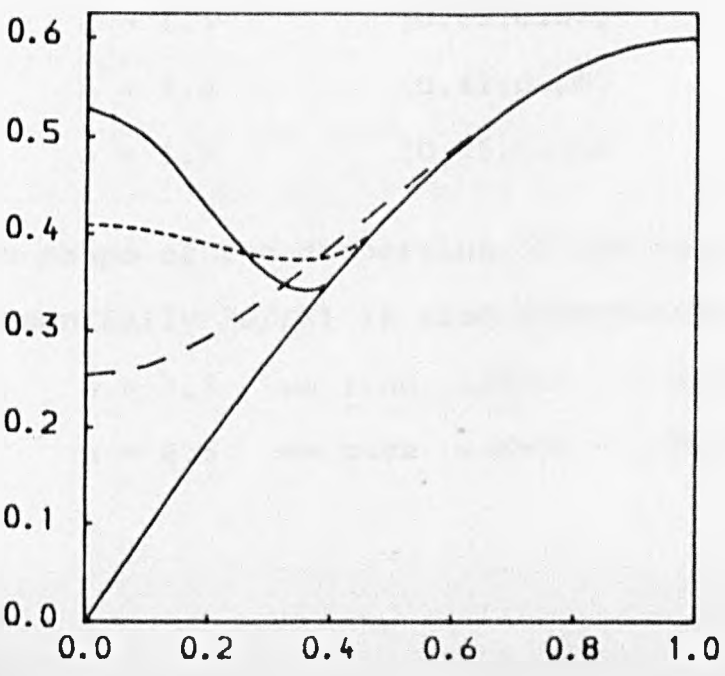

u = -0,05

Examination of the excitation spectra shows that our choice of parameters has produced a full range of many electron effects and we describe some of them below.

(100) Direction

For each of the nine values of u / a the plasmon mode lies above the electron hole continuum at every point along this direction. Indeed at small K the many electron excitation is to be found high up in the energy scale so that it is difficult to excite a plasmon mode for these values of wave vector. Notice how changes in electron density gives rise to a wide variation in the shape and extent of the dispersion of a plasmon mode for a given value of hopping parameter. It is interesting to look at the width of the frequency intervals in which we can find the many electron excitation for u = -0.05 (the electron hole continuum is confined to an interval width of 0.2 Hartree). We show below: the value of the lattice parameter, the frequency interval in which we can find the plasmon mode, and the width of the interval relative to that of the continuum.

a = 1.5	[0.53,0.21]	1.60
a = 2.5	[0.41,0.26]	0.75
a = 6.5	[0.25,0.31]	0.30

The shape of the dispersion of the many electron excitation (essentially $\partial\omega/\partial K$) is also interesting

at a = 1.5 we find $\omega(K=0) > \omega(K=\pi/a)$ and at

a = 6.5 we have $\omega(K=0) < \omega(K=\pi/a)$.

(110) Direction

We observe that for the six metals of high electron density (a = 1.5 and a = 2.5), the plasmon mode either merges with the continuum (decaying into electron hole pairs) or is just above the continuum, for K > 0.5 π/a. The absolute and relative extent of plasmon dispersion is reduced for these metals (in going from the (100) direction to the (110) direction) as a consequence of the increase in the magnitude of the maximum single particle excitation energy. Figures for u = -0.05 corresponding to those given above are as follows:

a = 1.5	[0.53,0.31]	0.55
a = 2.5	[0.41,0.35]	0.15
a = 6.5	[0.25,0.45]	0.50

We note that the extent of plasmon dispersion for the low density metals (a = 6.5) has increased, signalling a significant change in $\partial\omega/\partial K$. In contrast to this, the shape of the plasmon dispersion for the high density metals is largely unaffected by the change in direction.

(111) Direction

Spectra for this direction further highlight the sensitivity of the magnitude of the maximum single particle excitation energy to changes in direction - making it difficult to predict the extent to which the plasmon mode contributes to electronic properties such as the interaction energy

and exchange correlation energy. It is also apparent that when a plasmon excitation merges with the continuum, it does so smoothly. This is compatible with the electron electron interaction lifting the single particle excitation with maximum frequency from the Hartree spectrum. Only two of our choices of u / a (-0.01 / 6.5 and -0.03 / 6.5) yield plasmon modes which are above the electron hole continuum over the entire Brillouin zone.

TABLE 5

This table displays the results of the first, second and third stages of calculation of the dielectric function method, for a selection of values of u / a and wave vector (K is incremented in units of 0.1 π/a starting at 0.1 π/a and finishing at π/a).

'NIT' refers to the number of iterations required by the third stage of the calculation

'PE' is the plasmon energy correct to 10^{-4} Hartree

'EDMAX' is the maximum value of the energy difference $\varepsilon(k+\kappa)-\varepsilon(k)$

The meaning of the other symbols in the table should be apparent.

Features to Notice

(100) Direction: We see that for metals of small hopping parameter, u = -0.01, the third stage of the calculation is not required along this direction (look at NIT). In fact the first stage alone (the determination of W4) gives very good values of the plasmon energy for the majority of the points. This is a direct result of a low continuum edge.

(110) Direction: This direction demonstrates the need for the calculation of the full dielectric function for plasmon energies near the continuum. Look at the values of W4, W9, and PE for u = -0.03, a = 1.5, and K = 1.26.

W4	W9	NIT	PE
0.1809	0.1954	6	0.2010

Although W9 is relatively close to PE, it still takes six iterations to obtain the desired accuracy (the accuracy of PE is generally slightly better than 10^{-4} Hartree). This indicates that WTRAIL needs to be as good as we can make it - in order to keep the number of iterations down.

(111) Direction: Examination of the data for this direction shows just how poor the ninth order approximation can be. For u = -0.05, a = 6.5 and K = 0.29 the value of W9 is in error by about 11%.

KAPPA = (K,0.0)	K	W1	W2	W3	W4	W9	WTRAIL	NIT	PE	EDMAX
U = -0.01 A = 1.5										
	0.21	0.2306	0.2306	0.2306	0.2306	0.2306	0.0	0	0.2306	0.0063
	0.42	0.2136	0.2139	0.2139	0.2139	0.2139	0.0	0	0.2139	0.0124
	0.63	0.1889	0.1896	0.1896	0.1896	0.1896	0.0	0	0.1896	0.0182
	0.84	0.1603	0.1616	0.1616	0.1616	0.1616	0.0	0	0.1616	0.0235
	1.05	0.1314	0.1336	0.1337	0.1337	0.1337	0.0	0	0.1337	0.0283
	1.26	0.1049	0.1083	0.1086	0.1086	0.1086	0.0	0	0.1086	0.0324
	1.47	0.0822	0.0872	0.0878	0.0879	0.0879	0.0	0	0.0879	0.0356
	1.68	0.0646	0.0711	0.0722	0.0725	0.0726	0.0	0	0.0726	0.0380
	1.88	0.0529	0.0606	0.0624	0.0629	0.0632	0.0632	1	0.0632	0.0395
	2.09	0.0487	0.0568	0.0589	0.0596	0.0600	0.0600	2	0.0600	0.0400
U = -0.01 A = 2.5										
	0.13	0.1811	0.1812	0.1812	0.1812	0.1812	0.0	0	0.1812	0.0063
	0.25	0.1749	0.1752	0.1752	0.1752	0.1752	0.0	0	0.1752	0.0124
	0.38	0.1651	0.1658	0.1658	0.1658	0.1658	0.0	0	0.1658	0.0182
	0.50	0.1525	0.1539	0.1539	0.1539	0.1539	0.0	0	0.1539	0.0235
	0.63	0.1382	0.1404	0.1404	0.1405	0.1405	0.0	0	0.1405	0.0283
	0.75	0.1234	0.1265	0.1266	0.1266	0.1266	0.0	0	0.1266	0.0324
	0.88	0.1094	0.1134	0.1137	0.1137	0.1137	0.0	0	0.1137	0.0356
	1.01	0.0976	0.1025	0.1030	0.1030	0.1030	0.0	0	0.1030	0.0380
	1.13	0.0896	0.0951	0.0958	0.0959	0.0959	0.0	0	0.0959	0.0395
	1.26	0.0867	0.0925	0.0932	0.0933	0.0933	0.0	0	0.0933	0.0400
U = -0.01 A = 6.5										
	0.05	0.1137	0.1139	0.1139	0.1139	0.1139	0.0	0	0.1139	0.0063
	0.10	0.1140	0.1145	0.1145	0.1145	0.1145	0.0	0	0.1145	0.0124
	0.14	0.1143	0.1154	0.1154	0.1154	0.1154	0.0	0	0.1154	0.0182
	0.19	0.1147	0.1165	0.1166	0.1166	0.1166	0.0	0	0.1166	0.0235
	0.24	0.1151	0.1176	0.1178	0.1178	0.1178	0.0	0	0.1178	0.0283
	0.29	0.1155	0.1187	0.1189	0.1189	0.1189	0.0	0	0.1189	0.0324
	0.34	0.1158	0.1196	0.1199	0.1199	0.1199	0.0	0	0.1199	0.0356
	0.39	0.1161	0.1203	0.1206	0.1206	0.1206	0.0	0	0.1206	0.0380
	0.43	0.1162	0.1207	0.1211	0.1211	0.1211	0.0	0	0.1211	0.0395
	0.48	0.1163	0.1208	0.1212	0.1212	0.1212	0.0	0	0.1212	0.0400

KAPPA = (K,K,0)	K	W1	W2	W3	W4	W9	WTRAIL	NIT	PE	EDMAX
U = -0.03 A = 1.5										
	0.21	0.3903	0.3919	0.3919	0.3919	0.3919	0.0	0	0.3919	0.0375
	0.42	0.3408	0.3455	0.3456	0.3456	0.3456	0.0	0	0.3456	0.0742
	0.63	0.2755	0.2871	0.2882	0.2883	0.2883	0.0	0	0.2883	0.1090
	0.84	0.2105	0.2320	0.2363	0.2373	0.2377	0.2377	1	0.2377	0.1411
	1.05	0.1550	0.1876	0.1930	0.2023	0.2065	0.2065	2	0.2068	0.1697
	1.26	0.1124	0.1541	0.1717	0.1809	0.1954	0.1954	6	0.2010	0.1942
	1.47	SINGLE - PARTICLE MODES ONLY								0.2138
	1.68	SINGLE - PARTICLE MODES ONLY								0.2283
	1.88	SINGLE - PARTICLE MODES ONLY								0.2370
	2.09	SINGLE - PARTICLE MODES ONLY								0.2400
U = -0.03 A = 2.5										
	0.13	0.3114	0.3127	0.3127	0.3127	0.3127	0.0	0	0.3127	0.0375
	0.25	0.2940	0.2994	0.2997	0.2997	0.2997	0.0	0	0.2997	0.0742
	0.38	0.2682	0.2800	0.2811	0.2813	0.2813	0.0	0	0.2813	0.1090
	0.50	0.2377	0.2576	0.2609	0.2616	0.2618	0.2618	1	0.2618	0.1411
	0.63	0.2065	0.2351	0.2421	0.2444	0.2457	0.2457	2	0.2457	0.1697
	0.75	0.1784	0.2149	0.2265	0.2313	0.2360	0.2360	2	0.2363	0.1942
	0.88	0.1562	0.1990	0.2149	0.2225	0.2324	0.2324	3	0.2344	0.2138
	1.01	0.1411	0.1882	0.2074	0.2172	0.2323	0.2323	5	0.2378	0.2283
	1.13	0.1328	0.1823	0.2035	0.2147	0.2333	0.2394	4	0.2421	0.2370
	1.26	0.1302	0.1805	0.2023	0.2140	0.2338	0.2424	4	0.2443	0.2400
U = -0.03 A = 6.5										
	0.05	0.1980	0.2001	0.2001	0.2001	0.2001	0.0	0	0.2001	0.0375
	0.10	0.2012	0.2087	0.2093	0.2094	0.2094	0.0	0	0.2094	0.0742
	0.14	0.2064	0.2208	0.2229	0.2233	0.2233	0.0	0	0.2233	0.1090
	0.19	0.2134	0.2347	0.2386	0.2398	0.2402	0.2402	1	0.2402	0.1411
	0.24	0.2216	0.2491	0.2554	0.2572	0.2582	0.2582	1	0.2582	0.1697
	0.29	0.2305	0.2629	0.2711	0.2738	0.2755	0.2755	2	0.2755	0.1942
	0.34	0.2389	0.2752	0.2848	0.2882	0.2905	0.2905	2	0.2906	0.2138
	0.39	0.2460	0.2848	0.2955	0.2993	0.3021	0.3021	2	0.3022	0.2283
	0.43	0.2507	0.2910	0.3022	0.3063	0.3095	0.3095	2	0.3096	0.2370
	0.48	0.2524	0.2932	0.3045	0.3087	0.3120	0.3120	2	0.3121	0.2400

KAPPA = (K,K,K)	K	W1	W2	W3	W4	W9	WTRAIL	NIT	PE	EDMAX
U = -0.05 A = 1.5										
	0.21	0.4939	0.4979	0.4979	0.4980	0.4980	0.0	0	0.4980	0.0939
	0.42	0.4065	0.4234	0.4251	0.4254	0.4254	0.0	0	0.4254	0.1854
	0.63	0.3038	0.3422	0.3522	0.3556	0.3581	0.3581	2	0.3581	0.2724
	0.84	SINGLE - PARTICLE MODES ONLY								0.3527
	1.05	SINGLE - PARTICLE MODES ONLY								0.4243
	1.26	SINGLE - PARTICLE MODES ONLY								0.4854
	1.47	SINGLE - PARTICLE MODES ONLY								0.5346
	1.68	SINGLE - PARTICLE MODES ONLY								0.5706
	1.88	SINGLE - PARTICLE MODES ONLY								0.5926
	2.09	SINGLE - PARTICLE MODES ONLY								0.6000
U = -0.05 A = 2.5										
	0.13	0.3989	0.4038	0.4039	0.4039	0.4039	0.0	0	0.4039	0.0939
	0.25	0.3687	0.3869	0.3892	0.3895	0.3896	0.0	0	0.3896	0.1854
	0.38	0.3260	0.3628	0.3717	0.3745	0.3763	0.3763	2	0.3763	0.2724
	0.50	0.2791	0.3356	0.3552	0.3643	0.3760	0.3760	3	0.3784	0.3527
	0.63	SINGLE - PARTICLE MODES ONLY								0.4243
	0.75	SINGLE - PARTICLE MODES ONLY								0.4854
	0.88	SINGLE - PARTICLE MODES ONLY								0.5346
	1.01	SINGLE - PARTICLE MODES ONLY								0.5706
	1.13	SINGLE - PARTICLE MODES ONLY								0.5926
	1.26	SINGLE - PARTICLE MODES ONLY								0.6000
U = -0.05 A = 6.5										
	0.05	0.2568	0.2640	0.2645	0.2646	0.2646	0.0	0	0.2646	0.0939
	0.10	0.2646	0.2878	0.2924	0.2936	0.2941	0.2941	1	0.2941	0.1854
	0.14	0.2773	0.3176	0.3291	0.3335	0.3372	0.3372	2	0.3374	0.2724
	0.19	0.2942	0.3494	0.3678	0.3761	0.3859	0.3859	3	0.3875	0.3527
	0.24	0.3136	0.3804	0.4047	0.4165	0.4335	0.4335	4	0.4392	0.4243
	0.29	0.3334	0.4087	0.4375	0.4522	0.4335	0.4903	3	0.4894	0.4854
	0.34	SINGLE - PARTICLE MODES ONLY								0.5346
	0.39	SINGLE - PARTICLE MODES ONLY								0.5706
	0.43	SINGLE - PARTICLE MODES ONLY								0.5926
	0.48	SINGLE - PARTICLE MODES ONLY								0.6000

Computer Times for the Dielectric Function Method

The computer unit processing times associated with the dielectric function method are listed on the following page. The CPU time, shown in secs, relates to the time required to execute the program outlined by the flow chart given earlier in this section, for ten values of the wave vector κ. We put κ = (K,0,0), (K,K,0) or (K,K,K) and allowed K to scan through the set $\{ m\pi/10a : m = 1,2,...,10 \}$.

The results are rather surprising, in that stage 2 of the calculation is found to have only a minor effect on the overall efficiency of the method. To understand why this is so, let us return to the values of W4, W9, NIT and PE shown on page 74

W4	W9	WTRAIL	NIT	PE	EDMAX
0.1809	0.1954	0.1954	6	0.2010	0.1942

We see that because the fourth order approximation is such a poor guess (i.e. W4 < EDMAX) WTRAIL is set equal to (1.0+0.01)EDMAX, which is a better approximation to PE than W9 - so that there are fewer iterations with stage 2 of the calculation omitted. The above discussion relates to the plasmon mode near the electron hole continuum. Away from the continuum, stage 2 reduces NIT. The net effect of stage 2 is to reduce the computer time by a smaller amount than we might have expected. A bigger saving in computer time is brought about by summing over occupied states only (referred to as Method A), this reduces the CPU time by 50%.

u / a	κ = (K,O,O) A	B	C	κ = (K,K,O) A	B	C	κ = (K,K,K) A	B	C
-0.01 / 1.5	55	27	31	89	41	42	77	37	38
-0.01 / 2.5	45	22	21	77	36	44	84	40	41
-0.01 / 6.5	45	22	18	45	22	34	63	31	41
-0.03 / 1.5	80	38	48	90	42	44	80	38	38
-0.03 / 2.5	66	31	37	120	57	62	87	41	41
-0.03 / 6.5	59	28	37	87	41	51	115	54	68
-0.05 / 1.5	99	46	57	93	44	47	76	37	38
-0.05 / 2.5	75	35	44	105	50	53	84	40	43
-0.05 / 6.5	75	34	46	110	52	64	104	49	51

Method A Sum over both occupied and unoccupied states

Method B Sum over occupied states only

Method C Sum over occupied states only, with stage 2 of the calculation omitted

We close this section on the dielectric function method with a graphical study of the frequency dependence of the trace of the polarisation kernel. Let us choose a model for which the plasmon mode lies well above the electron hole continuum at small κ, but is close to the continuum at large κ. An appropriate choice is

u / a = -0.05 / 1.5 and $\underline{\kappa}$ = (K,0,0)

K	PE	EDMAX
0.1 π/a	0.5163	0.0313
0.7 π/a	0.2430	0.1782
1.0 π/a	0.2149	0.2000

We begin by considering the frequency dependence of the trace of the polarisation kernal at K = 0.7 π/a. The kernel has asymptotes at frequencies equal to the energy difference $\varepsilon(k+\kappa)-\varepsilon(k)$. Clearly, the number of asymptotes is related to the number of k vectors in the Brillouin zone, M^3 say. On the next page we plot this energy difference along the 100 direction in k space for three different values of M:

M = 18 (upper histogram), 30, and 40 (lower histogram)

The histograms peak at 0.1769 Hartree (M = 18), 0.1780 Hartree (M = 30), and 0.1782 Hartree. The low points of the histograms are at the negative of these values.

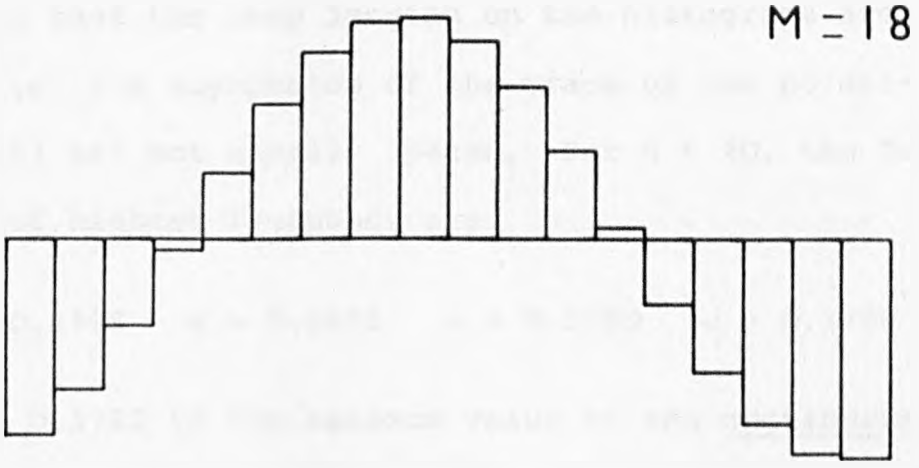
M = 18

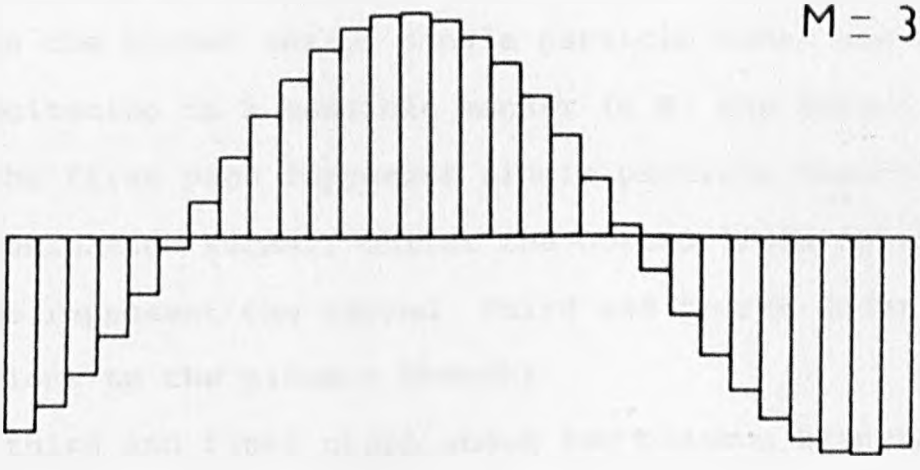
M = 30

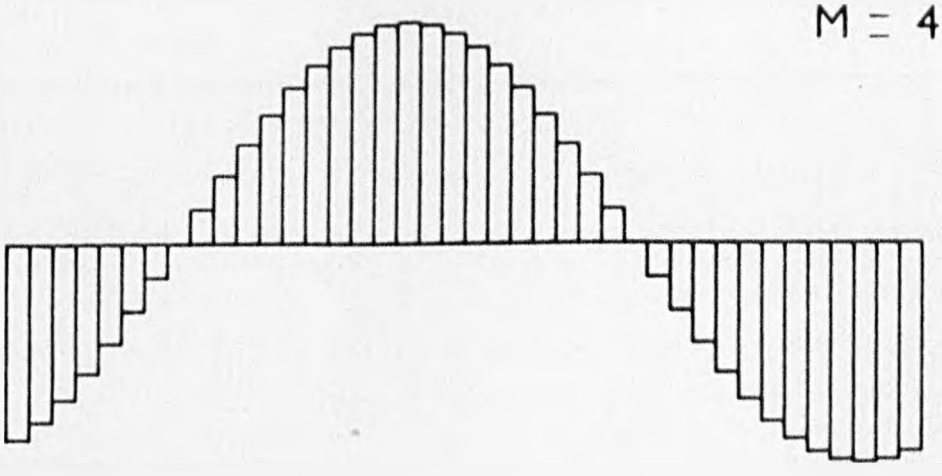
M = 40

We see that the step lengths on the histograms are not equal i.e. the asymptotes of the trace of the polarisation kernel are not equally spaced. For M = 40, the four asymptotes of highest frequency are

$$\omega = 0.1588 \quad \omega = 0.1695 \quad \omega = 0.1760 \quad \omega = 0.1782$$

Since 0.1782 is the maximum value of the continuous function $\varepsilon(k+\kappa)-\varepsilon(k)$, we take $(40)^3$ k vectors in the Brillouin zone in plotting the trace of the polarisation kernel at $\kappa_x = 0.7\pi/a$. The plot is given over two pages so as to accommodate the higher energy single particle modes and the plasmon excitation in a sensible manner (N.B. the dotted lines on the first page represent single particle branches of the polarisation kernel, whilst the dotted lines on the second page represent the second, third and fourth order approximations to the plasmon branch).

The third and final graph shows two plasmon branches of the trace of the polarisation kernel; one at $\kappa_x = 0.1\pi/a$. (dotted line) and one at $\kappa_x = \pi/a$.

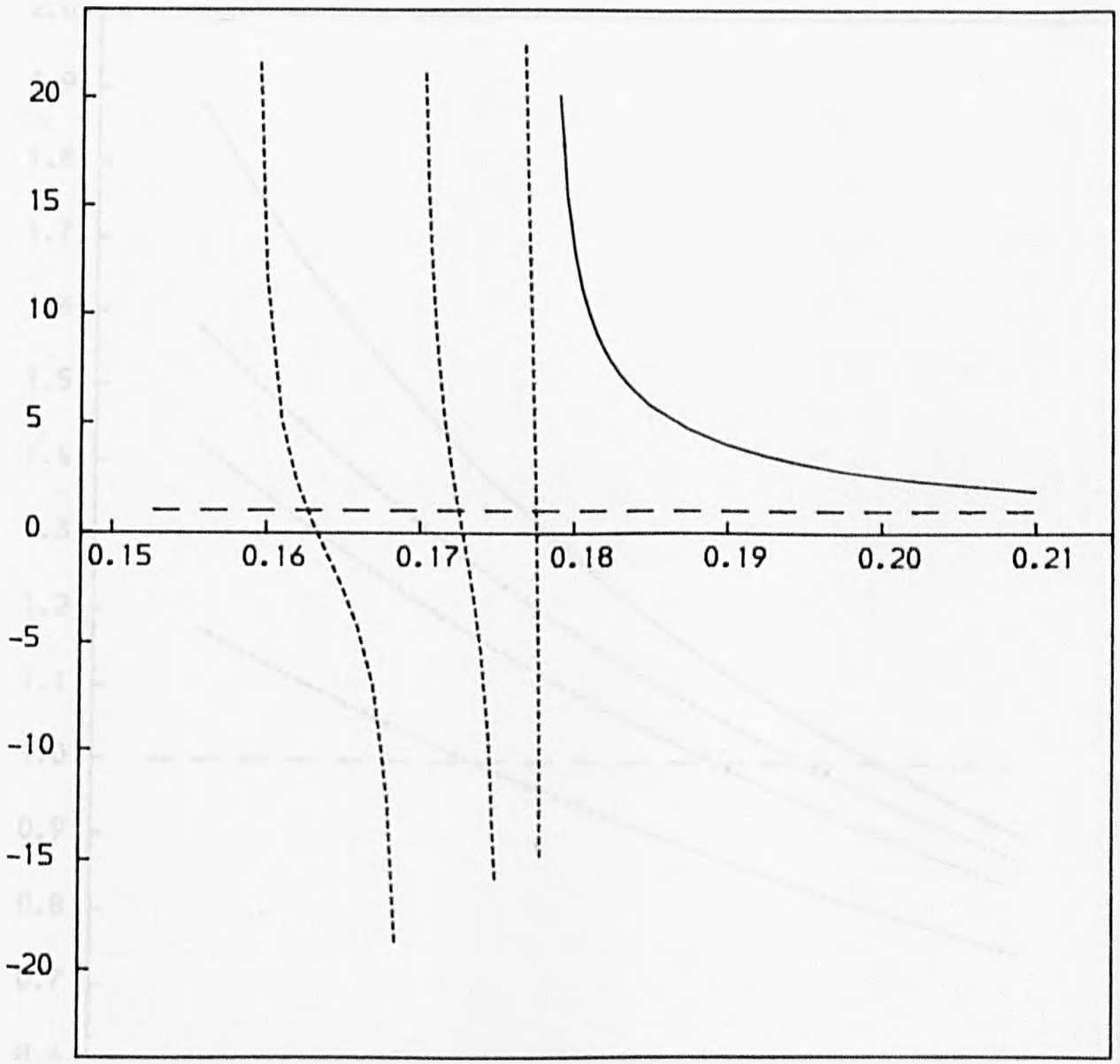
20
15
10
5
0
-5
-10
-15
-20
0.15
0.16
0.17
0.18
0.19
0.20
0.21

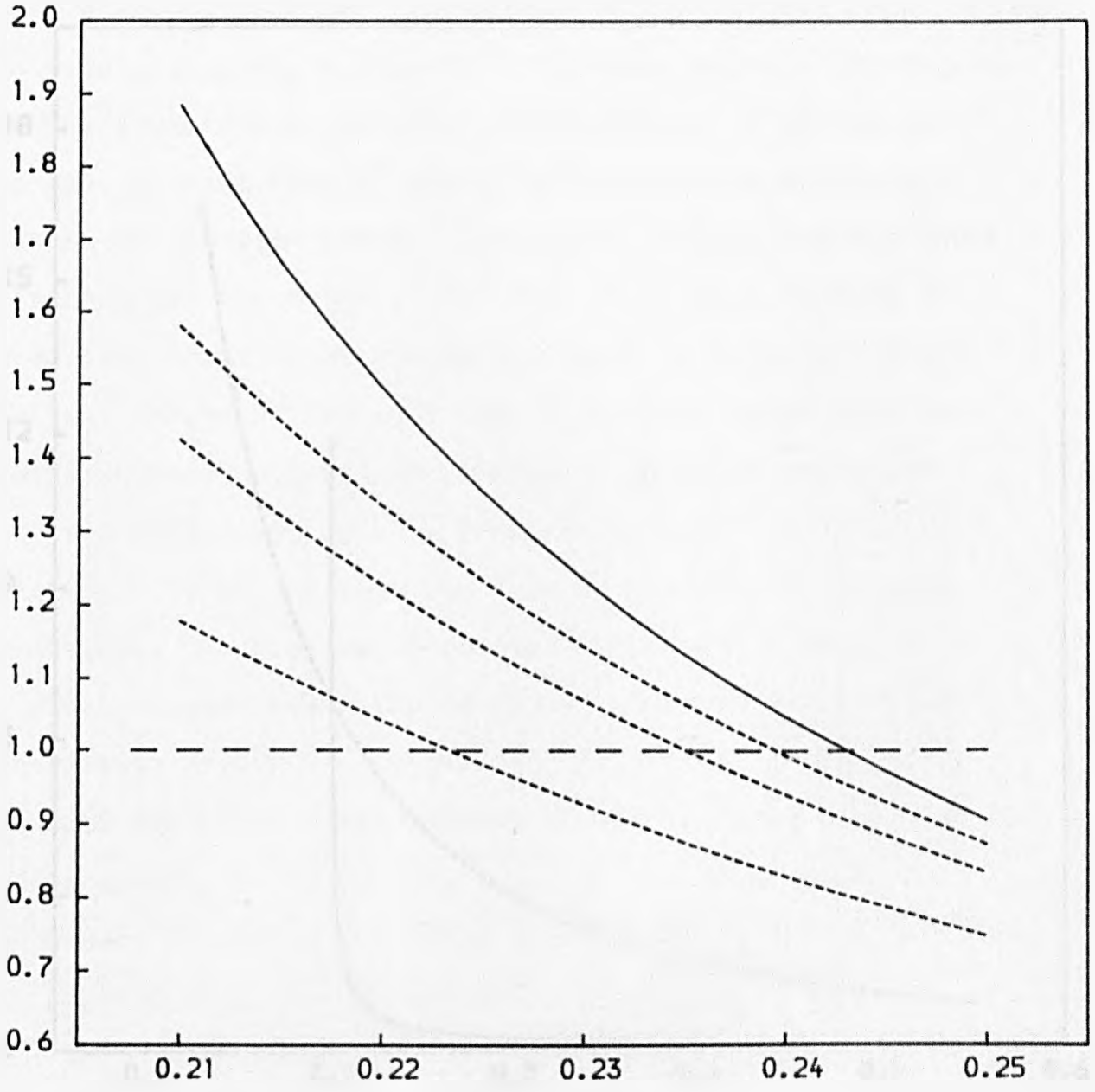
2.0
1.9
1.8
1.7
1.6
1.5
1.4
1.3
1.2
1.1
1.0
0.9
0.8
0.7
0.6
0.21
0.22
0.23
0.24
0.25

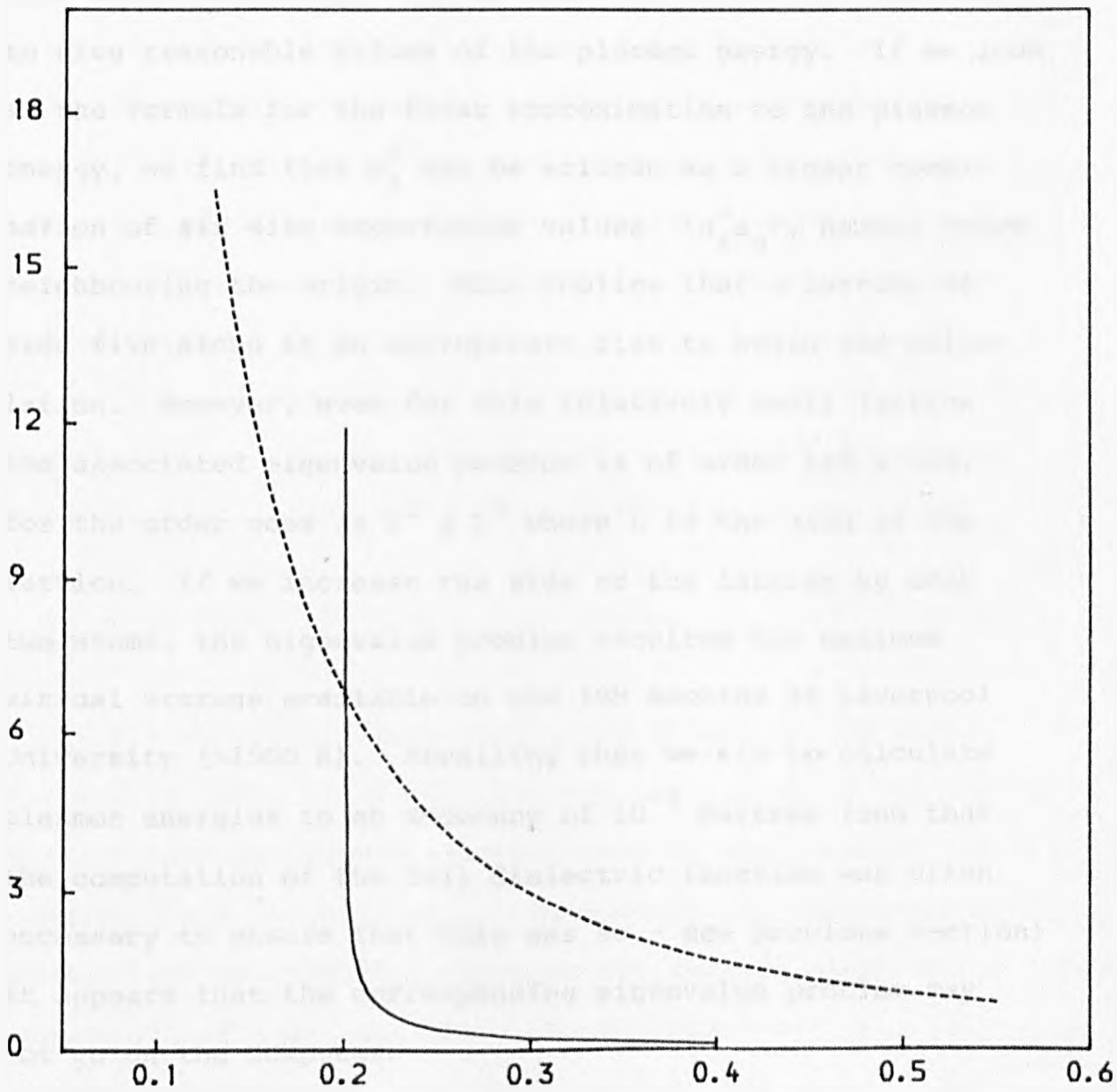
18
15
12
9
6
3
0
0.1
0.2
0.3
0.4
0.5
0.6

The Site Space Calculation

One of the first considerations in setting up the site space calculation is the size of the lattice required to give reasonable values of the plasmon energy. If we look at the formula for the first approximation to the plasmon energy, we find that ω_1^2 can be written as a linear combination of six site expectation values $\langle a_\ell^+ a_o \rangle$, namely those neighbouring the origin. This implies that a lattice of side five atoms is an appropriate size to begin the calculation. However, even for this relatively small lattice the associated eigenvalue problem is of order 125 x 125, for the order goes as $L^3 \times L^3$ where L is the side of the lattice. If we increase the side of the lattice by only two atoms, the eigenvalue problem requires the maximum virtual storage available on the IBM machine at Liverpool University ($\sim$1500 K). Recalling that we aim to calculate plasmon energies to an accuracy of 10^{-4} Hartree (and that the computation of the full dielectric function was often necessary to ensure that this was so - see previous section) it appears that the corresponding eigenvalue problem may not go on the computer.

Problems of storage and computer time meant that for many years solving an eigenvalue problem on a lattice was not an attractive proposition. Generally speaking, quantum mechanics gives rise to eigenvalue problems associated with matrices of high symmetry e.g. Hermitian matrices or block

diagonal matrices, and this can be used to ameliorate storage problems and reduce computer time. Unfortunately, the matrix associated with the site space formulation of the many electron problem is neither Hermitian nor block diagonal and any symmetry properties of the matrix are model dependent. In spite of this, there are physical systems well suited to the site space method, and these are tight binding systems. The important feature of tight binding systems is that they generate eigenvalue problems based on sparse matrices.

It is to sparse matrices that we now turn our attention. The plasmon energy (at wave vector κ) of the tightly bound metal is the eigenvalue of maximum modulus of the matrix $\underline{a}$

$$a_{\ell,\ell'} = u\left[1 - e^{-i\kappa.(\ell-\ell')}\right]\delta_{\ell',\ell} + 2\Omega(\kappa)\langle a^{+}_{\ell,\uparrow}a_{0,\uparrow}\rangle\left[e^{-i\kappa.\ell} - 1\right]\delta_{\ell',0}$$

The number of atoms (NC) along a side of the cubic lattice is taken to be odd, so that the origin of the system ℓ_x,ℓ_y,ℓ_z can be located at the centre of the lattice. For computational purposes it is inconvenient to work with the direct lattice vectors $\underline{\ell}$, because for certain atoms the components of $\underline{\ell}$ are negative. We therefore set up a right handed orthogonal set of axes I, J, K at the edge of the cube for which ℓ_x, ℓ_y and ℓ_z are all negative, and take this to be the point (1,1,1). The position vectors of the lattice with respect to this co-ordinate system are the members of the set R

$$R = \{ (I,J,K) : I, J \text{ and } K = 1,2,...NC \}$$

The centre atom has position vector (NO,NO,NO) where NO = (NC+1)/2. The vectors r = (I,J,K) can be used to label the rows and columns of $\underline{a}$. However, it is better to have a scalar index for this purpose, and so we introduce the bijective mapping M

$$M : (I,J,K) \longrightarrow I + (J-1)NC + (K-1)(NC)^2$$

By acting on the vectors r with the mapping M we generate the natural numbers 1,2,...,N where N is the number of lattice points, $N = (NC)^3$. This is illustrated over the page for a lattice of side five. The first grid shows each lattice point labelled with its position vector (I,J,K) whilst the second grid shows the lattice points labelled by the scalar index M(I,J,K).

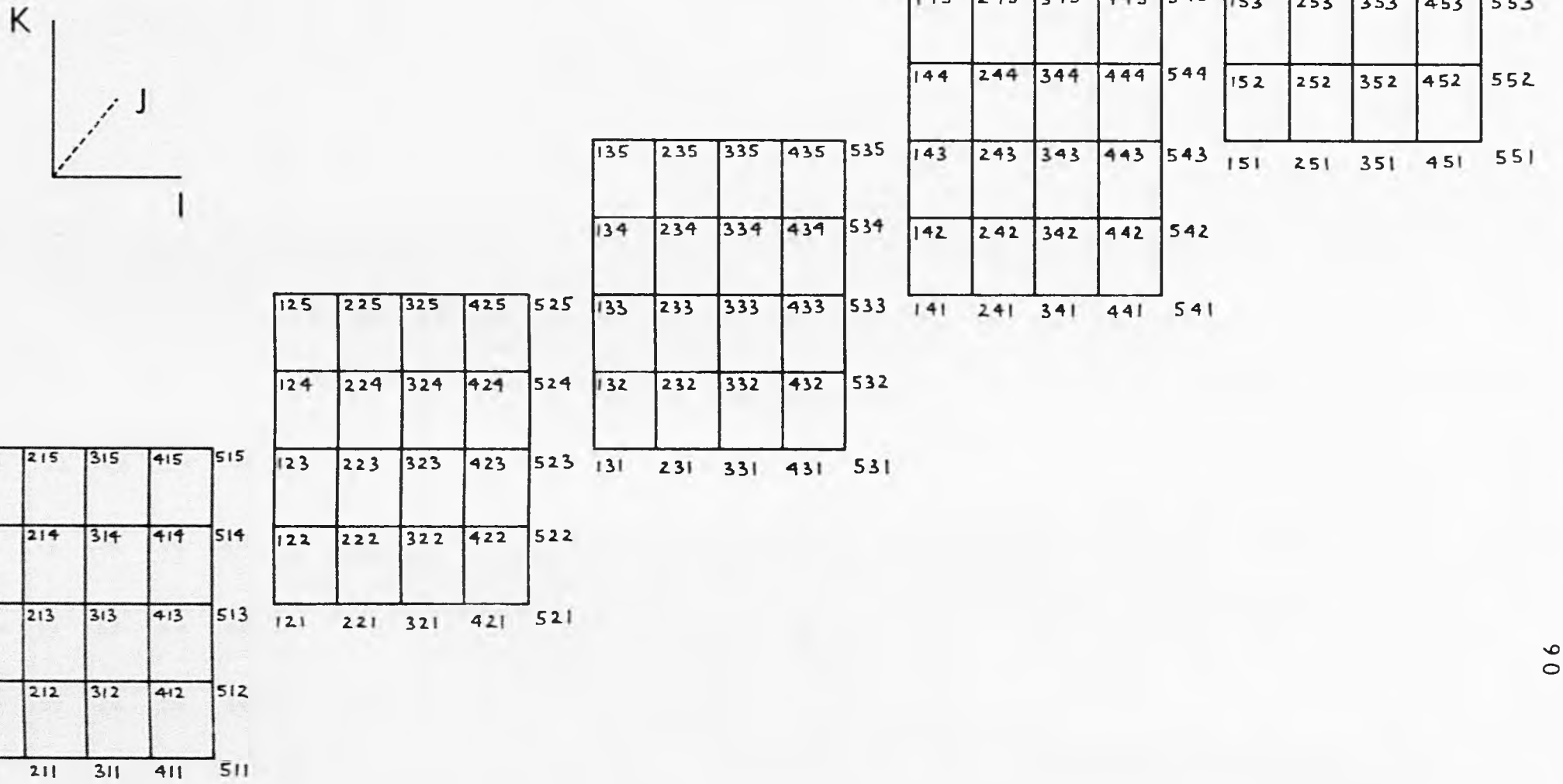
K
J
I
115 215 315 415 515
114 214 314 414 514
113 213 313 413 513
112 212 312 412 512
111 211 311 411 511
125 225 325 425 525
124 224 324 424 524
123 223 323 423 523
122 222 322 422 522
121 221 321 421 521
135 235 335 435 535
134 234 334 434 534
133 233 333 433 533
132 232 332 432 532
131 231 331 431 531
145 245 345 445 545
144 244 344 444 544
143 243 343 443 543
142 242 342 442 542
141 241 341 441 541
155 255 355 455 555
154 254 354 454 554
153 253 353 453 553
152 252 352 452 552
151 251 351 451 551

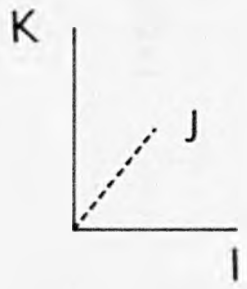

101	102	103	104	105
76	77	78	79	80
51	52	53	54	55
26	27	28	29	30
1	2	3	4	5

106	107	108	109	110
81	82	83	84	85
56	57	58	59	60
31	32	33	34	35
6	7	8	9	10

111	112	113	114	115
86	87	88	89	90
61	62	63	64	65
36	37	38	39	40
11	12	13	14	15

116	117	118	119	120
91	92	93	94	95
66	67	68	69	70
41	42	43	44	45
16	17	18	19	20

121	122	123	124	125
96	97	98	99	100
71	72	73	74	75
46	47	48	49	50
21	22	23	24	25

Since the lattice is of finite extent, we need to impose boundary conditions on the eigenvalue equation. In principle, the nature of the boundary conditions for this problem are unimportant because we are searching for the frequency of a bulk plasmon mode. In practise, we impose boundary conditions which are likely to be helpful from a computation point of view. We know that in the absence of the electron-electron interaction, the eigenvalue problem can be solved analytically and we make use of this fact in helping us to choose suitable boundary conditions. Consider the following simple example:

$$\omega X_n = \alpha (X_{n-1} + X_{n+1}) \qquad n = 2,3,\ldots, (N-1)$$

	cyclic boundary conditions	kill off boundary conditions
	$\omega X_1 = \alpha (X_0 + X_2)$	$\omega X_1 = \alpha X_2$
	$\omega X_N = \alpha (X_{N-1} + X_{N+1})$	$\omega X_N = \alpha X_{N-1}$
	$X_n = X_{n+N}$	
Solution	$X_n = A e^{in\theta}$	$X_n = A \sin n\theta$
provided	$\omega = 2\alpha\cos\theta$	$\omega = 2\alpha\cos\theta$
where	$\theta = 2m\pi/N \quad m = 0,1,..$	$\tan N\theta = -\tan\theta$

N.B. $\theta \in [0, 2\pi[$

The above system of equations describes a linear chain of atoms in which each atom is coupled only to its neighbour(s) by the tight binding parameter α. It is essentially the one dimensional form of our eigenvalue problem with the Coulomb interaction between electrons switched off. We see from this example that cyclic boundary conditions are to be followed on the grounds of mathematical convenience. Kill off boundary conditions produce a transcendental equation for the variable θ. In three dimensions the cyclic boundary conditions are

$$X(\ell_x,\ell_y,\ell_z) = X(\ell_x+NCa,\ell_y,\ell_z)$$

$$X(\ell_x,\ell_y,\ell_z) = X(\ell_x,\ell_y+NCa,\ell_z)$$

$$X(\ell_x,\ell_y,\ell_z) = X(\ell_x,\ell_y,\ell_z+NCa)$$

The non-interacting amplitudes, $X_\ell(e^2=0)$, for our tightly bound metal are plane waves $Aexp(ip\ell)$. It is clear that these amplitudes are easily determined by the imposition of cyclic boundary conditions, for $p_x a = 2m\pi/NC$ where $m = 0,1,\ldots,(NC-1)$ likewise p_y,p_z. This is useful in carrying out checks on the computer program for the site space method.

So far in this section, we have set up a co-ordinate system I,J,K and used this to assign a natural number to each lattice site via the mapping M.

$$\underline{a} = \begin{vmatrix} a_{11} & \cdots & a_{1N} \\ \vdots & & \vdots \\ a_{N1} & \cdots & a_{NN} \end{vmatrix}$$

We then imposed cyclic boundary conditions on the eigenvalue equation. The matrix $\underline{a}$ for the finite lattice is now completely defined. In each row there are at most seven non-zero elements: six one electron terms and one many electron term. The matrix describing a lattice of 125 atoms appears on the following pages. The elements of the matrix $\underline{a}$ are shown in accordance with the prescription detailed below.

$$1 \equiv u[(1-\cos\kappa_x a) - i\sin\kappa_x a] \qquad 2 \equiv u[(1-\cos\kappa_x a) + i\sin\kappa_x a]$$

$$3 \equiv u[(1-\cos\kappa_y a) - i\sin\kappa_y a] \qquad 4 \equiv u[(1-\cos\kappa_y a) + i\sin\kappa_y a]$$

$$5 \equiv u[(1-\cos\kappa_z a) - i\sin\kappa_z a] \qquad 6 \equiv u[(1-\cos\kappa_z a) + i\sin\kappa_z a]$$

$$7 \equiv 2\Omega(\kappa)\langle a^{+}_{\ell,\uparrow} a_{O,\uparrow}\rangle [e^{-i\kappa\cdot\ell} - 1]$$

Notice that the diagonal lines, which are typical of a tight binding regime, are broken at the surfaces of the lattice, and that the many electron terms are confined to a single column, the 63rd column infact ($\underline{\ell} = \underline{0}$ is mapped to 63).

The most important feature of the matrix is that it is sparse, 90% of its elements are zero. To define a sparse matrix we need only record the position and values of the non-zero elements. There are a variety of 'address systems' we could employ to do this and the one we shall use is the simplest. It is based on the two matrices INDEX and VALS.

INDEX(I,J) is the number of the column of the non-zero element with 'name' J in row I of matrix $\underline{a}$

VALS(I,J) is the value of the non-zero element with name J in row I of matrix $\underline{a}$.

As we have seen, there are seven different types of elements so J = 1,7.

To show how easy it is to define the INDEX matrix (taking account of cyclic boundary conditions) we reproduce a section of the computer program for the site space method. The centre element of the matrix is at (IC,IC) where IC = (N+1)/2.

```
      DO 6 K = 1,NC,1
      DO 7 J = 1,NC,1
      DO 8 I = 1,NC,1

      IA = I+(J-1)*NC+(K-1)*NC*NC

      INDEX(IA,1) = IA+1
      INDEX(IA,2) = IA-1
      INDEX(IA,3) = IA+NC
      INDEX(IA,4) = IA-NC
      INDEX(IA,5) = IA+(NC*NC)
      INDEX(IA,6) = IA-(NC*NC)
      INDEX(IA,7) = IC

      IF(I.EQ.NC) INDEX(IA,1) = INDEX(IA,1)-NC
      IF(I.EQ.1) INDEX(IA,2) = INDEX(IA,2)+NC
      IF(J.EQ.NC) INDEX(IA,3) = INDEX(IA,3)-(NC*NC)
      IF(J.EQ.1) INDEX(IA,4) = INDEX(IA,4)+(NC*NC)
      IF(K.EQ.NC) INDEX(IA,5) = INDEX(IA,5)-(NC*NC*NC)
      IF(K.EQ.1) INDEX(IA,6) = INDEX(IA,6)+(NC*NC*NC)

8     CONTINUE
7     CONTINUE
6     CONTINUE
```

The VALS matrix similarly presents no difficulty.

Having looked at the way in which we can store matrix a, we turn our attention to the methods available for the computation of the plasmon energy. One method is to do no work at all i.e. use a black box subroutine to solve the eigenvalue problem. For a low order approximation (small lattice) we can store the entire matrix and call a subroutine from the NAGFLIB. For better approximations we store only the non-zero elements and use one of the subroutines produced by the Harwell group for example. So if we want to use a black box subroutine we can do, but there is a more efficient route to the plasmon energy, for we can employ the POWER METHOD.

We know that there are two eigenvalues of $\underline{a}$ which are related to the plasmon energy namely:

λ_1 = + plasmon energy λ_2 = - plasmon energy

Thus $|\lambda_1| = |\lambda_2|$. By applying a shift to the diagonal elements of $\underline{a}$ we remove the degeneracy, and the plasmon energy becomes the eigenvalue of maximum modulus. This eigenvalue is obtained very efficiently by operating repeatedly with the matrix $\underline{a}$ on a given starting vector $\underline{v}$; normalising after each operation so that the element of maximum modulus in the resulting vector is unity. When the absolute value of the difference of two normalisation factors from successive operations is less than a set tolerance (10^{-4} Hartree), the final normalisation factor will be the eigenvalue of maximum modulus to that accuracy. This is the power method.

Let $\underline{v}_{max}$ be the eigenvector going with the eigenvalue of maximum modulus of $\underline{a}$ (more precisely of $\underline{a}_{shift}$). Operating repeatedly with $\underline{a}$ on $\underline{v}$ builds up the component $\underline{v}_{max}$ contained in $\underline{v}$, so that eventually

$$\underline{a}^n \underline{v} \propto \underline{v}_{max} \quad \text{for some number n.}$$

The problem of the proportionality constant is overcome by normalising after each matrix multiplication. Also, the starting vector $\underline{v}$ is not entirely arbitrary since the method requires $\underline{v}_{max}$ to be a component of $\underline{v}$.

It is clear that all we require for the calculation of the eigenvalue of maximum modulus is a formula for the matrix product $\underline{a}\ \underline{v}$ in terms of INDEX and VALS. This is easily established.

$$(\underline{a}\ \underline{v})_I = \sum_{J=1}^{7} \mathrm{VALS}(I,J)\ \underline{v}(\mathrm{INDEX}(I,J))$$

In writing the above equation we have assumed that there are seven non-zero elements in every row, if this is not true then the appropriate terms are ignored.

The power method therefore provides a very simple route to the plasmon energy.

The next comment about the site space method concerns the computation of the expectation value of the operator $a_\ell^+ a_o$. We have seen that this expectation value is the Fourier lattice transform of the occupation number n_k, thus to compute the set $\{\langle a_\ell^+ a_o \rangle\}$ we must carry out N Brillouin zone summations. For a large lattice, it is worth looking for symmetry properties of the expectation value with respect to interchange of lattice vectors, so as to minimise CPU time. In our model for example, the occupation number n_k is an even function of each of the components of the wave vector k, and is invariant under the interchange of the components. The Fourier lattice transform manifests this symmetry in site space: $\langle a_\ell^+ a_o \rangle$ is an even function of each of the components of the direct lattice vector ℓ, and is invariant under the interchange of the components. This means that the expectation value need only be computed for

a selection of lattice sites and not the entire lattice. Write $\underline{\ell} = \underline{L}\, a$ i.e.

$$L_x = -(NO-1),\ldots,O,\ldots,(NO-1) \quad \text{likewise } L_y, L_z$$

(recall that the total number of lattice vectors (N) is odd, and that NO = (NC+1)/2). It is sufficient to compute the expectation value for those values of $\underline{L}$ such that

$$O \leq L_z \leq (NO-1) \qquad O \leq L_y \leq L_z \qquad O \leq L_x \leq L_y$$

There are NO(NO+1)(NO+2)/6 values of $\underline{L}$ satisfying this condition

NO	NO(NO+1)(NO+2)/6	N
3	10	125
4	20	343
5	35	729
6	56	1331
7	84	2197
8	120	3375

So far, we have made use of the symmetry properties of $\langle a^{+}_{\ell} a_o \rangle$, we now investigate the possibility of determining the explicit functionality of the expectation value.

By definition $\langle a^{+}_{\ell} a_o \rangle = \frac{1}{N} \sum_k n_k \, e^{ik.\ell}$

Changing the summation to an integration, and writing $\underline{\ell} = \underline{L}a$, we can express the expectation value as follows

$$\langle a^{+}_{L} a_o \rangle = \frac{1}{(2\pi)^3} \int_{-\pi}^{\pi} dx \int_{-\pi}^{\pi} dy \int_{-\pi}^{\pi} dz \; \theta(\cos x+\cos y+\cos z)\cos(xL_x)\cos(yL_y)\cos(zL_z)$$

This formula is simplified by employing the integral representation of the step function

$$2\pi i \; \theta(t) = \lim_{\eta \to 0} \int_{-\infty}^{\infty} dw \; \frac{e^{iwt}}{(w-i\eta)}$$

The result is

$$2\pi i \langle a^{+}_{L} a_o \rangle =$$

$$i^{(L_x+L_y+L_z)} \{ P \int_{-\infty}^{\infty} dw \, \frac{1}{w} J_{L_x}(w) J_{L_y}(w) J_{L_z}(w) + i\pi J_{L_x}(0) J_{L_y}(0) J_{L_z}(0) \}$$

where J is a Bessel function of the first kind

$$2\pi i^{L} J_L(w) = \int_{-\pi}^{\pi} dx \, \cos xL \, \exp(iw\cos x)$$

Note that

$J_L(0) = 0$ for all L except $L = 0$ ($J_0(0) = 1$)

$J_L(-w) = (-1)^L J_L(w)$

Our brief excursion into the realms of Bessel functions has been profitable, for we see that

$$\langle a_L^+ a_o \rangle = 0 \qquad \text{if } L_x+L_y+L_z = \text{even}$$

$$(\langle a_L^+ a_o \rangle = \frac{1}{2} \qquad \text{for } \underline{L} = \underline{0}).$$

The computation of the set $\{\langle a_L^+ a_o \rangle\}$ therefore presents no difficulty for our model. But what about more complicated systems? Let us suppose the analogous expectation value(s) has no special symmetry properties and cannot be integrated for any value of L, and further that we are dealing with a large lattice N > 1000. There are two courses of action open to us. Firstly, we could compute the Fourier lattice transform by summing over occupied states only. Secondly, we could look for an alternative formula for the expectation value more amenable to computation e.g. we were able to express the expectation value in terms of a single integral over Bessel functions.

We underline that the computation of the set $\{\langle a_L^+ a_o \rangle\}$ takes place <u>once</u> for the whole excitation spectrum.

At this point we present the results of the site space method. For a small lattice, the value of the plasmon energy depends on the type of boundary conditions we impose on the problem. By taking a lattice of side 5 (125 atoms in all) we find that cyclic boundary conditions give a value of the plasmon energy which is roughly equivalent to the third order approximation, whilst kill off boundary

conditions produce slightly better values. However, to work to an accuracy of 10^{-4} H we require a lattice of side 13; this was confirmed by increasing the lattice side to 15 (an addition of over 1000 atoms), and for large lattices cyclic boundary conditions are preferred.

TABLE 6

This table displays the real and imaginary parts (EIGR and EIGI) of the eigenvalue of maximum modulus of the excitation spectrum. For comparison purposes we have selected the same values of u / a and wave vector that appear in the table of plasmon energies as determined by the dielectric function method. (The lattice size is $(15)^3$).

'IT' is the number of operations required to deliver the modulus of the eigenvalue to an accuracy of 'ACC'.

An arrow pointing to a value of EIGR indicates that EIGR < EDMAX i.e. the plasmon mode is no longer well defined.

KAPPA = (K,0,0) U = -0.01

K	EDMAX	EIGR	EIGI	ACC	IT
A = 1.5					
0.21	0.0063	0.2306D+00	0.7753D-07	0.73374D-05	12
0.42	0.0124	0.2139D+00	0.1542D-05	0.46827D-05	11
0.63	0.0182	0.1896D+00	0.5470D-05	0.96155D-05	10
0.84	0.0235	0.1616D+00	0.3197D-05	0.43815D-05	11
1.05	0.0283	0.1337D+00	0.5018D-05	0.58715D-05	11
1.26	0.0324	0.1086D+00	0.8249D-05	0.80949D-05	11
1.47	0.0356	0.8789D-01	0.7955D-05	0.62234D-05	12
1.68	0.0380	0.7256D-01	0.1535D-04	0.93674D-05	12
1.88	0.0395	0.6319D-01	0.1798D-04	0.84364D-05	13
2.09	0.0400	0.6304D-01	0.2251D-04	0.95445D-05	13
A = 2.5					
0.13	0.0063	0.1012D+00	0.7529D-08	0.76183D-06	14
0.25	0.0124	0.1752D+00	0.1056D-05	0.55514D-05	11
0.38	0.0182	0.1658D+00	0.3700D-05	0.96079D-05	10
0.50	0.0235	0.1539D+00	0.5026D-05	0.83710D-05	10
0.63	0.0283	0.1404D+00	0.6893D-05	0.92941D-05	10
0.75	0.0324	0.1266D+00	0.4335D-05	0.49940D-05	11
0.88	0.0356	0.1137D+00	0.5994D-05	0.61718D-05	11
1.01	0.0380	0.1030D+00	0.7832D-05	0.72467D-05	11
1.13	0.0395	0.9587D-01	0.9159D-05	0.78088D-05	11
1.26	0.0400	0.9334D-01	0.8851D-05	0.73783D-05	11
A = 6.5					
0.05	0.0063	0.1139D+00	0.5800D-07	0.53640D-05	12
0.10	0.0124	0.1145D+00	0.7620D-05	0.54545D-05	11
0.14	0.0182	0.1154D+00	0.1146D-05	0.35481D-05	11
0.19	0.0235	0.1166D+00	0.4011D-05	0.82658D-05	10
0.24	0.0283	0.1178D+00	0.5302D-05	0.79955D-05	10
0.29	0.0324	0.1189D+00	0.6491D-05	0.83684D-05	10
0.34	0.0356	0.1199D+00	0.7425D-05	0.88315D-05	10
0.39	0.0380	0.1206D+00	0.8052D-05	0.91502D-05	10
0.43	0.0395	0.1211D+00	0.8367D-05	0.92649D-05	10
0.48	0.0401	0.1212D+00	0.8368D-05	0.91804D-05	10

KAPPA = (K,K,0) U = -0.03

K	EDMAX		EIGR	EIGI	ACC	IT
A = 1.5						
0.21	0.0375		0.3919D+00	0.4363D-05	0.97020D-05	12
0.42	0.0742		0.3455D+00	0.5163D-05	0.63522D-05	12
0.63	0.1090		0.2883D+00	0.6559D-05	0.54769D-05	14
0.84	0.1411		0.2377D+00	0.1918D-04	0.93251D-05	16
1.05	0.1697		0.2068D+00	0.3165D-04	0.86165D-05	23
1.25	0.1942		0.2009D+00	0.2098D-04	0.99789D-05	51
1.47	0.2138	->	0.2123D+00	-0.3573D-07	0.13033D-04	70
1.68	0.2283	->	0.2243D+00	0.7345D-08	0.34474D-04	70
1.88	0.2370	->	0.2357D+00	0.1564D-08	0.37766D-04	70
2.09	0.2400	->	0.2353D+00	0.1308D-09	0.95658D-05	42
A = 2.5						
0.13	0.0375		0.3127D+00	0.1048D-05	0.38937D-05	13
0.25	0.0742		0.2997D+00	0.4134D-05	0.56161D-05	12
0.38	0.1090		0.2813D+00	0.8123D-05	0.71993D-05	13
0.50	0.1411		0.2618D+00	0.1292D-04	0.76224D-05	15
0.63	0.1697		0.2457D+00	0.2182D-04	0.79916D-05	18
0.75	0.1942		0.2363D+00	0.3624D-04	0.89096D-05	22
0.88	0.2138		0.2343D+00	0.3938D-04	0.99744D-05	29
1.01	0.2283		0.2376D+00	0.3357D-04	0.94863D-05	44
1.13	0.2370		0.2421D+00	0.2810D-04	0.97627D-05	57
1.26	0.2400		0.2436D+00	0.1161D-03	0.97199D-05	42
A = 6.5						
0.05	0.0375		0.2001D+00	0.6340D-07	0.40712D-05	13
0.10	0.0742		0.2094D+00	0.5906D-05	0.80767D-05	12
0.14	0.1090		0.2233D+00	0.1180D-04	0.90427D-05	13
0.19	0.1411		0.2402D+00	0.1420D-04	0.78069D-05	15
0.24	0.1697		0.2582D+00	0.1665D-04	0.70293D-05	17
0.29	0.1942		0.2755D+00	0.2156D-04	0.78596D-05	19
0.34	0.2138		0.2906D+00	0.2814D-04	0.97468D-05	18
0.39	0.2283		0.3022D+00	0.2301D-04	0.75812D-05	19
0.43	0.2370		0.3096D+00	0.3097D-04	0.99987D-05	18
0.48	0.2400		0.3121D+00	0.3104D-04	0.96947D-05	18

KAPPA = (K,K,K) U = -0.05

K	EDMAX		EIGR	EIGI	ACC	IT
A = 1.5						
0.21	0.0939		0.4979D+00	-0.8195D-05	0.944181D-05	12
0.42	0.1854		0.4254D+00	-0.1469D-04	0.992959D-05	15
0.63	0.2724		0.3581D+00	-0.3085D-04	0.858171D-05	23
0.84	0.3527	->	0.3509D+00	0.6889D-07	0.342091D-04	70
1.05	0.4243	->	0.4136D+00	0.2854D-08	0.682361D-04	70
1.26	0.4854	->	0.4766D+00	-0.1607D-07	0.136311D-03	70
1.47	0.5346	->	0.5260D+00	-0.2023D-08	0.628171D-04	70
1.68	0.5706	->	0.5644D+00	0.1477D-08	0.301561D-04	70
1.88	0.5926	->	0.5710D+00	0.6700D-08	0.661351D-03	70
2.09	0.6000	->	0.5858D+00	-0.6811D-09	0.466791D-04	70
A = 2.5						
0.13	0.0939		0.4039D+00	-0.1477D-08	0.614691D-07	17
0.25	0.1854		0.3996D+00	-0.1409D-04	0.918631D-05	15
0.38	0.2724		0.3763D+00	-0.2467D-04	0.808691D-05	21
0.50	0.3527		0.3783D+00	-0.1741D-04	0.912971D-05	38
0.63	0.4243	->	0.4168D+00	0.6803D-07	0.665661D-04	70
0.75	0.4854	->	0.4770D+00	0.3374D-07	0.126581D-03	70
0.88	0.5346	->	0.5260D+00	0.1032D-07	0.562071D-04	70
1.01	0.5706	->	0.5690D+00	-0.1535D-07	0.748761D-04	70
1.13	0.5926	->	0.5801D+00	0.9390D-08	0.295501D-03	70
1.26	0.6000	->	0.5862D+00	0.1387D-08	0.393141D-04	70
A = 6.5						
0.05	0.0939		0.2646D+00	-0.5977D-07	0.817841D-05	13
0.10	0.1854		0.2941D+00	-0.2019D-04	0.907601D-05	17
0.14	0.2724		0.3373D+00	-0.3297D-04	0.841151D-05	23
0.19	0.3527		0.3874D+00	-0.3875D-04	0.863791D-05	29
0.24	0.4243		0.4390D+00	-0.1348D-04	0.976451D-05	49
0.29	0.4854		0.4886D+00	-0.1858D-04	0.186361D-04	70
0.34	0.5346	->	0.5319D+00	0.2731D-07	0.261401D-04	70
0.39	0.5706	->	0.5643D+00	0.2673D-08	0.387371D-04	70
0.43	0.5926	->	0.5868D+00	0.1643D-09	0.683781D-04	70
0.48	0.6000	->	0.5925D+00	-0.3233D-10	0.201851D-04	70

Two striking features of Table 6 are the columns EIGI and IT. We see that at small κ, it takes about 12 iterations to deliver ABS(EIG + iEIGI) to an accuracy of 10^{-5} Hartree, whereas for those values of κ corresponding to the plasmon mode lying close to the electron hole continuum, it takes upwards of 70 iterations to obtain this accuracy (and so the maximum number of iterations was set at 70). Since each iteration involves the multiplication of a column vector with <u>complex</u> elements, and in view of the fact that the eigenvalue of maximum modulus is <u>real</u> to the order of 10^{-4} Hartree, it makes sense to investigate the possibility of determining the plasmon energy from an eigenvalue problem based on a real matrix.

Let us return to equation II.1.30 and write

$$\langle M|a^{+}_{\ell,\uparrow}a_{O,\uparrow}|O\rangle = e^{-i\kappa.\ell/2}\, Y_{\ell}$$

The equation for Y_{ℓ} is

$$\begin{aligned} i\omega Y_{\ell} = {} & 2u \sin\kappa_x a \left[Y_{(\ell_x+a,\ell_y,\ell_z)} - Y_{(\ell_x-a,\ell_y,\ell_z)} \right] \\ & -2u \sin\kappa_y a \left[Y_{(\ell_x,\ell_y+a,\ell_z)} - Y_{(\ell_x,\ell_y-a,\ell_z)} \right] \\ & -2u \sin\kappa_z a \left[Y_{(\ell_x,\ell_y,\ell_z+a)} - Y_{(\ell_x,\ell_y,\ell_z-a)} \right] \\ & -4\Omega(\kappa) \langle a^{+}_{\ell} a_{O} \rangle \sin(\underline{\kappa}.\ell/2) Y_{O} \end{aligned}$$

By equating real and imaginary parts of this equation we establish an eigenvalue problem based on a real matrix.

The eigenvectors are the real part of Y, whilst the eigenvalues are of the form

$$\omega' = 8u^2[\sin^2(\kappa_x a/2)+\sin^2(\kappa_y a/2)+\sin^2(\kappa_z a/2)] - \omega^2$$

$$\omega' Y_{\ell}^{real} =$$

$$4u^2\sin^2(\kappa_x a/2)\{ Y^{real}_{(\ell_x \pm 2a, \ell_y, \ell_z)} \}$$

$$+8u^2\sin(\kappa_x a/2)\sin(\kappa_y a/2)\{ Y^{real}_{(\ell_x \pm a, \ell_y \pm a, \ell_z)} \}$$

$$+8u\Omega(\kappa)\sin(\kappa_x a/2)\{<a^{+}_{\ell_x \pm a, \ell_y, \ell_z} a_O>\sin(\kappa.\ell/2 \pm \kappa_x a/2)\}\ Y_O^{real}$$

$$+8u\Omega(\kappa)\sin(\kappa_x a/2)\sin(\kappa.\ell/2)<a^{+}_{\ell} a_O>\{ Y^{real}_{(\pm a, O, O)} \}$$

The right hand side of the above equation isn't in fact complete, but since the terms to be added only correspond to various permutations of x, y and z, it does indicate the general structure of the real matrix. N.B. Curly brackets are an instruction to take linear combinations e.g.

$\{ Y^{real}_{(\pm, ,)} \}$ is shorthand for $\{ Y^{real}_{(+, ,)} + Y^{real}_{(-, ,)} \}$

The reader is now invited to return to the grid shown on page 91. Focus on site 57 say. The real eigenvalue problem connects Y^{real}_{57} to the following Y^{real}'s

$$(Y^{real}_{59} + Y^{real}_{60})$$

$$(Y^{real}_{51} - Y^{real}_{53} - Y^{real}_{61} + Y^{real}_{63})$$

$$[<a^{+}_{58}a_O>\sin(\kappa.\ell/2+\kappa_x a/2) - <a^{+}_{56}a_O>\sin(\kappa.\ell/2-\kappa_x a/2)]Y^{real}_{63}$$

$$<a^{+}_{57}a_O>\ (Y^{real}_{64} - Y^{real}_{62})$$

Recalling that if $\ell = 0$ is mapped to an odd(even) number then

$$\langle a_m^+ a_0 \rangle = 0 \text{ for } m = \text{odd/even}$$

we see that lattice sites going with an odd number are connected only to their fellow sites with odd numbers i.e. 'odd is connected to odd' and 'even is connected to even'. The eigenvalue problem has <u>separated</u>. (If the total number of sites is even, the odd/even symmetry is broken, but the eigenvalue problem still separates of course. Note also that the presence of Y_{60}^{real} is a consequence of cyclic boundary conditions, they are therefore dropped).

Table 7

The results of the real matrix eigenvalue problem are shown in this table for a lattice of side 13. Notice the reduction in IT.

KAPPA = (K,0.0) U = -0.01

K	EDMAX	EIG	ACC	IT
A = 1.5				
0.21	0.0063	0.2306D+00	0.71095D-05	3
0.42	0.0124	0.2139D+00	0.93676D-05	10
0.63	0.0182	0.1896D+00	0.61545D-06	3
0.84	0.0235	0.1616D+00	0.35160D-05	2
1.05	0.0283	0.1337D+00	0.65968D-05	2
1.26	0.0324	0.1086D+00	0.85988D-05	2
1.47	0.0356	0.8793D-01	0.78649D-05	2
1.68	0.0380	0.7258D-01	0.30019D-05	2
1.88	0.0395	0.6315D-01	0.46106D-05	2
2.09	0.0400	0.6000D-01	0.69458D-05	2
A = 2.5				
0.13	0.0063	0.1812D+00	0.70461D-05	3
0.25	0.0124	0.1752D+00	0.41032D-05	10
0.38	0.0182	0.1658D+00	0.59176D-06	3
0.50	0.0235	0.1539D+00	0.37008D-05	2
0.63	0.0283	0.1405D+00	0.70909D-05	2
0.75	0.0324	0.1267D+00	0.97646D-05	2
0.88	0.0356	0.1137D+00	0.41236D-05	3
1.01	0.0380	0.1030D+00	0.64577D-05	2
1.13	0.0395	0.9588D-01	0.50299D-05	2
1.26	0.0400	0.9335D-01	0.24223D-05	2
A = 6.5				
0.05	0.0063	0.1137D+00	0.42843D-05	1
0.10	0.0124	0.1145D+00	0.53932D-05	8
0.14	0.0182	0.1154D+00	0.52456D-06	3
0.19	0.0235	0.1166D+00	0.37279D-05	2
0.24	0.0283	0.1178D+00	0.72957D-05	2
0.29	0.0324	0.1189D+00	0.34558D-05	3
0.34	0.0356	0.1199D+00	0.91516D-05	2
0.39	0.0380	0.1206D+00	0.33483D-05	3
0.43	0.0395	0.1211D+00	0.59532D-05	2
0.48	0.0400	0.1212D+00	0.36138D-05	2

KAPPA = (K,K,0) U = -0.03

K	EDMAX	EIG	ACC	IT
A = 1.5				
0.21	0.0375	0.3919D+00	0.87210D-05	6
0.42	0.0742	0.3456D+00	0.15815D-05	2
0.63	0.1090	0.2883D+00	0.71131D-05	3
0.84	0.1411	0.2377D+00	0.70246D-05	6
1.05	0.1697	0.2068D+00	0.81524D-05	10
1.26	0.1942	0.2008D+00	0.88013D-05	19
1.47	0.2138	0.2117D+00	0.88906D-05	23
1.68	0.2283	0.2238D+00	0.98836D-05	18
1.88	0.2370	0.2319D+00	0.82337D-05	14
2.09	0.2400	0.2346D+00	0.96397D-05	8
A = 2.5				
0.13	0.0375	0.3127D+00	0.76345D-05	6
0.25	0.0742	0.2997D+00	0.11693D-05	2
0.38	0.1090	0.2813D+00	0.77553D-05	3
0.50	0.1411	0.2618D+00	0.12432D-05	2
0.63	0.1697	0.2457D+00	0.58476D-05	7
0.75	0.1942	0.2363D+00	0.95076D-05	8
0.88	0.2138	0.2343D+00	0.93311D-05	12
1.01	0.2283	0.2376D+00	0.86315D-05	17
1.13	0.2370	0.2413D+00	0.92928D-05	17
1.26	0.2400	0.2425D+00	0.23043D-05	1
A = 6.5				
0.05	0.0375	0.2001D+00	0.66343D-05	6
0.10	0.0742	0.2094D+00	0.92588D-05	2
0.14	0.1090	0.2233D+00	0.37624D-05	2
0.19	0.1411	0.2402D+00	0.26952D-05	3
0.24	0.1697	0.2582D+00	0.19605D-05	4
0.29	0.1942	0.2755D+00	0.56187D-05	6
0.34	0.2138	0.2906D+00	0.57746D-05	7
0.39	0.2283	0.3022D+00	0.57240D-05	7
0.43	0.2370	0.3096D+00	0.79926D-05	6
0.48	0.2400	0.3121D+00	0.64311D-05	5

KAPPA = (K,K,K) U = -0.05

K	EDMAX	EIG	ACC	IT
A = 1.5				
0.21	0.0939	0.4979D+00	0.58963D-05	3
0.42	0.1854	0.4254D+00	0.73656D-05	4
0.63	0.2724	0.3581D+00	0.96061D-05	9
0.84	0.3527	0.3510D+00	0.40336D-04	30
1.05	0.4243	0.4134D+00	0.64714D-04	30
1.26	0.4854	0.4727D+00	0.90210D-05	28
1.47	0.5346	0.5205D+00	0.93845D-05	16
1.68	0.5706	0.5554D+00	0.75861D-05	10
1.88	0.5926	0.5768D+00	0.84715D-05	7
2.09	0.6000	0.5840D+00	0.86110D-05	5
A = 2.5				
0.13	0.0939	0.4039D+00	0.60923D-05	11
0.25	0.1854	0.3896D+00	0.46250D-05	13
0.38	0.2724	0.3763D+00	0.54739D-05	15
0.50	0.3527	0.3782D+00	0.92640D-05	18
0.63	0.4243	0.4161D+00	0.12147D-03	30
0.75	0.4854	0.4737D+00	0.55438D-04	30
0.88	0.5346	0.5214D+00	0.11073D-04	30
1.01	0.5706	0.5563D+00	0.92395D-05	28
1.13	0.5926	0.5774D+00	0.12742D-05	11
1.26	0.6000	0.5843D+00	0.16032D-05	7
A = 6.5				
0.05	0.0939	0.2646D+00	0.26669D-05	8
0.10	0.1854	0.2941D+00	0.50624D-05	12
0.14	0.2724	0.3373D+00	0.68857D-05	14
0.19	0.3527	0.3874D+00	0.89136D-05	11
0.24	0.4243	0.4388D+00	0.98783D-05	26
0.29	0.4854	0.4885D+00	0.28525D-04	30
0.34	0.5346	0.5317D+00	0.29799D-04	30
0.39	0.5706	0.5650D+00	0.31587D-04	30
0.43	0.5926	0.5849D+00	0.67464D-05	17
0.48	0.6000	0.5915D+00	0.23086D-05	10

Tables 5 and 7 represent only one third of the total data analysed; we looked at results for 270 wave vectors in all (9 choices of u / a, 3 directions, 10 increments of wave vector per direction). Examination of the larger data set shows that to an accuracy of 10^{-4} Hartree, the value of the plasmon energy determined by the site space method (EIG) is in perfect agreement with that obtained by the dielectric function approach (PE) for 91% of the wave vectors.

The accuracy of agreement at the exceptional wave vectors is detailed below

at 14 wave vectors, EIG and PE agree to within 0.0004 H and at 5 wave vectors, agreement is worse than 0.0005 H:

u / a	KAPPA	W9	PE	EIG
-0.05 / 1.5	(0.6,0.6,0)	0.3066	0.3258	0.3239
-0.01 / 1.5	(0.8,0.8,0)	0.0722	0.0768	0.0761
-0.05 / 2.5	(0.8,0.8,0)	0.3498	0.3837	0.3813
-0.03 / 2.5	(1.0,1.0,0)	0.2338	0.2443	0.2425
-0.05 / 6.5	(0.6,0.6,0.6)		0.4894	0.4885

The components of κ are in units of π/a.

Concerning the accuracy of EIG, we discuss the comparison of CPU times for the site space method with those for the dielectric function approach. Strictly speaking, for each choice of u / a, we search for the minimum numbers of atoms (N_{min}) required by the site space calculation to ensure that PE and EIGR agree to a set accuracy (10^{-4} Hartree), and then quote computer times as determined by $N_{min}(u,a)$. However, it is reasonable to work with only one size of lattice, some average value of $\{N_{min}(u,a)\}$, provided this does not significantly effect CPU times. A consequence of working with an average value of $\{N_{min}(u,a)\}$ would be that for certain values of u and a, EIG and PE would differ by more than 10^{-4} H at a small number of wave vectors. A lattice of side 13 is therefore an appropriate choice, because for 4 pairings of u and a agreement is perfect for all wave vectors, whereas for 5 pairings of u and a agreement at a small number of wave vectors is not perfect but still of the order of 10^{-3} H.

We emphasise that for 22 of the 27 wave vectors in our data set which are on or near the surface of the domain of the plasmon excitation in the Brillouin zone, PE and EIG agree to within 0.0001 H. Particular attention was paid to this point. Accordingly, computer times are quoted for a lattice of side 13.

Computer Times for the Site Space Method

The CPU times shown over the page are the analogous results to those given on page 80 for the dielectric function approach. The times are in seconds.

u / a	κ = (K,0,0)	κ = (K,K,0)	κ = (K,K,K)
-0.01 / 1.5	52	70	98
-0.01 / 2.5	54	53	94
-0.01 / 6.5	51	56	66
-0.03 / 1.5	67	107	125
-0.03 / 2.5	61	84	138
-0.03 / 6.5	61	66	91
-0.05 / 1.5	75	125	137
-0.05 / 2.5	67	122	156
-0.05 / 6.5	63	75	154

Comparing CPU times for the site space and momentum space calculations, we find that the site space program runs more slowly by a factor of between 1.4 and 3.9 depending on the choice of parameters and directions. As we have mentioned, solving an eigenvalue problem on a lattice was for many years not an attractive proposition because of storage problems or equivalently, high CPU times. In view of this, the CPU times for the site space method are very encouraging, particularly when we recall that

(i) all reasonable steps were taken to optimise the efficiency of the momentum space program: WTRAIL was set equal to the best available approximation to the plasmon energy; Brillouin zone summations were executed over occupied states only

(ii) the results include the computation of plasmon energies very close to the electron hole continuum to an accuracy of 1 part in 10,000.

Widening our discussion to overall computing effort i.e. taking account of the work involved in writing and debugging programs, there can be no doubt that it is more convenient to solve the RPAE equations in site space than to compute the dielectric function, for whereas the pole structure of the dielectric function is a potential source of underflow/overflow problems, the site space program runs smoothly near and over the continuum.

Throughout this chapter we have paid particular attention to the mathematical and computational features of the site space method. It is appropriate at this stage, whilst discussing the results of the method, to redress the balance by looking at a physical reason for wanting to solve the RPAE equations in site space.

The peak positions of surface plasmon modes in high resolution electron energy loss spectra (HREELS) are described quite accurately by means of a surface loss function

$$\text{Im}\,[1/(1+\varepsilon)]$$

It is a more difficult proposition to account for details of the lineshape of such spectra. In 1983 a paper appeared in Surface Science (Egri et al) which looked specifically at this point. Spectra were examined for cleaved GaAs(110) surfaces prepared in situ in ultrahigh vacuum by the double wedge technique. There is a surface plasmon peak at 20 meV and a surface phonon peak at 40 meV. The gross structure of the spectra can be explained by a dispersionless phonon oscillator combined with a Drude term representing the conduction electrons. However, the assumption of a plasmon free surface layer produced a very good description of the lineshape of the spectra. The width of the surface layer was a 'fit' parameter, the optimum fit occurring at 150 Å. The authors made firm contact between theory and experiment by demonstrating theoretically that the radius of the plasmon wavefunction is of the order of 150 Å.

The model they adopt is simply a Lindhard electron gas, and their final formula for the plasmon wavefunction is essentially that for the matrix element $\langle M|a^{+}_{\ell,\uparrow}a_{o,\uparrow}|0\rangle$, namely (II.2.10), where for the direct lattice vector read the position vector of the electron relative to the hole. Since the authors are concerned with small momentum transfers of the single particle excitations (the physically relevant situation), it is possible to integrate the formula for the Lindhard plasmon to obtain an explicit expression for the spatial extent of the plasmon wavefunction ('$\langle M|a^{+}_{\ell,\uparrow}a_{o,\uparrow}|0\rangle$') normal to the surface

$$\phi(R) \sim J_1(R)/R$$

The first zero of ϕ is at 185 $\mathring{A}$ which is approximately the width of the plasmon free surface layer. The work of Egri, Matz, Luth and Stahl indicates the usefulness of the matrix elements of the operator $(a^{+}_{\ell,\uparrow}a_{o,\uparrow})$.

The site space method delivers the plasmon wavefunction and the plasmon energy from the same calculation (the dielectric theory approach requires usto compute a Fourier lattice transform once the plasmon energy has been determined), so that solving the RPAE equations in site space provides physically useful information (the spatial extent of the plasmon wavefunction) with an economy of effort.

The conventional way of displaying the variation and localisation of the plasmon matrix element as a function of lattice vector, is to plot the matrix element along a

given direction in the lattice. An alternative approach is to present a 3D view of the two dimensional array of spot heights corresponding to the absolute values of the matrix elements over a particular plane in the lattice. The isometric projections shown over the next twelve pages illustrate how the appreciation of more than 30,000 matrix elements can be realised almost at a glance. In consequence, such projections can be used to fingerprint elementary excitations (see also Rogan and Inglesfield, 1981).

Isometric Projections

The absolute values of the matrix elements $\langle M|a^{+}_{\ell,\uparrow}a_{o,\uparrow}|O\rangle$ for a lattice of side 15, are presented in the form of isometric projections on planes of fixed L_z (in accordance with the convention given over the page) for a comprehensive selection of parameters:

u	a	KAPPA	K in π/a	EIGR	EDMAX	Page
-0.05	2.5	(K,K,0)	0.1	0.4049	0.0626	126
-0.05	2.5	(K,K,0)	0.4	0.3586	0.2351	127
-0.05	2.5	(K,K,0)	0.8	0.3819	0.3804	128
-0.01	1.5	(0,0,K)	0.1	0.2306	0.0063	129
-0.01	1.5	(0,0,K)	0.9	0.0632	0.0395	130
-0.01	1.5	(K,K,0)	0.1	0.2259	0.0125	131
-0.01	1.5	(K,K,0)	0.9	0.0788	0.0790	132
-0.01	1.5	(K,K,K)	0.1	0.2212	0.0188	133
-0.01	1.5	(K,K,K)	0.9	0.1158	0.1185	134

The matrix element of maximum modulus is unity.

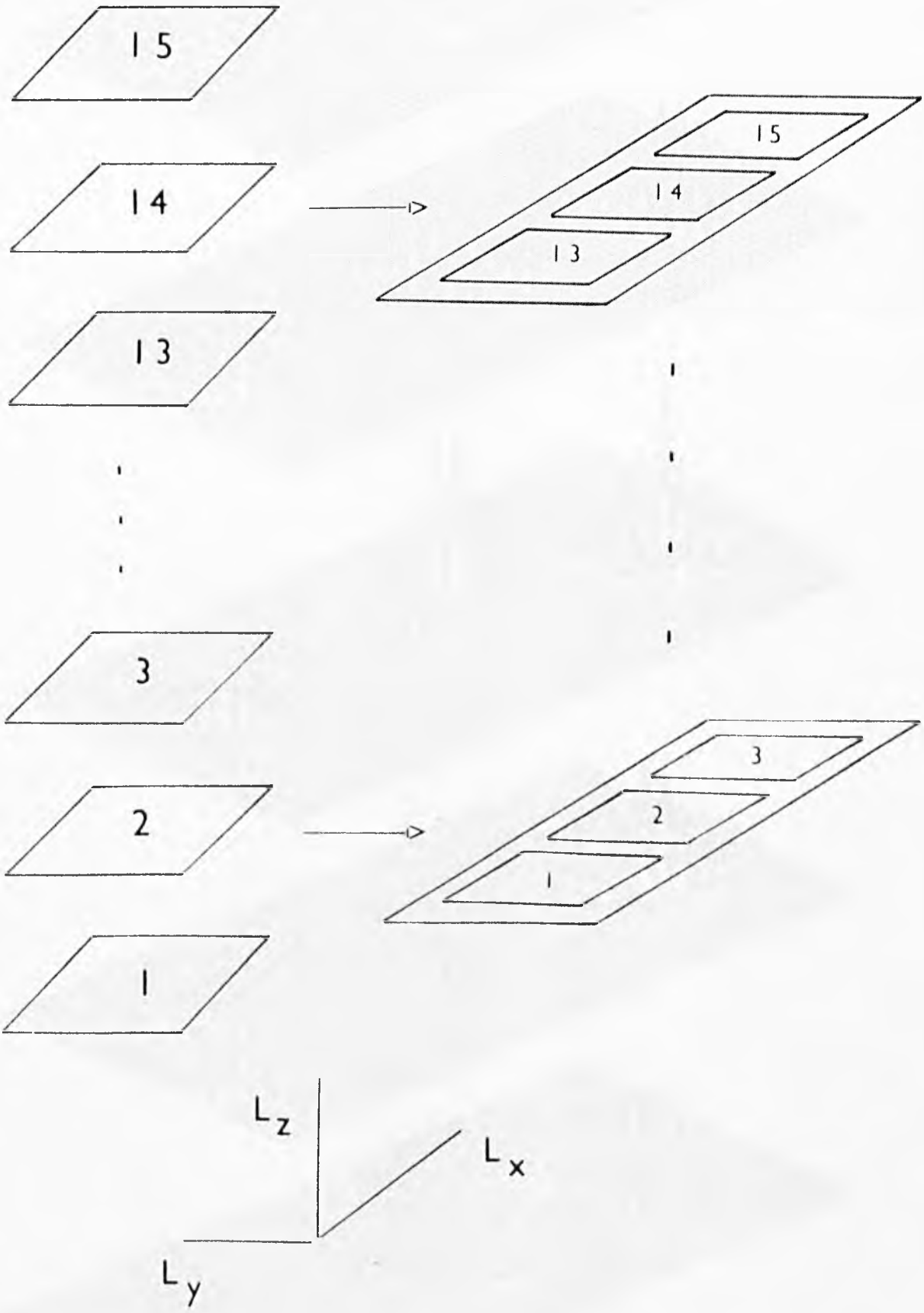
15
14
13
3
2
1
15
14
13
3
2
1
L_z
L_x
L_y

110

$k = 0,1$

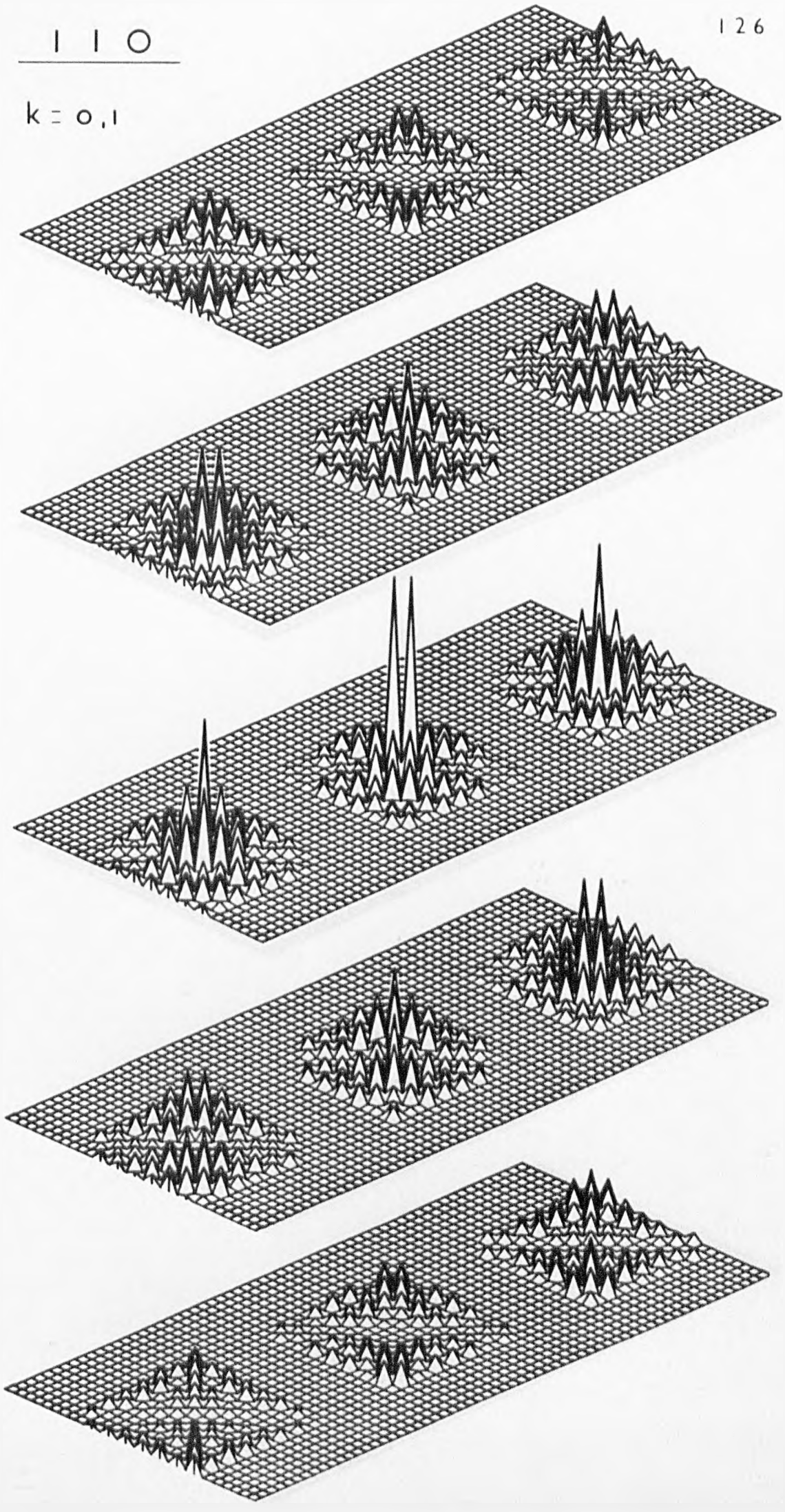

110

$k = 0{,}4$

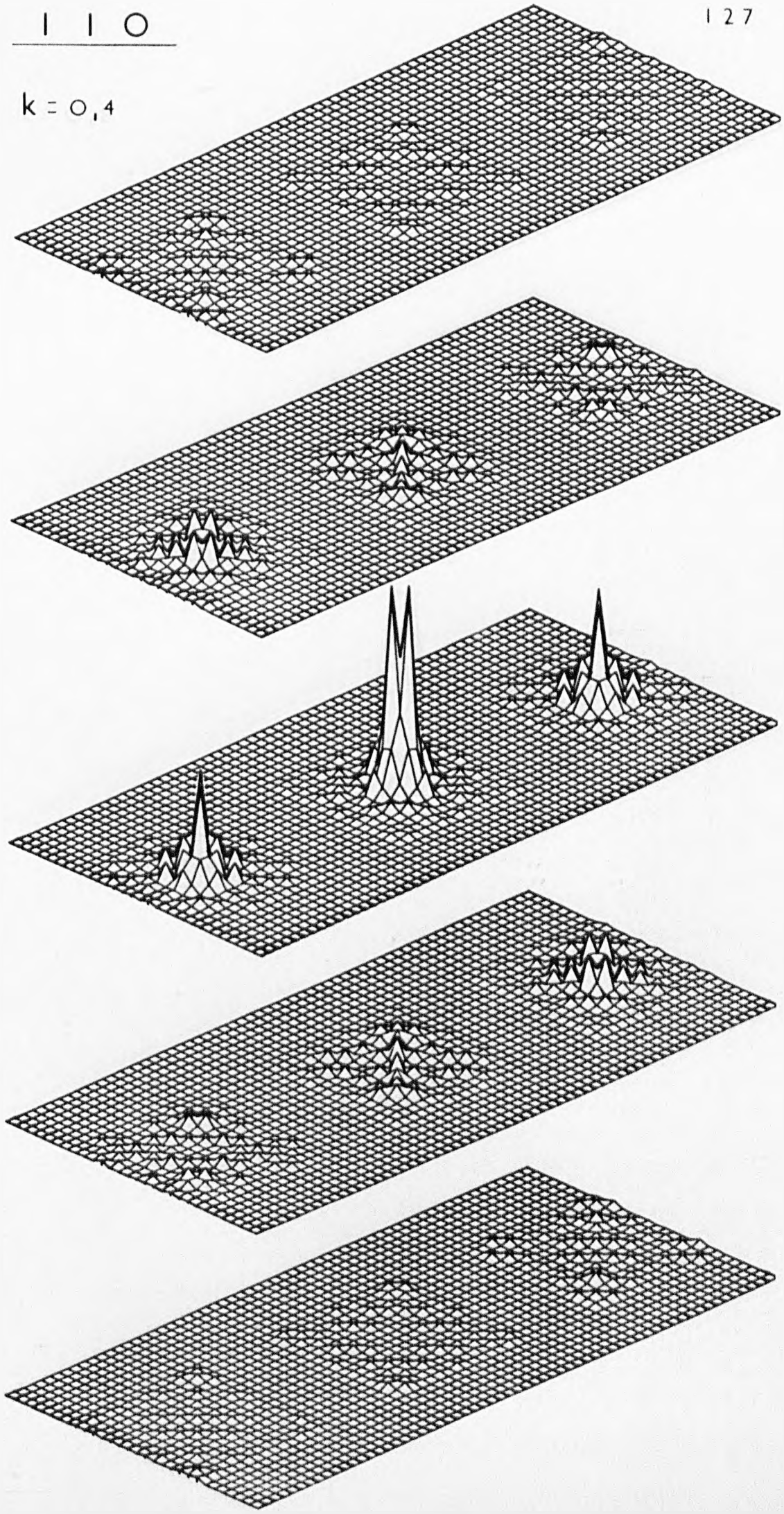

k = 0,8

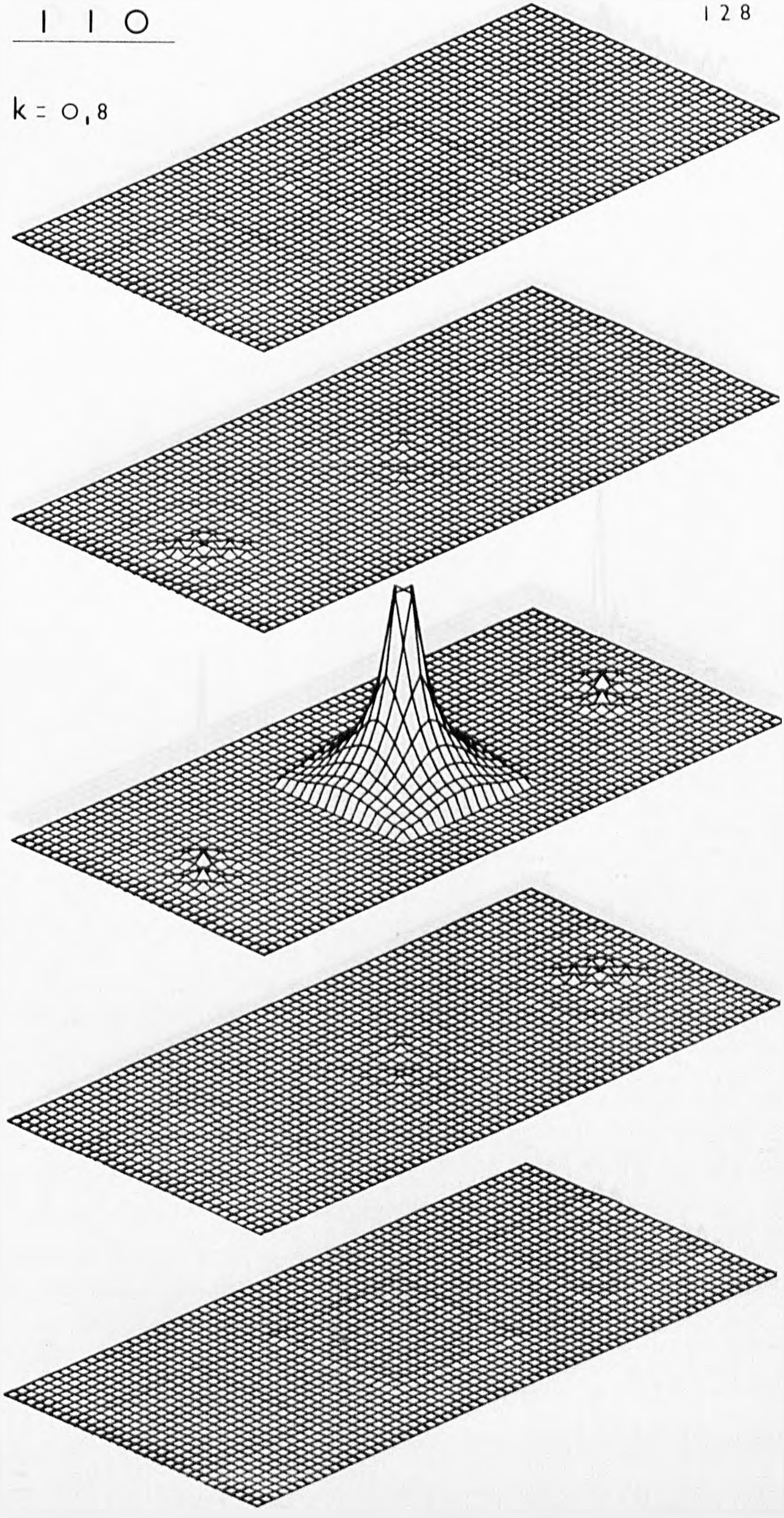

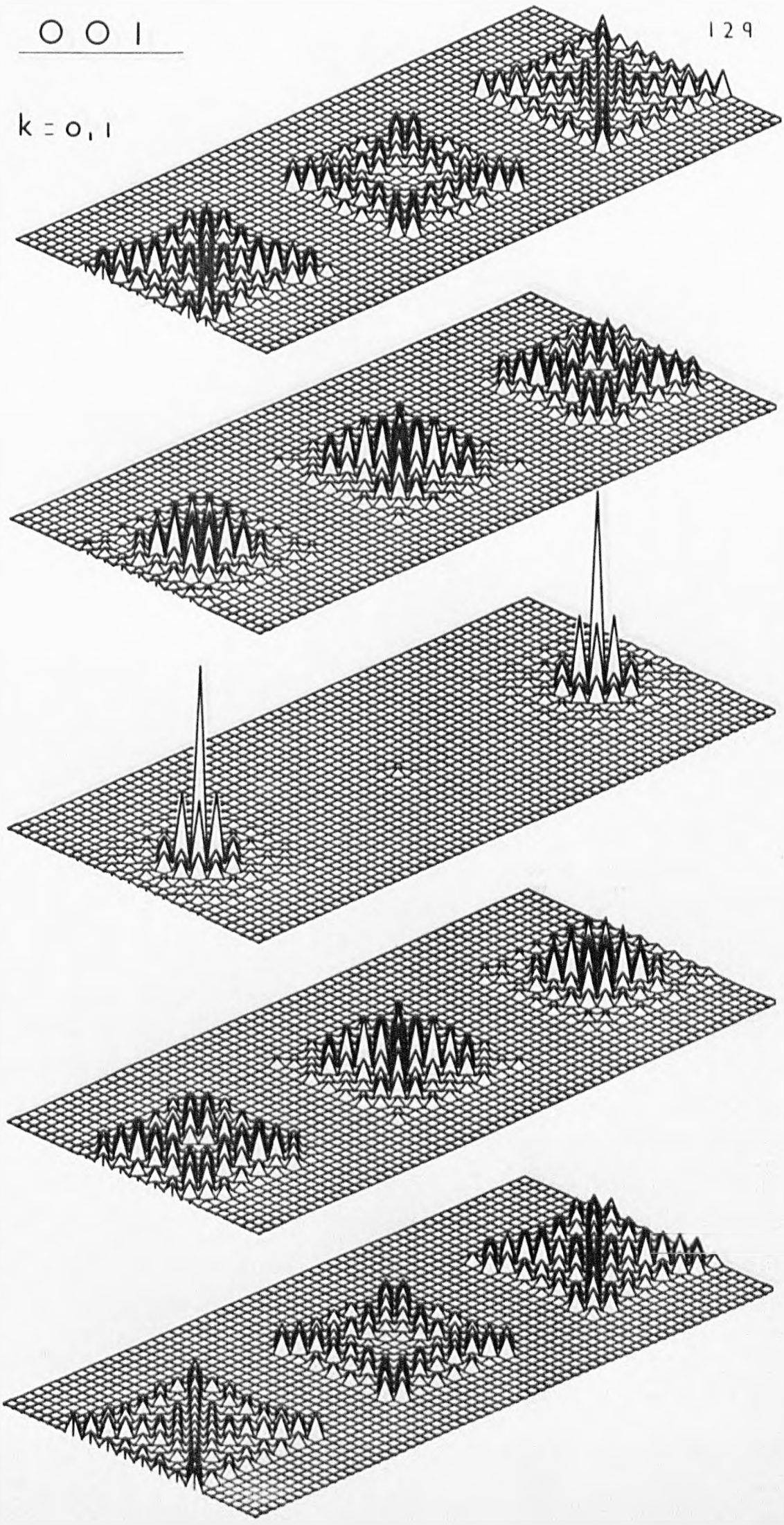
0 0 1
k = 0, 1

001

k = 0,9

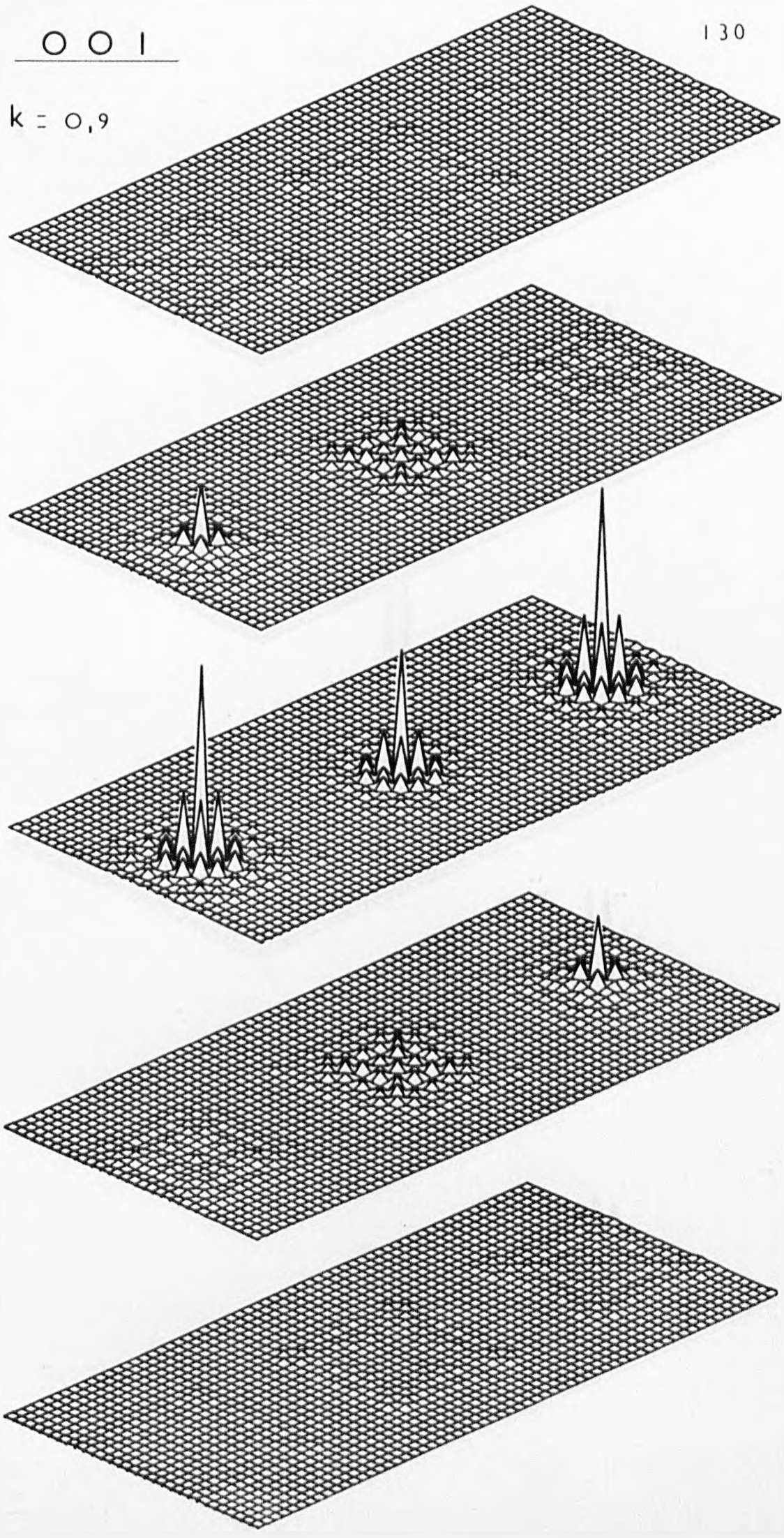

110

$k = 0,1$

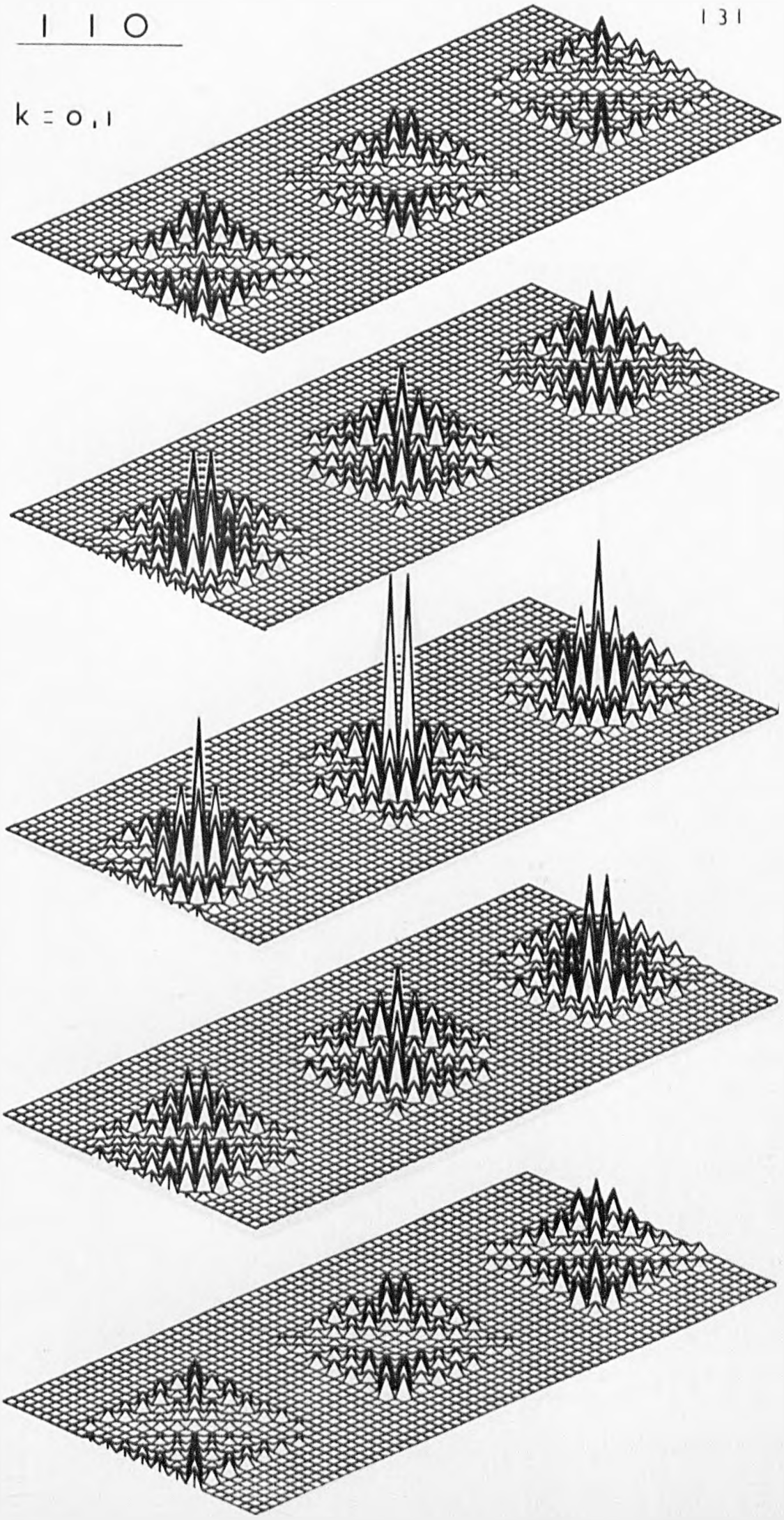

110

$k = 0,9$

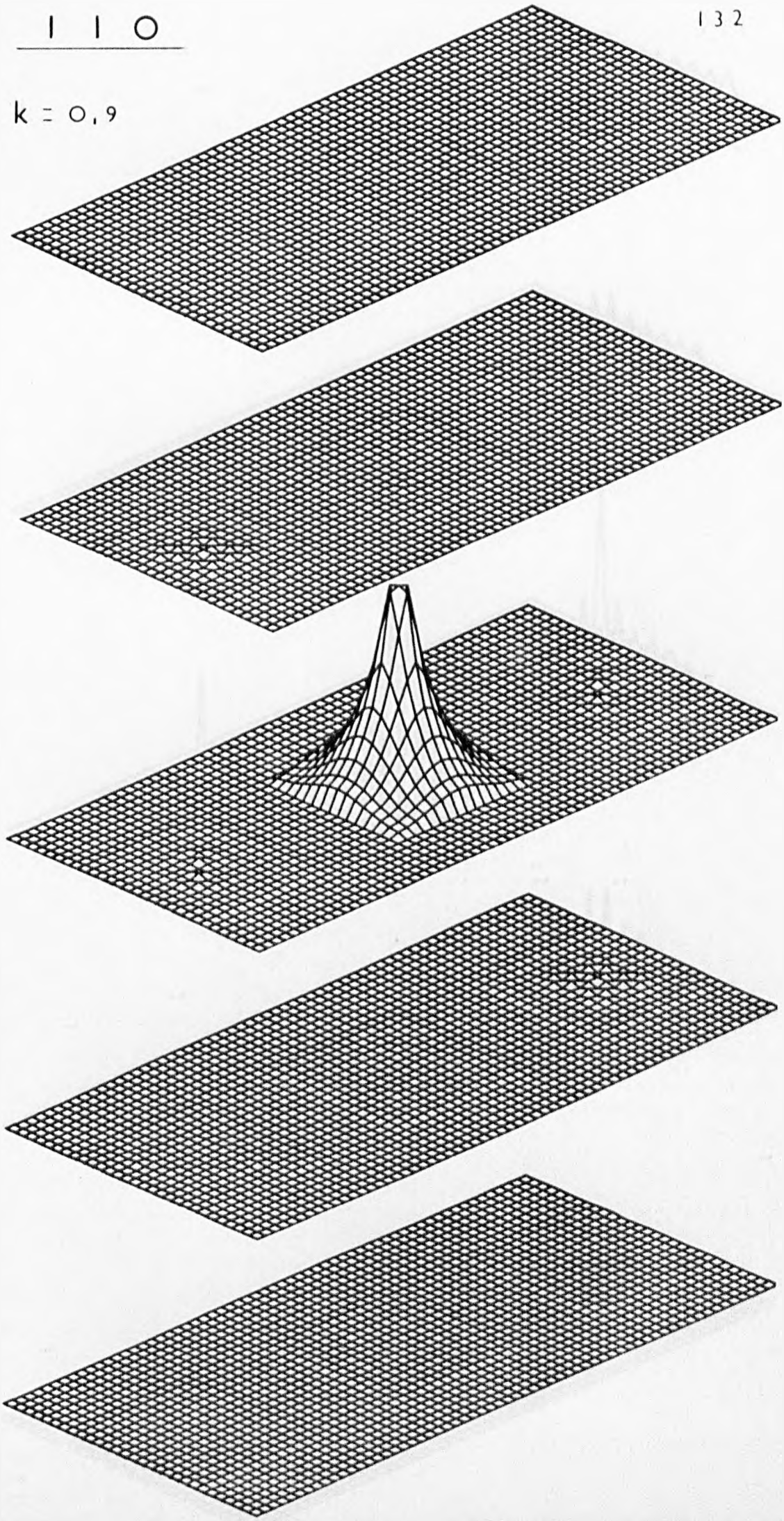

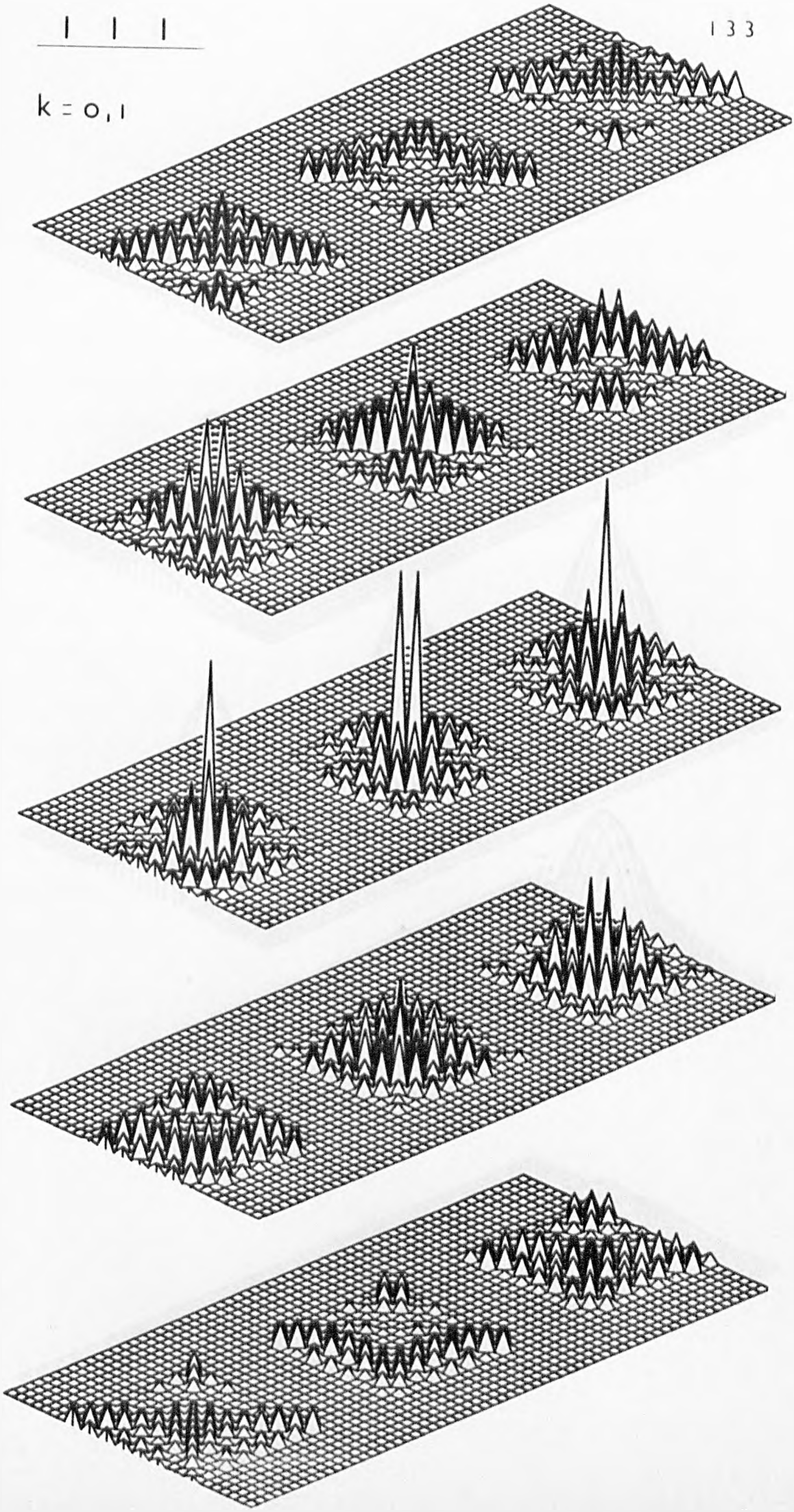
k = o,1

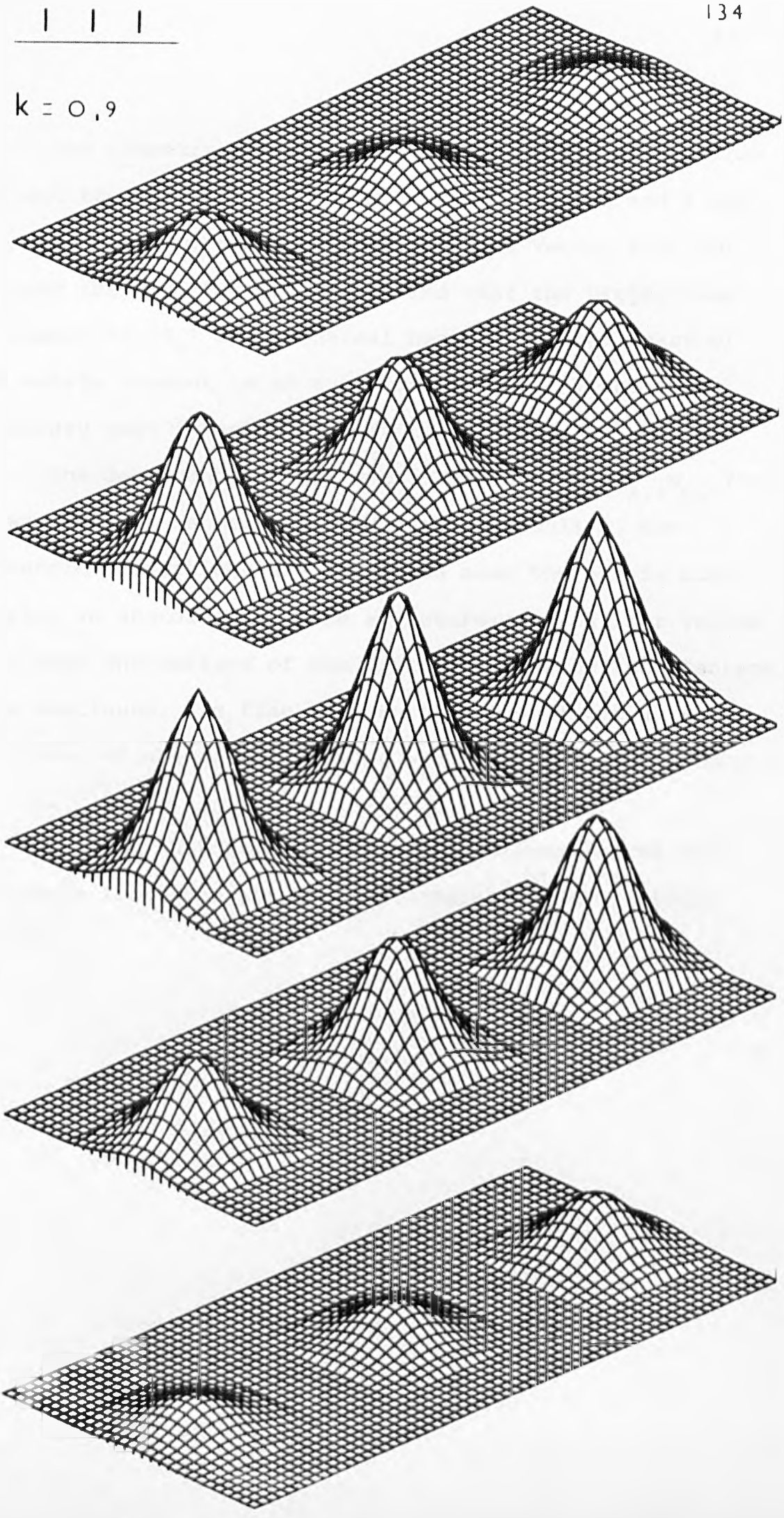
1 1 1
k = 0,9

The symmetry properties of the isometric projections reflect the direction of κ, and the fact that n and ε are even functions of the components of wave vector e.g. for κ along the (001) direction we find that the projections on planes of $|\ell_z|$ are identical because the real part of the matrix element is an even function of ℓ_z, and the imaginary part is an odd function.

The dependence of the matrix element $\langle M|a^{+}_{\ell,\uparrow}a_{o,\uparrow}|O\rangle$ on wave vector is most transparent. At small κ, the isometric projections are localised near the origin displaying an abundance of fine structure; whereas for values of κ near the surface of the Brillouin zone or the electron hole continuum, the fine structure is washed out as the real part of the matrix element becomes large away from the origin.

We note that the isometric projections depend surprisingly little on the hopping parameter and electron density.

II.3 A Sum Rule and Spectral Strengths

Our discussion of the single particle aspects of the tightly bound metal has hitherto been limited. We have mentioned that within the random phase approximation, one electron transitions are elementary excitations of the interacting system to the order of 1/N, so that modal sums incorporate a term specific to quasi electrons. In this section we investigate the role played by one electron transitions in determining the exchange correlation energy and interaction energy of the metal. To do this, we calculate the spectral strengths ($|C_M|^2$) of the trace of the response function

$$\text{Tr } F(\kappa+G,\kappa+G';\omega) = \sum_m \{ \frac{|C_m(\kappa)|^2}{[\ \omega-\omega_m(\kappa)\ ]} - \frac{|C_m(-\kappa)|^2}{[\ \omega+\omega_m(-\kappa)\ ]} \} \quad 3.1$$

$$\int dx\ \langle M|\rho(x,x)|0\rangle e^{i(Q+G).r} = F(\kappa+G)\delta_{Q,\kappa}\{\ 2N\langle M|a^{+}_{0,\uparrow}a_{0,\uparrow}|0\rangle\ \} \quad 3.2$$

The above result depends on the tight binding approximation and the Bloch property.

The computation of the spectral strength of the plasmon mode is based on the relation

$$|C_M|^2 = e^2\ \partial\omega_M/\partial e^2$$

For a site space calculation, the plasmon energy is computed at two values of the coupling constant (unity, and unity plus one per cent say) and the spectral strength is then the

difference in the two energies multiplied by a factor of 100. Within a dielectric theory framework, we recall that the relation

$$1 - \mathrm{Tr}\ \Lambda(e^2,\omega) = 0 \qquad \text{at } \omega = \omega_M$$

determines the frequency of an elementary excitation as an implicit function of the coupling constant. By totally differentiating this equation with respect to the coupling constant, we arrive at an expression for the spectral strength

$$|C_M|^2 = -1/\{\ \partial/\partial\omega\ \mathrm{Tr}\Lambda(e^2,\omega)\ \} \quad \text{at } \omega = \omega_M$$

The frequency derivative of the trace of the polarisation kernel is a quantity which has already been computed, for it was required by the Newton method, and so the spectral strength of the plasmon mode is readily accessible in momentum space. (Successive approximations to the spectral strength can be obtained by expanding the trace of the polarisation kernel as in Section II.2. The second order approximation for example is $\omega_2^3/[4\omega_2^2-2\omega_1^2]$).

To determine the spectral strength of a single particle mode, we use a scattering theory approach. Let us reserve the symbols s and p to label the single particle and plasmon modes respectively. The single particle matrix elements of the charge density operator satisfy the following equation

$$\omega_s \langle s|\rho(x,x')|0\rangle = (H_o(x')-H_o(x))\ \langle s|\rho(x,x')|0\rangle + \langle\rho(x,x')\rangle \int dy\ (v(x',y)-(v(x,y))\langle s|\rho(y,y)|0\rangle$$

To simplify notation, we introduce matrices ρ, h and v

$$\omega\rho = h\rho + v$$

Switching off the electron-electron interaction, $\rho \to \rho_o$ where

$$\omega\rho_o = h\rho_o$$

In writing this equation we have assumed that the single particle excitation spectrum is continuous. The matrix ρ can be expressed in terms of ρ_o in the standard way

$$\rho = \rho_o + (\omega 1 - h)^{-1} v$$

and by referring to the definition of the polarisation kernel (I.1.15), we deduce that

$$\langle s|\rho(x,x)|O\rangle = \langle s|\rho(x,x)|O\rangle_o + \int dy\, F(x,y;\omega_s)\langle s|\rho(y,y)|O\rangle_o$$

or equivalently

$$\langle s|a^+_{o,\uparrow}a_{o,\uparrow}|O\rangle = [1 + \mathrm{Tr}\, F(\kappa+G,\kappa+G';\omega_s)]\langle s|a^+_{o,\uparrow}a_{o,\uparrow}|O\rangle_{ni}$$

The subscript for the non-interacting system has been changed from 'o' to ni. The normalisation condition (I.1.39) establishes the link to the spectral strength of a single particle mode

$$|C_s|^2 = |\, 1 + \mathrm{Tr}F\,|^2\, |C_s|^2_{ni}$$

$$|C_s|^2_{ni} = 4N\Omega(\kappa)\; |\langle s|a^+_{o,\uparrow}a_{o,\uparrow}|O\rangle_{ni}|^2$$

There are three comments to make about this result. Firstly, the spectral strength of the single particle mode is of the order of 1/N, for:

$$\langle s(k,\kappa)|a^{+}_{o,\uparrow}a_{o,\uparrow}|O\rangle_{ni} = \frac{1}{N}\frac{1}{\sqrt{2}}n_k(1-n_{k+\kappa})$$

Secondly, because the spectral strength is related to the response function, it is better to compute this quantity in momentum space. Thirdly, to evaluate the response function we employ the plasmon pole approximation i.e. we sum over plasmon modes only

$$|C(k,\kappa)|^2 = \frac{4}{N}\Omega(\kappa)n_k(1-n_{k+\kappa})\left|1 + \frac{|C_p(\kappa)|^2}{[\varepsilon(k+\kappa)-\varepsilon(k)-\omega_p(\kappa)]} - \frac{|C_p(-\kappa)|^2}{[\varepsilon(k+\kappa)-\varepsilon(k)+\omega_p(-\kappa)]}\right|^2$$

To test the reliability of this expression we look to a sum rule. This is easily established from the following Kramers-Kronig relation

$$\lim_{\omega\to\infty} \mathrm{Re}\,\varepsilon^{-1}(\kappa;\omega) = 1 - (2/\omega^2\pi)\int_0^\infty d\omega'\ \mathrm{Im}\,\varepsilon^{-1}(\kappa;\omega') + O(1/\omega^4)$$

By expressing the real part of the inverse dielectric function in terms of the polarisation kernel, and the imaginary part in terms of the spectral resolution of the response function, we arrive at the sum rule

$$\sum_m \omega_m(\kappa)|C_m(\kappa)|^2 = (1/2)\ \omega_1^2$$

where m denotes mode type.

Consider the left hand side of the sum rule, and in particular look at the single particle contribution. The factor of unity in our expression for $|C(k,\kappa)|^2$ gives an overall contribution of $1/2\ \omega_1^2$, whilst the remaining terms cancel the plasmon contribution. The sum rule is therefore satisfied exactly over all the Brillouin zone.

Before going on to use our expressions for the spectral strengths to compute E_{xc} and E_{int}, we investigate the percentage plasmon contribution to the sum rule. On the following page we find a table displaying the spectral strength of the plasmon mode (abbreviated to C_p) and its absolute and percentage contribution to the sum rule (PE*CP and % respectively). We also display various successive approximations to these quantities. The table highlights the importance of an accurate determination of the plasmon energy, for %9 is in error by 34% near the electron hole continuum. A graphical study of the percentage plasmon contribution to the sum rule follows

% ≡ ordinate ; K(O→1 in units of π/a) ≡ abscissa

The plasmon contribution in the (100) direction is always over 70% (this is due to the plasmon mode being well defined everywhere along this direction). In the (110) and (111) directions, the plasmon mode is not well defined everywhere for certain choices of u / a, and the plasmon contribution falls accordingly. For the high density metals the tail off is quite rapid.

KAPPA = (K,K,0) U = -0.03 A = 1.5

K	C1 W1*C1 %1	C2 W2*C2 %2	C3 W3*C3 %3	C4 W4*C4 %4	C9 W9*C9 %9	IT	CP PE*CP %
0.21	0.19542 0.07638 100.00	0.19488 0.07638 100.00	0.19487 0.07638 100.00	0.19487 0.07638 100.00	0.19487 0.07638 100.00	0	0.19487 0.07638 100.00
0.42	0.17039 0.05806 100.00	0.16819 0.05811 100.07	0.16797 0.05806 99.99	0.16796 0.05805 99.98	0.16796 0.05805 99.98	0	0.16796 0.05805 99.98
0.63	0.13777 0.03796 100.00	0.13305 0.03820 100.63	0.13175 0.03796 100.01	0.13150 0.03791 99.86	0.13145 0.03790 99.83	0	0.13145 0.03790 99.83
0.84	0.10525 0.02216 100.00	0.09858 0.02237 103.23	0.09467 0.02237 100.95	0.09299 0.02207 99.61	0.09190 0.02185 98.61	1	0.09189 0.02185 98.60
1.05	0.07750 0.01201 100.00	0.07120 0.01336 111.18	0.06518 0.01290 107.43	0.06115 0.01237 102.96	0.05408 0.01117 92.96	2	0.05282 0.01092 90.93
1.26	0.05620 0.00632 100.00	0.05248 0.00809 127.99	0.04667 0.00801 126.81	0.04199 0.00760 120.23	0.03002 0.00587 92.84	6	0.01838 0.00369 58.48
1.47	SINGLE - PARTICLE MODES ONLY						
1.68	SINGLE - PARTICLE MODES ONLY						
1.88	SINGLE - PARTICLE MODES ONLY						
2.09	SINGLE - PARTICLE MODES ONLY						

KAPPA = (K,0,0)

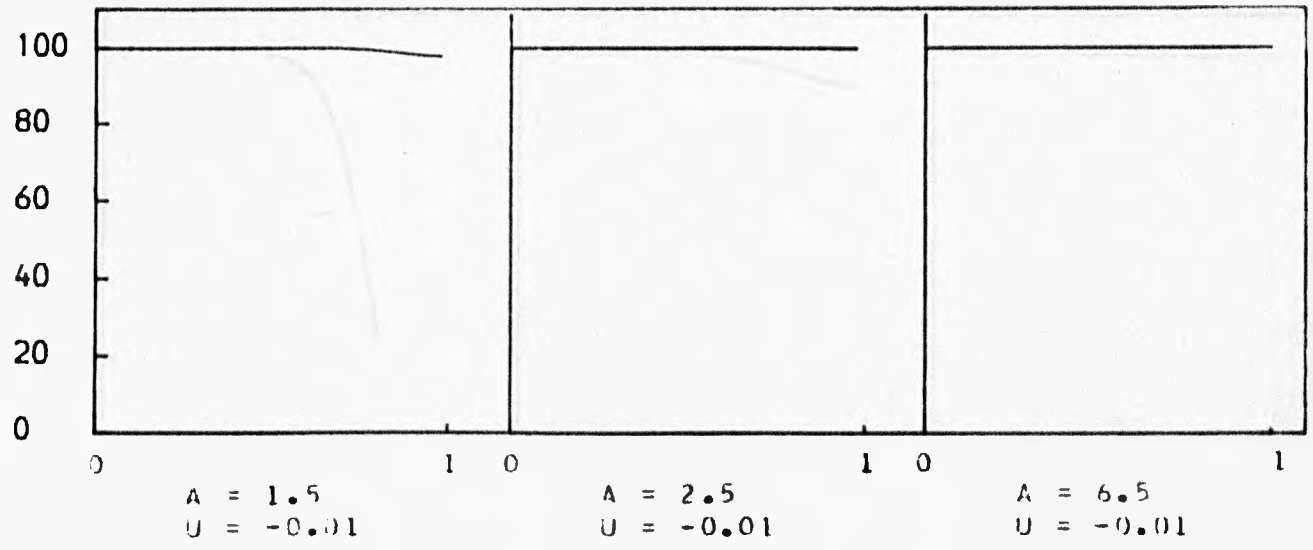

A = 1.5
U = -0.01

A = 2.5
U = -0.01

A = 6.5
U = -0.01

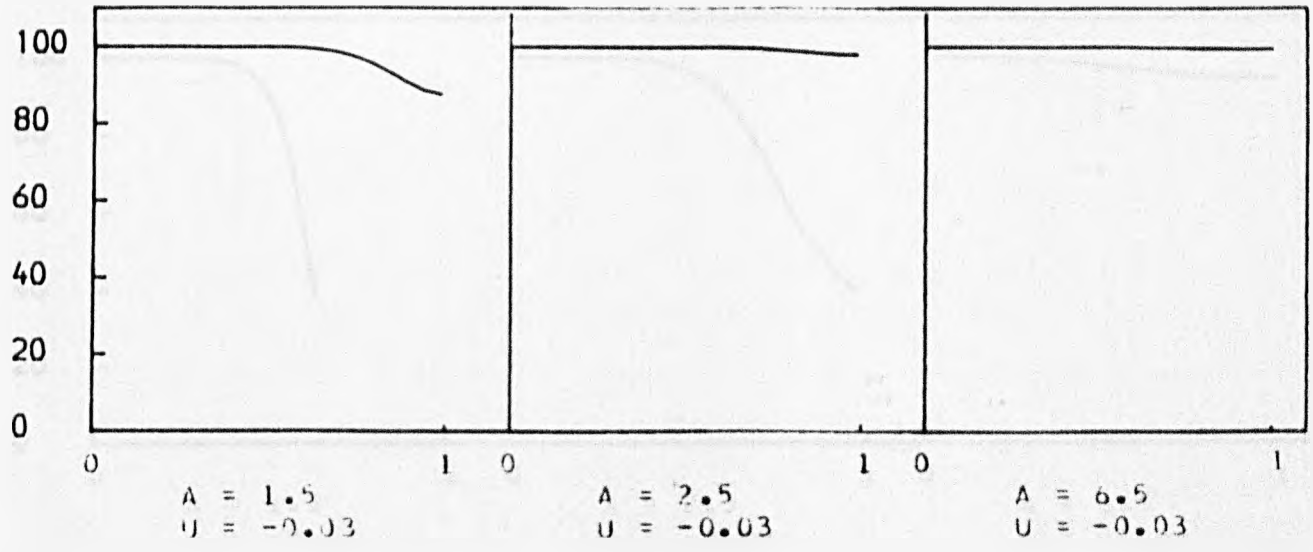

A = 1.5
U = -0.03

A = 2.5
U = -0.03

A = 6.5
U = -0.03

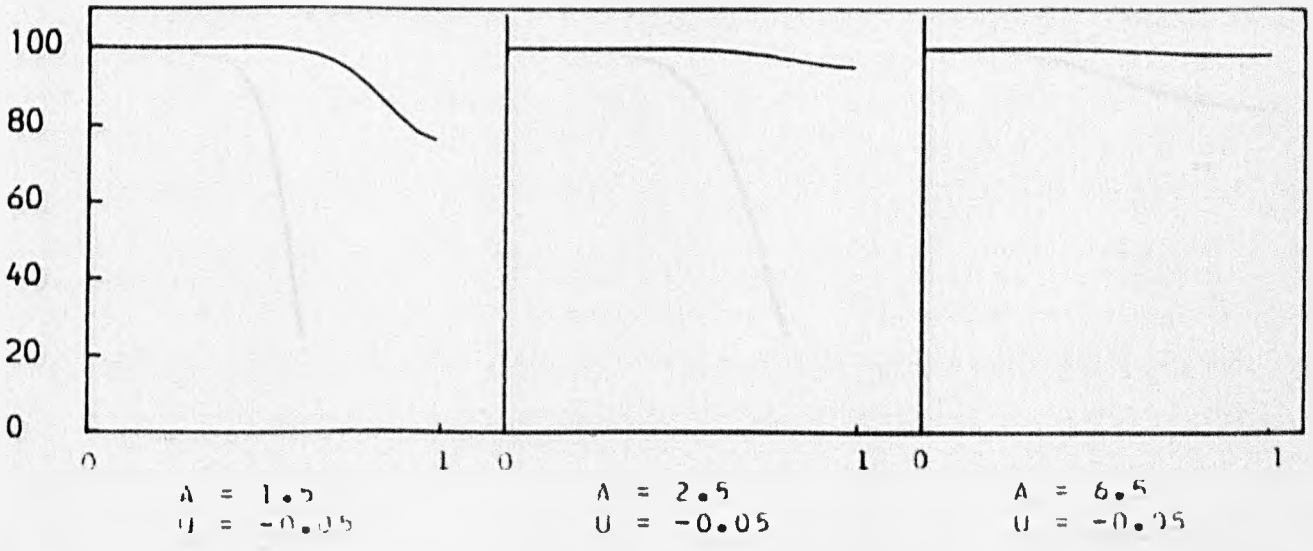

A = 1.5
U = -0.05

A = 2.5
U = -0.05

A = 6.5
U = -0.05

KAPPA = (K,K,0)

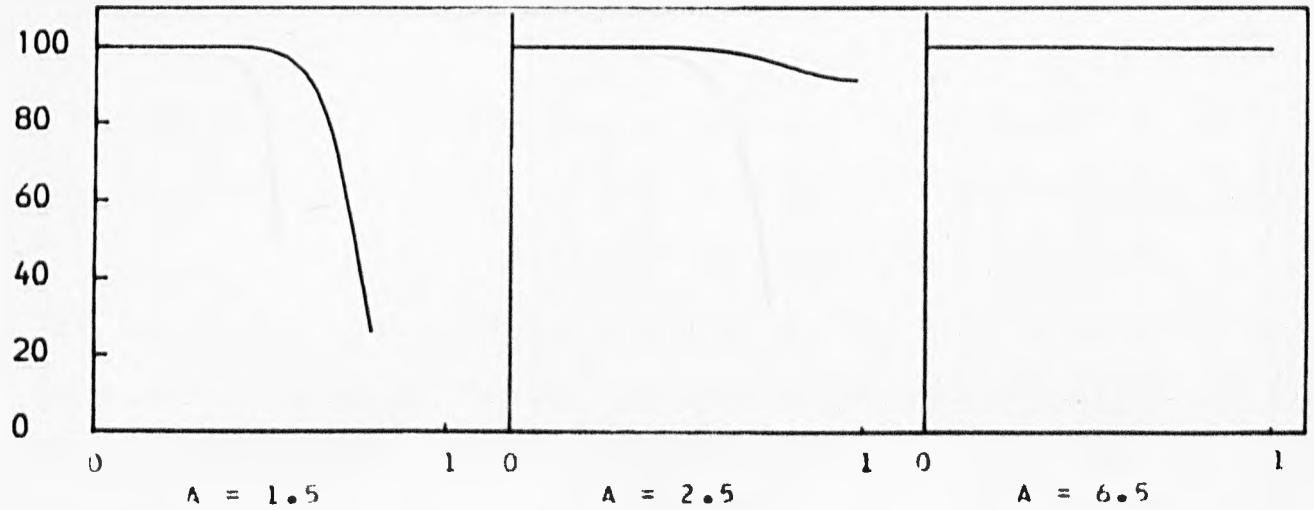

A = 1.5 U = -0.01 | A = 2.5 U = -0.01 | A = 6.5 U = -0.01

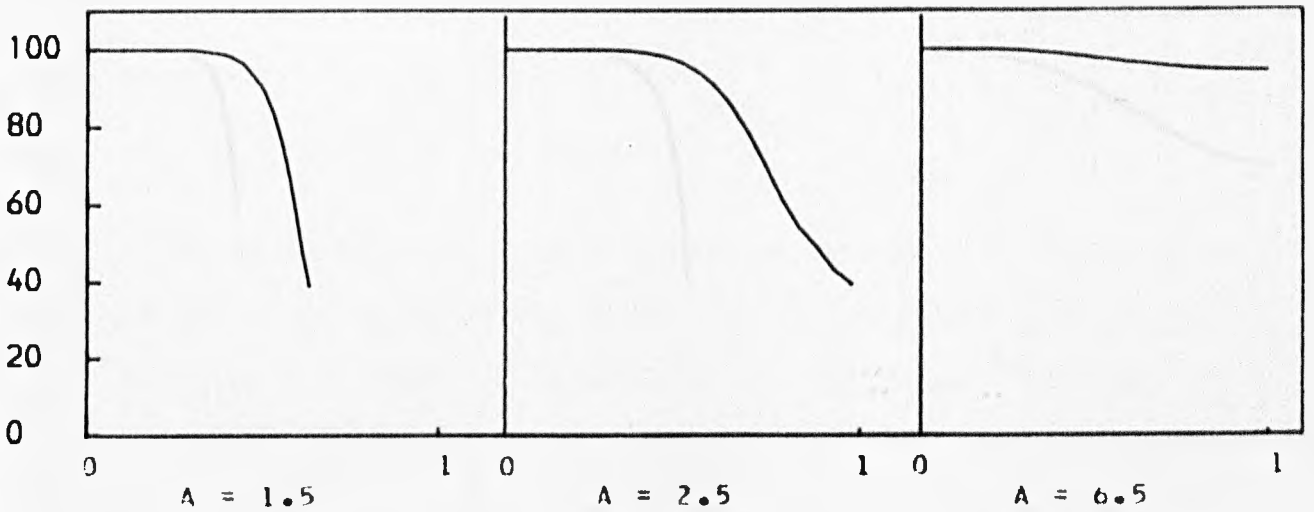

A = 1.5 U = -0.03 | A = 2.5 U = -0.03 | A = 6.5 U = -0.03

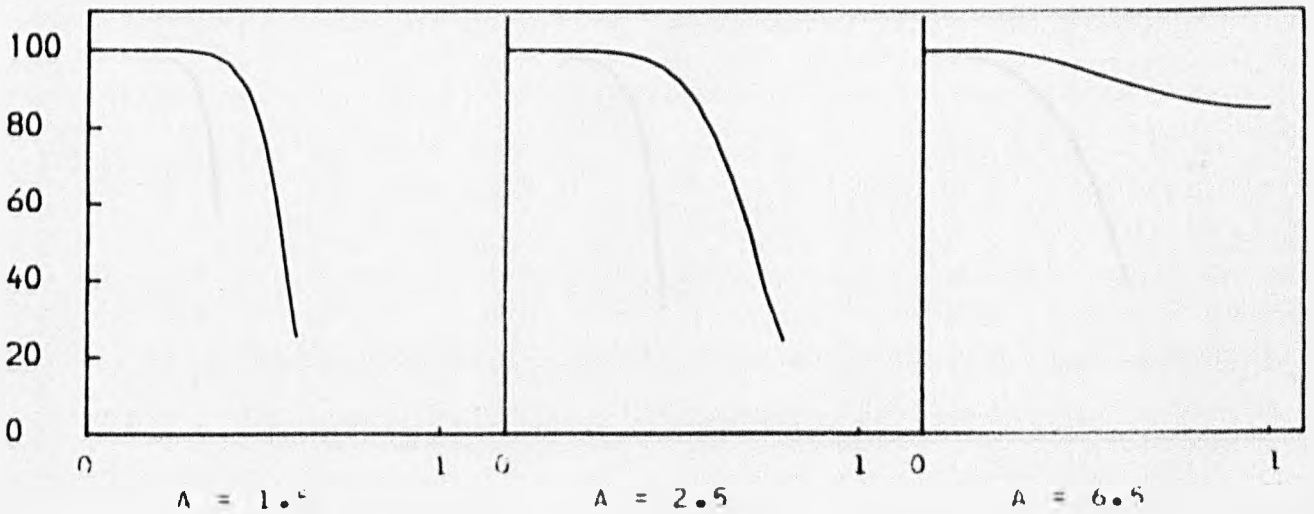

A = 1.5 U = -0.05 | A = 2.5 U = -0.05 | A = 6.5 U = -0.05

KAPPA = (K,K,K)

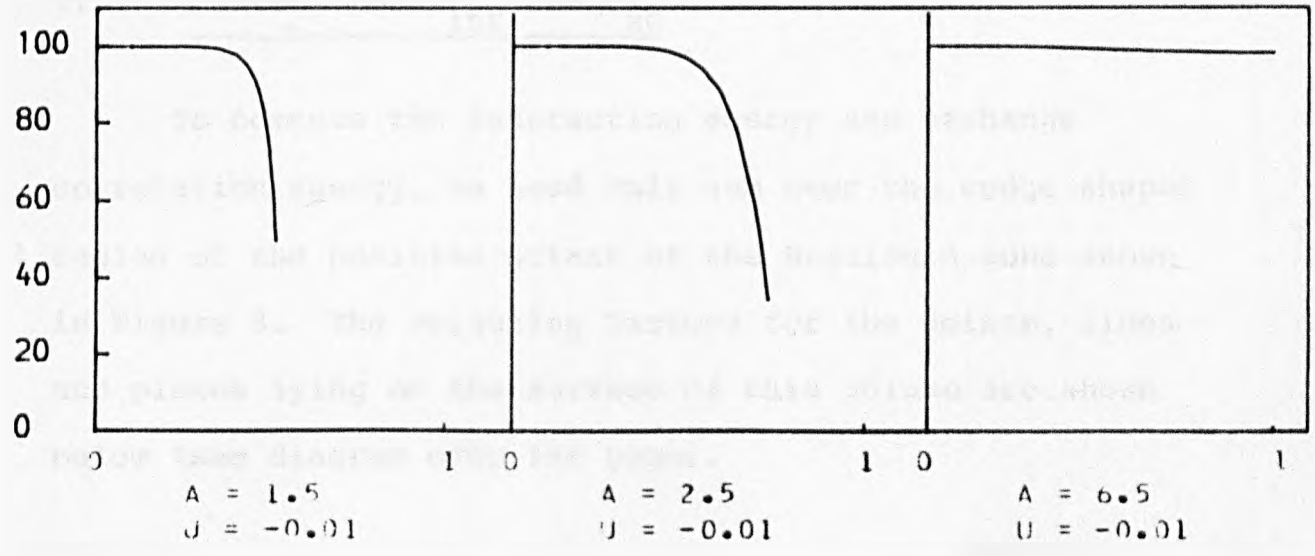

A = 1.5 U = -0.01 | A = 2.5 U = -0.01 | A = 6.5 U = -0.01

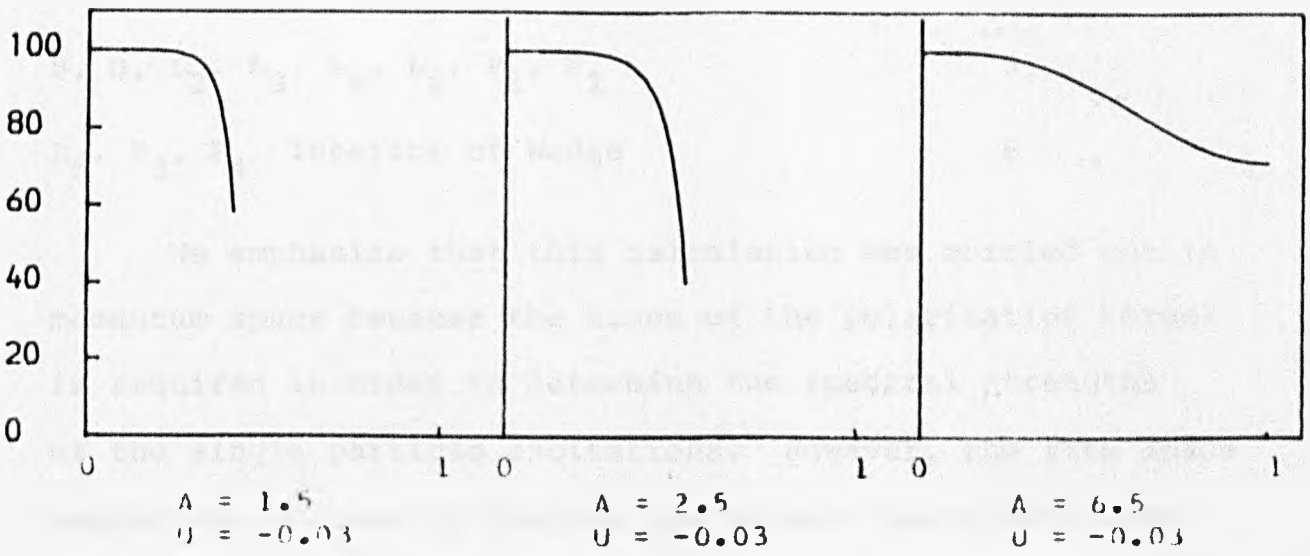

A = 1.5 U = -0.03 | A = 2.5 U = -0.03 | A = 6.5 U = -0.03

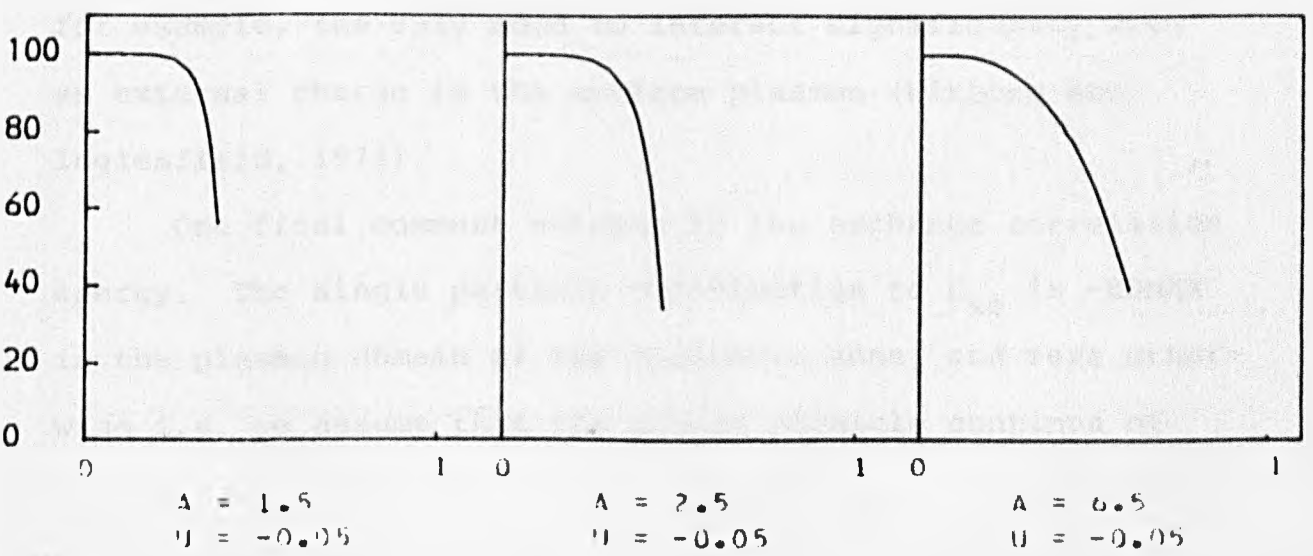

A = 1.5 U = -0.05 | A = 2.5 U = -0.05 | A = 6.5 U = -0.05

II.4 Results for E_{int} and E_{xc}

To compute the interaction energy and exchange correlation energy, we need only sum over the wedge shaped region of the positive octant of the Brillouin zone shown in Figure 3. The weighting factors for the points, lines and planes lying on the surface of this volume are shown below (see diagram over the page).

	Weight
A, C, L_1	1
B, D, L_2, L_3, L_4, L_6, P_1, P_2	3
L_5, P_3, P_4 Interior of Wedge	6

We emphasise that this calculation was carried out in momentum space because the trace of the polarisation kernel is required in order to determine the spectral strengths of the single particle excitations. However, the site space method can be used to compute the plasmon contribution to such modal sums, which is important since at metal surfaces for example, the only mode to interact significantly with an external charge is the surface plasmon (Wikborg and Inglesfield, 1974).

One final comment relates to the exchange correlation energy. The single particle contribution to E_{xc} is -EDMAX in the plasmon domain of the Brillouin zone, and zero otherwise i.e. we assume that the single particle continua of

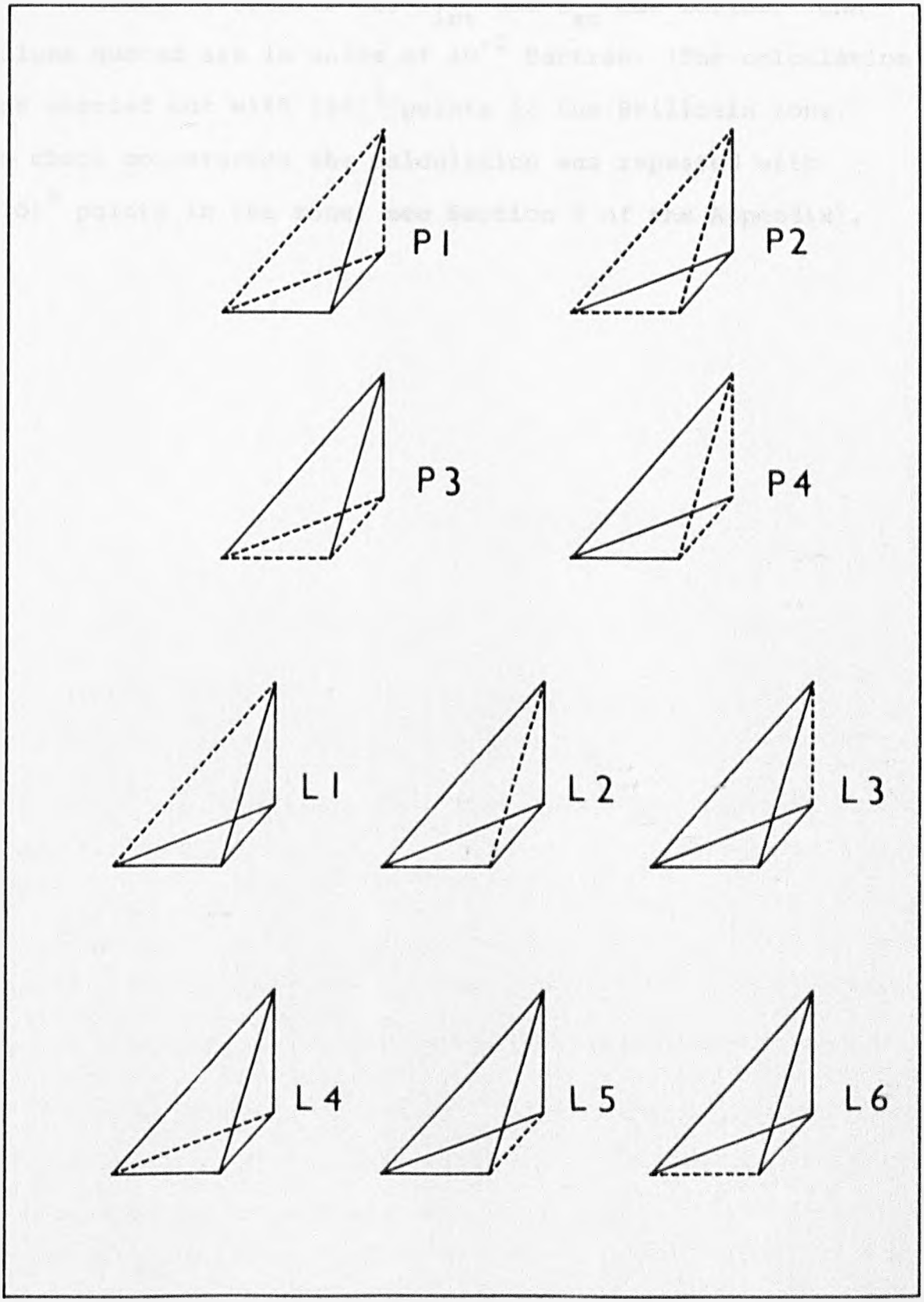
P1
P2
P3
P4
L1
L2
L3
L4
L5
L6

the interacting and non-interacting systems overlap.

Tables of results for E_{int} and E_{xc} now follow. The values quoted are in units of 10^{-2} Hartree. (The calculation was carried out with $(18)^3$ points in the Brillouin zone. To check convergence the calculation was repeated with $(30)^3$ points in the zone; see Section 2 of the Appendix).

INTERACTION ENERGIES (EINT).

	A = 1.5	A = 2.5	A = 6.5
U = -0.01	1.437	2.435	3.276
U = -0.03	2.164	4.148	5.588
U = -0.05	2.543	4.947	8.010

PLASMON CONTRIBUTION TO EINT.

	A = 1.5	A = 2.5	A = 6.5
U = -0.01	0.951 (66.2%)	1.949 (80.0%)	3.179 (97.0%)
U = -0.03	1.166 (53.9%)	2.045 (49.3%)	4.498 (80.5%)
U = -0.05	1.253 (49.3%)	1.944 (39.3%)	3.874 (48.4%)

SINGLE PARTICLE CONTRIBUTIONS TO EINT.

	A = 1.5	A = 2.5	A = 6.5
U = -0.01	0.486	0.487	0.097
U = -0.03	0.998	2.102	1.090
U = -0.05	1.291	3.004	4.137

EXCHANGE CORRELATION ENERGIES (EXC).

	A = 1.5	A = 2.5	A = 6.5
U = -0.01	1.130	1.962	3.534
U = -0.03	1.276	1.797	3.042
U = -0.05	1.320	1.647	2.142

PLASMON CONTRIBUTION TO EXC.

	A = 1.5	A = 2.5	A = 6.5
U = -0.01	2.727 (1.71X)	5.365 (1.58X)	7.272 (1.94X)
U = -0.03	3.797 (1.51X)	7.150 (1.34X)	14.256 (1.27X)
U = -0.05	4.363 (1.43X)	7.877 (1.26X)	17.519 (1.14X)

SINGLE PARTICLE CONTRIBUTIONS TO EXC.

	A = 1.5	A = 2.5	A = 6.5
U = -0.01	-1.597	-3.403	-3.738
U = -0.03	-2.521	-5.353	-11.214
U = -0.05	-3.043	-6.229	-15.377

The most interesting feature about the results for E_{int} and E_{xc} is that the single particle contribution to these sums is always significant (there is one exception to this: for u / a = -0.01 / 6.5 the plasmon contribution to E_{int} is 97%. The plasmon mode is well-defined over all the Brillouin zone for this choice of parameters, but note that this result corresponds to a low density metal and the RPA is strictly valid for $r_s < 1$).

The plasmon contribution to E_{int} and E_{xc} falls as u is increased for a given value of a, reflecting that EDMAX is directly proportional to u. Even so, it is surprising that for u / a = -0.05 / 6.5 the single particle contribution to E_{int} is about 50%.

CHAPTER III

A MODEL INSULATOR - CHARGE TRANSFER STATES AND EXCITONS

III.1 Opening Remarks

Two types of elementary excitation to be found in semi-conductors and insulators are charge transfer states and excitons. An exciton is a stationary state of the many electron system in which a single electron hole pair travels through the crystal lattice. The degree of separation of the electron and hole characterises the internal structure of the exciton. A Frenkel exciton consists of an electron hole pair excitation hopping from atom to atom, the mechanism for the transfer of energy being dipolar interaction. In contrast to this, a Mott-Wannier exciton corresponds to a conduction band electron and a valence band hole moving through the crystal with considerable separation.

The theory of exciton structure has developed along two distinct lines; for in the Frenkel exciton the electron sees both the hole and details of the lattice potential, whereas in the Wannier exciton the electron moves around the hole in an average lattice potential (Knox, 1963). It is therefore standard to describe a Frenkel exciton by retaining only dipolar terms in the Hamiltonian i.e. terms of the form

$$V_{\ell\ell',\ell'\ell}\ (a^{+}_{\ell 1}a_{\ell 2})^{+}\ (a^{+}_{\ell' 1\ell' 2})$$

and thence to perform a multipolar expansion of the Coulomb interaction (by hypothesis, the wavefunctions of electrons on neighbouring atoms do not overlap significantly)

$$V_{\ell\ell',\ell'\ell} \simeq x_i^* x_j T_{ij}(\ell-\ell')$$

where x_i is the ith component of the dipole moment matrix of the levels 1 and 2, and (T_{ij}) is the dipole tensor (we adopt Einstein summation convention for repeated indices Anderson, 1963). The Bogolyubov transformation then diagonalises the Hamiltonian

$$\omega_\kappa^2 = E_{gap}^2 + 2E_{gap} x_i x_j t_{ij}(\kappa)$$

$$\Psi_\kappa = \frac{1}{\sqrt{N}} \sum_\ell e^{i\kappa.\ell}(b_\ell^+|O\rangle) \qquad b_\ell = a_{\ell 1}^+ a_{\ell 2}$$

t_{ik} is the Fourier lattice transform of the dipole tensor and $b_\ell^+|O\rangle$ is a many electron state describing a lattice in which there is an electron hole pair excitation at site ℓ. By taking linear combinations of such states (so as to satisfy translational invariance) we arrive at a stationary state of the system: Ψ_κ. Frenkel called these running waves of excitation 'excitons'.

The large radius exciton is treated quite differently. The excited electron and hole unit is regarded as a two particle system in which the electron and hole have effective masses (m_e^*, m_h^*) and interact via a modified Coulomb potential due to the remaining valence electrons and ion cores

$$(-\nabla^2/2m_e^* - \nabla^2/2m_h^* - e^2/\varepsilon r_{eh})\Psi = \omega\Psi$$

The solutions of this equation, Wannier excitons, are modified hydrogenic functions.

Theoretically, it is unsatisfactory to view the same elementary excitations from two such differing standpoints; indeed, as Knox has pointed out, the alkali halides cannot be described accurately by either the Frenkel or Wannier models. The Frenkel model is invalid since a bound state of the negative halide ion does not exist. The Wannier model is also inappropriate because the effective Bohr radius of the exciton in alkali halides is relatively small (for ϵ is small) and so Bloch functions going with large κ are required to construct the exciton (the Wannier model assumes that κ is small). It is therefore essential to establish a workable unified theory of elementary excitations in semi-conductors and insulators so as to be able to describe excitons of intermediate radius. The difficulty with a dielectric theory approach is that exchange interactions are not easily accommodated (Hubbard, 1957; Hanke, 1978).

In this chapter, we demonstrate that by solving the RPAE equations in site space, both Frenkel and Wannier excitons can be obtained from the same set of equations in a straightforward manner. Furthermore, by looking at limiting cases we recover the results of the canonical transformation technique of the Frenkel model, and the effective mass theory of the Wannier model. Egri went some way towards this unified approach in 1979, but his model was one dimensional and he started with a simplified Hamiltonian from the outset so as to effect a diagonalisation.

Consider a model insulator in which each atom has an occupied 1s orbital and unoccupied $2p_z$ orbital. We take the lattice to be simple cubic, and employ the tight binding approximation. Since the valence band is full and the conduction band is empty, then

$$n_{k,b} = \delta_{b,1} \qquad \text{for all } k$$

b is a band index; b is 1 for the s band and 2 for p band. The electron hole amplitudes for this many electron system satisfy the following set of coupled linear equations

$$(\omega+\varepsilon_{gap})X_\ell = u\sum_{\ell'} [1+e^{-i\kappa.(\ell-\ell')}]\gamma_{\ell,\ell'}X_{\ell'}-PX_\ell-QY_\ell$$

$$(\omega-\varepsilon_{gap})Y_\ell = -u\sum_{\ell'} [1+e^{-i\kappa.(\ell-\ell')}]\gamma_{\ell,\ell'}Y_{\ell'}+PY_\ell+QX_\ell$$

where $X_\ell = \langle M|a^+_{\ell 1}a_{o2}|O\rangle$ $\qquad$ $Y_\ell = \langle M|a^+_{\ell 2}a_{o1}|O\rangle$

In writing this equation we have made the simplifying, though unnecessary, assumption that the hopping parameter for the overlap of valence orbitals on neighbouring atoms (s-s) is equal to that for the overlap of conduction electron orbitals (pσ-pσ, pπ-pπ; s-p mixing has been ignored). We stress that although the tight binding approximation does not provide a good description of most semi-conductor valence bands, the solid rare gases are in fact relatively tight binding in the ground state.

We have taken $|M\rangle$ to be a singlet state and defined ε_{gap} as the difference in the atomic energy levels $\varepsilon_2-\varepsilon_1$,

corrected by Hartree Fock terms. P and Q are many electron coefficients

$$P = 2\delta_{\ell,o} N \sum_{G} v(\kappa+G)|F_{12}(\kappa+G)|^2 - \sum_{k} v_k F_{11}(-k)F_{22}(k)e^{ik.\ell} \qquad 1.1$$

(direct) (exchange)

$$Q = 2\delta_{\ell,o} \sum_{G} v(\kappa+G)|F_{12}(\kappa+G)|^2 - \sum_{k} v_k |F_{12}(k)|^2 e^{ik.\ell}$$

(direct) (exchange)

F_{12} is the Fourier transform of the orbital density $\chi_1^* \chi_2$, likewise F_{11} and F_{22}. The derivation of the key system of equations for the insulator model follows the same route as that for the tightly bound metal of Chapter II, and since this was discussed in some detail we do not look at the associated mathematics here (the full derivation appears in a paper by the author and J.E. Inglesfield, 1981). In this chapter we concern ourselves solely with the physical aspects of the model.

III.2. The Extreme Tight Binding Approximation

Let us assume that the atoms in the model insulator are sufficiently far apart, that we may neglect the hopping integral (u) in the RPAE equations. This is the so-called extreme tight binding approximation. The object of this section is to investigate the nature of the elementary excitations in such a model. Setting the hopping integral to zero, the RPAE equations for the electron hole amplitudes become

$$(\omega+\varepsilon_{gap}+P)X_{\ell} = -QY_{\ell}$$

$$(\omega-\varepsilon_{gap}-P)Y_{\ell} = QY_{\ell}$$

The dispersion relation of the elementary excitations in the extreme tight binding insulator is therefore

$$\omega^2(\kappa,\ell) = \varepsilon_{gap}^2 + 2\varepsilon_{gap}P + P^2 - Q^2$$

where P and Q are of the form

$$P = 2\delta_{\ell,o}\,\Omega_{12}(\kappa) - E_a(\ell)$$

$$Q = 2\delta_{\ell,o}\,\Omega_{12}(\kappa) - E_b(\ell)$$

We see that there are two types of many electron excitation present; one type depending on wave vector alone, and the other type depending on the direct lattice vector ℓ. Consider first the dispersive modes; take ℓ to be the zero vector, so that the electron and hole are confined to the

same atom. Under such circumstances we anticipate that the elementary excitation under consideration is the Frenkel exciton. This is indeed the case, for if we set the exchange terms equal to zero the dispersion relation becomes

$$\omega^2(\kappa) = \varepsilon_{gap}^2 + 2\varepsilon_{gap}\{2\Omega_{12}(\kappa)\}$$

which is the Anderson formula for the Frenkel exciton ($2\Omega_{12} \equiv x_i^* x_j t_{ij}$). We reinstate the exchange terms into the dispersion relation and comment that they are readily evaluated by integrating over the appropriate Fourier transforms

$$\left.\begin{aligned} \chi_{1s} &= (\alpha^{3/2}/\sqrt{\pi})\exp(-\alpha r) \\ \chi_{2p} &= (\beta^{5/2}/\sqrt{\pi})r_3\exp(-\beta r) \end{aligned}\right\} \begin{aligned} F_{11}(k/a_o) &= 16z^4/[4z^2+k^2]^2 \\ F_{12}(k/a_o) &= i384\sqrt{2}z^5k_3/[9z^2+4k^2]^3 \\ F_{22}(k/a_o) &= [z^8+z^6(k^2-6k_3^2)]/[z^2+k^2]^4 \end{aligned}$$

$$\alpha = z/a_o \qquad \beta = z/2a_o$$

$$\underline{E_a(0) = 59/243\ z} \qquad \underline{E_b(0) = 7(2/9)^4 z}$$

Setting the value of the gap energy to unity (measured in Hartree) and taking the G = 0 term only, in the sum over reciprocal lattice vectors Ω_{12} (a very good approximation in the 001 direction), the final result for the energy of the Frenkel exciton is

$$\omega^2(\kappa) = 1 - 0.486z + 0.059z^2 + (a_o/a)^3 \pi z^{10} \frac{1152(1-0.226z)\,\kappa_3^2}{[2.25z^2+a_o^2\kappa^2]^6\kappa^2}$$

A plot of this function is to be found in the paper by the author and J.E. Inglesfield (see Section 3 of Appendix). Notice that the effective nuclear charge is an important quantity in determining the exciton energy e.g. $\omega(0)$ for z = 2 is approximately half the value of $\omega(0)$ for z = 1 (with $a = 4a_o$). To understand why this is so, we recall that the mechanism for the transfer of energy associated with the Frenkel exciton is dipolar interaction; the electron and hole always sitting on the same atom. The 'local' situation is therefore important. Now z defines the local situation in that it is an expansion parameter characterising the atomic orbitals and in consequence the magnitude of the atomic dipole moment. In fact, $(x_{sp})_3$ is inversely proportional to z. Thus, for small values of z, we have a correspondingly large dipole moment and hence a large potential energy of interaction and so it costs less energy to excite a Frenkel exciton with z = 2 than with z = 1.

In addition to the Frenkel exciton, it is possible to excite charge transfer states in the model insulator. These are dispersionless modes corresponding to non-zero values of ℓ in the expressions for the many electron coefficients P and Q

$$\omega_{\ell}^2 = [\ 1+E_a(\ell)\ ]^2 - E_b^2(\ell) \quad ; \quad \varepsilon_{gap} = 1H$$

We see that the frequency of a charge transfer state is determined by the exchange terms in the equation of motion of a^+a

$$E_a(\ell) = \int d^3r \int d^3r' \frac{\chi_1^*(r)\chi_1(r)\chi_2^*(r')\chi_2(r')}{|\ r+\ell-r'\ |}$$

$$E_b(\ell) = \int d^3r \int d^3r' \frac{\chi_1^*(r)\chi_2(r)\chi_1^*(r')\chi_2(r')}{|\ r+\ell-r'\ |}$$

The standard method of evaluating two centre Coulomb integrals is to expand the Coulomb potential as a Taylor series and integrate successive terms. In the case of $E_b(\ell)$ only one term survives; the quadrupole term, so that $E_b(\ell)$ represents the mutual potential energy of two interacting dipoles (Heller and Marcus, 1951)

$$E_b(\ell) = \frac{2^{15}}{3^{10}} \frac{1}{z^2} \left(\frac{a_o}{\ell}\right)^3 \left(1-3\cos^2\theta_{\ell} \right) \qquad 2.1$$

We can establish this result directly from dipole theory with a potential of the form

$$\phi(r) = \frac{\sqrt{(\alpha^3\beta^5)}^{1/2}}{\pi} \int d^3r' \frac{z' e^{-(\alpha+\beta)r'}}{|r-r'|}$$

An alternative approach is to Fourier transform the Coulomb potential to obtain $E_b(\ell)$. On performing the momentum space integration we recover the right hand side of (2.1) plus extra terms involving $\exp(-3z\ell/2a_o)$ and powers of ℓ. The Fourier transform method gives the precise value of the two centre Coulomb integral; whereas the multipolar expansion technique fails to pick up higher order terms because it rests on the assumption that

$$|\ell| >> |r-r'-\ell|$$

However, within the context of the model (2.1) is sufficient. A similar discussion holds for $E_a(\ell)$, we find that

$$E_a(\ell) = \frac{a_o}{\ell} - \frac{6}{z^2}\left(\frac{a_o}{\ell}\right)^3 (1-3\cos^2\theta_\ell)$$

Thus $E_a(\ell)$ is the dominant term and corresponds to the potential energy of interaction of an s type dipole at the origin, and a p type dipole at site ℓ

$$E_a(\ell) = (x_{ss})_i^* (x_{pp})_j T_{ij}(\ell)$$

Since the dipoles cannot de-excite, the electron hole unit cannot hop from atom to atom. The modes are therefore dispersionless.

If the $2p_x$ and $2p_y$ orbitals are included in the model, the frequencies ω_ℓ are obtained from a 6 x 6 determinant.

By writing down the dipole tensor with respect to principal axes (two axes parallel to ℓ; one perpendicular to ℓ) the determinant becomes tri-diagonal, and factorises into transverse and longitudinal modes.

The charge transfer states are important, for they are an extreme form of Wannier exciton, and it is Wannier excitons that we go on to consider in the next section.

III.3 One Electron Hopping and Wannier Excitons

Let us return to the 2N x 2N system of couplied linear equations (1.1) which take into account one electron hopping. It is possible to decouple the equations to obtain only the positive frequency solutions (for if ω is an eigenvalue, then so is $-\omega$) by defining new variables $X' = X+Y$ and $Y' = X-Y$. The eigenvalue problem then separates into two systems of equations, each of order N x N. This transformation is of interest computationally, but is unnecessary for the analytical work of this section. With one electron hopping included, there exists a continuum of single particle excitations (whereas only one electron transitions of frequency equal to ε_{gap} are possible in the extreme tight binding limit). In the absence of the electron electron interaction, we find that $Y_\ell \propto \exp(ik.\ell)$ provided

$$\omega(k,\kappa) = \varepsilon_{gap} - 2u[\ \cos k_x a + \cos(k_x+\kappa_x)a \quad \text{et cyclic}\ ]$$

At $\kappa = 0$, the continuum limits are therefore

$$(\varepsilon_{gap} + 12u) \quad \text{and} \quad (\varepsilon_{gap} - 12u)$$

We now look for modes below the frequency of the continuum edge by taking ℓ to be non-zero and ignoring the many electron coefficient $E_b(\ell)$

$$E_a(\ell) \sim 1/\ell \qquad E_b(\ell) \sim 1/\ell^3$$

The two equations for X and Y decouple, and it is sufficient to consider the equation for Y

$$(\omega-\varepsilon_{gap})Y_{\ell} = -u\sum_{\ell'} [1+e^{-i\kappa.(\ell-\ell')}]\delta_{\ell,\ell'}Y_{\ell'} + PY_{\ell}$$

If we regard the components of ℓ as continuous variables, then to first approximation we have

$$Y_{(\ell_x+a,\ell_y,\ell_z)} + Y_{(\ell_x-a,\ell_y,\ell_z)} = (2+a^2\partial^2/\partial\ell_x^2)\, Y_{\ell}$$

$$Y_{(\ell_x+a,\ell_y,\ell_z)} - Y_{(\ell_x-a,\ell_y,\ell_z)} = 2a\partial/\partial\ell_x$$

Likewise for the components ℓ_y,ℓ_z. The eigenvalue equation for Y in the vicinity of small $|\kappa|$ becomes

$$2ua^2\,(u\nabla^2+i\kappa.\nabla)Y_{\ell} - (a_o/\ell)Y_{\ell} = (\omega-\varepsilon_{gap}-12u)Y_{\ell}$$

The $\kappa.\nabla$ term is removed by writing

$$\psi_{\ell} = \exp(-i\kappa.\ell/2)Y_{\ell}$$

$$2ua^2\nabla^2\psi_{\ell} - (a_o/\ell)\psi_{\ell} = (\omega-\varepsilon_{gap}-12u-\tfrac{1}{2}ua^2\kappa^2)\psi_{\ell}$$

and so we deduce that

$$\omega_{\kappa} = \varepsilon_{gap} + 12u - \tfrac{1}{2}ua^2\kappa^2 + (a_o^2/8ua^2n^2)$$

where n is a natural number. This is the Rydberg-Wannier series. Clearly, the n = 1 (or s type) Wannier exciton is not expected to be described correctly by this result since

the $\ell = 0$ contribution will be important and this has been neglected. However, the energies of the $2p_z$ and 3d Wannier excitons are in good agreement with the full computer calculation.

Notice that by setting the hopping integral to zero in the equation for ψ_ℓ, we recover the charge transfer states to first approximation. As Inglesfield has pointed out (Rogan and Inglesfield, 1981) the Frenkel exciton is a resonance lying within the single particle continuum, and coexists with the Wannier exciton spectrum at each wave vector. To our knowledge this is a new conclusion. We found no evidence for the existence of a plasmon mode in this model.

CONCLUSION

The basic many electron problem associated with an inhomogeneous electron gas is how best to determine the excitation spectrum in light of the nature of the inhomogeneity under consideration. The many electron problem is not a formalistic problem, it is one of technique. We have demonstrated in this thesis that by solving the RPAE equations in site space, the excitation spectrum and one electron transition matrix elements of a tightly bound metal (or insulator) are obtained from a simple eigenvalue problem. The method is therefore computationally convenient; lending itself to black box subroutines, or the power method. Also, since one electron and many electron terms are treated on the same footing, the pole structure present in dielectric theory is missing, making the site space approach mathematically attractive. In addition, there is much physical insight to be gained from using the site space approach, because exchange interactions are readily accommodated. In consequence, plasmons, excitons and charge transfer states are obtained from the same key equation (in a straightforward manner).

We temper our enthusiasm for the site space approach with the realisation that it is inappropriate for the determination of the spectral strength of a single particle mode. Such modes are extended solutions of the RPAE equations. With this reservation, we highly recommend the site space approach for future research into many electron theory.

APPENDIX

SECTION 1

References

1. Anderson, P.W. Concepts in Solids (New York; Benjamin)(1963).
2. Baldereschi, A., Phys. Rev., B17, 4710 (1978).
3. Bohm, D. and Pines, D., Phys. Rev., 92, 609 (1953).
4. Brown, G.E. Many Body Problems (Amsterdam; North-Holland) (1972).
5. Egri, I.,JPhys. C: Solid State Phys., 12, 1843 (1979).
6. Egri, I., Matz, R., Luth, H. and Stahl, A., Surface Sci., 128, 51 (1983).
7. Ehrenreich, H. and Cohen, M., Phys. Rev., 115, 786 (1959).

7a Feibelman, P.J., Duke C.B. and Bagchi, A., Phys. Rev., B5, 2436 (1972).

8. Fetter, A.L. and Walecka, J.D. Quantum Theory of Many-Particle Systems (New York; McGraw-Hill)(1971).
9. Gell-Mann, M. and Brueckner, K., Phys. Rev., 106, 364 (1957).
10. Grimley, T.B., Proc. Phys. Soc., 72, 103 (1958).
11. Hanke, W., Adv. Phys., 27, 287 (1978).
12. Harris, J. and Griffin, A., Phys. Rev., B11, 3669 (1975).
13. Hedin, L. and Lundqvist, S., Solid State Phys., 23, 1 (1969).
14. Heller,R. and Marcus, A ., Phys. Rev., 84, 809 (1951).
15. Hubbard, J., Proc. Roy. Soc. A 240, 539 (1957).
16. Inglesfield, J.E. and Wikborg, E., Solid State Commun., 14, 661 (1974).
17. Knox, R.S., Theory of Excitons (Solid State Physics. Suppl. 5), (New York; Academic Press)(1963).
18. Kubo, R., J. Phys. Soc. Japan, 12, 570 (1957).

19. Kunz, C. Phys. Lett., 15, 312 (1965).

20. Oddershede, J., Adv. Quantum Chemistry, 11, 275 (1978).

21. Pines, D. Elementary Excitations in Solids, (New York; Benjamin)(1963).

22. Rogan, J. and Inglesfield, J.E., J. Phys. C., 14, 3585 (1981).

23. Sawada, K., Phys. Rev., 106, 372 (1957).

24. Sawada, K., Brueckner, K., Fukada, N. and Brout, R., Phys. Rev., 108, 507 (1957).

25. Schmidt, J. and Lucas, A.A., Solid State Commun., 11, 415 (1972).

26. Seitz, F. The Modern Theory of Solids (New York; McGraw-Hill)(1940).

27. Thouless, D.J., The Quantum Mechanics of Many-Body Systems (New York; Academic Press)(1961).

28. Wentzel, G., Helv. Phys. Acta, 15, 111 (1942).

29. Wikborg, E. and Inglesfield, J.E., Phys. Scr., 15, 37 (1977).

SECTION 2

INTERACTION ENERGIES (EINT).

	A = 1.5	A = 2.5	A = 6.5
U = -0.01	1.452		3.278
U = -0.03		4.157	
U = -0.05	2.552		8.034

PLASMON CONTRIBUTION TO EINT.

	A = 1.5	A = 2.5	A = 6.5
U = -0.01	0.945 (65.1%)		3.181 (97.0%)
U = -0.03		2.045 (49.2%)	
U = -0.05	1.218 (47.7%)		3.848 (47.9%)

SINGLE PARTICLE CONTRIBUTIONS TO EINT.

	A = 1.5	A = 2.5	A = 6.5
U = -0.01	0.508		0.098
U = -0.03		2.111	
U = -0.05	1.333		4.186

EXCHANGE CORRELATION ENERGIES (EXC).

	A = 1.5	A = 2.5	A = 6.5
U = -0.01	1.096		3.516
U = -0.03		1.742	
U = -0.05	1.250		2.056

PLASMON CONTRIBUTION TO EXC.

	A = 1.5	A = 2.5	A = 6.5
U = -0.01	2.702 (1.68X)		7.279 (1.94X)
U = -0.03		7.335 (1.31X)	
U = -0.05	4.175 (1.43X)		17.433 (1.13X)

SINGLE PARTICLE CONTRIBUTIONS TO EXC.

	A = 1.5	A = 2.5	A = 6.5
U = -0.01	-1.607		-3.761
U = -0.03		-5.593	
U = -0.05	-2.925		-15.377

SECTION 3

J. Phys. C: Solid State Phys., 14 (1981) 3585–3602. Printed in Great Britain

Electronic excitations in tight-binding systems

J Rogan† and J E Inglesfield‡

† Donnan Laboratories, University of Liverpool, PO Box 147, Liverpool L69 3BX, UK

‡ Science Research Council, Daresbury Laboratory, Daresbury, Warrington WA4 4AD, UK

Received 9 March 1981

Abstract. The excitation energies in the random phase approximation with exchange can be found from the linearised equations of motion of electron–hole pairs. This is expressed in a real space representation in which many-body interactions and one-electron hopping are treated on the same footing. In the real space representation both the direct and exchange interactions between electron–hole pairs are included, so excitons, plasmons and single-particle excitations are all contained in the formalism. This is applied to a model insulator, first without one-electron hopping: this shows a dispersive Frenkel exciton and charge transfer excitations. When one-electron hopping is included, the Frenkel exciton can lie within the single-particle continuum; the charge transfer states become Wannier excitons. Applied to metals, the real space technique gives exactly the same plasmon frequency as the usual dielectric function method

1. Introduction

The random phase approximation (RPA) is the starting point for most many-body theories of the electron gas (Pines 1963, Singwi *et al* 1968, Arponen and Pajanne 1975); it is equivalent to a time-dependent Hartree approach (Hedin and Lundqvist 1969) in which the electron–hole and plasmon excitations are self-sustaining charge density fluctuations (Wikborg and Inglesfield 1977). These can be found from the frequency-dependent dielectric response function, which can be calculated quite easily in simple inhomogeneous systems like a jellium metal with a surface (Inglesfield and Wikborg 1974). The dielectric function may also be used to find the excitations in a tightly bound solid, in which localised orbitals are used as basis functions for the one-electron wavefunctions. From the wavefunctions, a localised real space representation of the dielectric function can be found, and in this way Hanke and Sham (1975, Hanke 1978) have studied the optical properties of covalently bonded crystals.

An alternative approach to the RPA is to linearise the equations of motion of the electron–hole pairs (Brown 1972), and in a previous paper (Rogan *et al* 1981, referred to as I) we related this to the dielectric function approach in a general inhomogeneous system: the matrix elements of electron–hole creation and annihilation operators, ladder operators, and an effective boson Hamiltonian can be written down explicitly in terms of the charge density fluctuations. However, if localised basis functions are used it is possible to solve the equations of motion directly, in real space, without any previous calculation of the dielectric response function. We shall now show that the direct solution

0022-3719/81/253585 + 18 $01.50

of the equations of motion for electron–hole pairs, in which one-electron hopping and many-body effects are treated on the same footing, can be used to study excitations in metals and insulators.

We begin in § 2 by deriving the linearised equations of motion for electron–hole creation and annihilation operators in a local orbital representation. In an infinite crystal the excitations have a well defined wavevector $\boldsymbol{\kappa}$, and one class of excitations corresponds to taking an electron with Bloch wavevector $\boldsymbol{k}$ and putting it into state $\boldsymbol{k}+\boldsymbol{\kappa}$; as the electron and hole wavefunctions are extended, these modes cannot be found satisfactorily in real space. However, we shall see that a plasmon excitation in a metal consists of a superposition of electron–hole pairs which are localised around one another, and which can be found directly in a real-space, local-orbital representation. In a plasmon the dipole moment of the electron–hole pairs self-consistently excites other electron–hole pairs—this is the dominant interaction in metals, and is given by the direct interaction term in the equations of motion (the only term included in time-dependent Hartree–RPA). But in insulators, the Coulomb interaction between the electron and hole can dominate, producing bound state excitons (Knox 1963). This is given by the *exchange* term in the equations of motion; including this is equivalent to the time-dependent Hartree–Fock method (Hedin and Lundqvist 1969), or the random phase approximation with exchange (RPAE), and can be carried out in our real-space approach.

In § 3 we shall apply our method to an extreme tight-binding insulator with two orbitals per atom, an occupied s and an unoccupied p orbital, but without any one-electron hopping between atoms. This has been frequently used to study excitations in insulators (Giaquinta *et al* 1976a, Egri 1979), and in RPAE two types of excitations occur: the Frenkel exciton, corresponding to an electron excited into a conduction band orbital on the same atom, which shows dispersion, and dispersionless charge transfer states in which the electrons and holes are localised on separate atoms (Gunn and Inkson 1979). It is very easy to include one-electron band structure effects, simply by adding one-electron hopping terms to the equation of motion. We shall see in § 4 that this has surprisingly little effect on the frequency of the Frenkel exciton. The charge transfer states become Wannier excitons for which the standard effective mass equation (Knox 1963) can be derived from the electron–hole equations, giving approximate expressions for the exciton energies and wavefunctions. An advantage of our equation of motion method is that both the Frenkel and the Wannier excitons drop naturally out of the same equations.

In our RPAE results the Frenkel and Wannier excitons coexist. Moreover, for certain values of the parameters the Frenkel exciton lies within the particle–hole continuum. There is some experimental evidence of a collective excitation above the band gap, as well as excitons below (Schmidt 1971, Giaquinta *et al* 1976b), and this has usually been described as a plasmon (Giaquinta *et al* 1976a, b). Our results show that this excitation in the tight-binding insulator is a Frenkel exciton, with the electron well localised on the same atom as the hole, rather than a plasmon.

Finally in § 5 we shall turn to plasmons in tight-binding metals—our real space method gives just the same dispersion as the usual dielectric function approach (Hanke 1978) with much less computing effort. Moreover, this method gives the electron–hole wavefunction from which the plasmon is built up. The screening of the Coulomb interaction in metals (Hedin and Lundqvist 1969) means that the bare exchange interaction in the equations of motion should be dropped, leaving just the direct term (corresponding to RPA); we shall see in § 5 that including the exchange term (RPAE) (Brener and Fry 1980) is unsatisfactory. As the real-space method works so well we hope to apply it to

calculations of plasmons in more complicated tight-binding systems, for example transition metal surfaces, avoiding all calculations of surface dielectric functions.

2. RPAE in a local orbital representation

The linearised equation of motion of an electron–hole pair creation–annihilation operator is given by (1):

$$\begin{aligned}[a_\mu^+ a_\nu, H] = &\sum_\beta \left(h_{\nu\beta} + \sum_{\alpha,\gamma} \langle a_\alpha^+ a_\gamma \rangle \left[V_{\alpha\nu,\beta\gamma} - V_{\alpha\nu,\gamma\beta} \right] \right) a_\mu^+ a_\beta \\ &- \sum_\alpha \left(h_{\alpha\mu} + \sum_{\beta,\gamma} \langle a_\beta^+ a_\gamma \rangle \left[V_{\alpha\beta,\gamma\mu} - V_{\beta\alpha,\gamma\mu} \right] \right) a_\alpha^+ a_\nu \\ &+ \sum_{\alpha,\beta,\gamma} \left(\langle a_\mu^+ a_\gamma \rangle \left[V_{\alpha\nu,\gamma\beta} - V_{\alpha\nu,\beta\gamma} \right] - \langle a_\gamma^+ a_\nu \rangle \left[V_{\gamma\alpha,\beta\mu} - V_{\alpha\gamma,\beta\mu} \right] \right) a_\alpha^+ a_\beta \end{aligned} \tag{1}$$

$h_{\alpha\beta}$ is the matrix element of the one-electron part of the Hamiltonian, evaluated with a set of single-particle orbitals $\varphi_\alpha(x)$ (x includes spin as well as spatial coordinates)†:

$$h_{\alpha\beta} = \int \mathrm{d}x \varphi_\alpha^*(x) \left[-\tfrac{1}{2}\nabla^2 + V_{\mathrm{ion}}(r) \right] \varphi_\beta(x) \tag{2}$$

and the Coulomb matrix elements are defined by

$$V_{\alpha\beta,\gamma\delta} = \int \mathrm{d}x \int \mathrm{d}x' \varphi_\alpha^*(x)\, \varphi_\beta^*(x')\, v(r - r')\, \varphi_\gamma(x')\, \varphi_\delta(x) \tag{3}$$

where v is the Coulomb interaction. The terms $\langle a_\alpha^+ a_\gamma \rangle$ etc. in equation (1), which appear as a result of linearising four-particle operators (Brown 1972) (this linearisation corresponds to RPAE), are expectation values with respect to some calculable ground state, normally taken to be the Hartree–Fock ground state (Rowe 1968, Brown 1972, I). In the previous paper (I) we showed how this equation simplifies if the φ_α are taken to be the Hartree–Fock eigenfunctions, but we shall now take them to be local basis functions, so that we consider the one-electron and many-electron problem at the same time (Gunn and Inkson 1979, Gunn 1980). In the local orbital representation we shall replace the single orbital label (α) by (α, i), meaning orbital α on atom i.

To find the excitations of the system we take the matrix element of (1) between the ground state $|0\rangle$ and excited state $|N\rangle$, giving:

$$\begin{aligned}\omega_N \langle N | a_{j\mu}^+ a_{i\eta} | 0 \rangle = &\sum_{\alpha m} \left(h_{\alpha m,j\mu} + \sum_{\beta n,\gamma p} \langle a_{\beta n}^+ a_{\gamma p} \rangle \left[V_{\alpha m\beta n,\gamma p j\mu} - V_{\beta n\alpha m,\gamma p j\mu} \right] \right) \langle N | a_{\alpha m}^+ a_{i\eta} | 0 \rangle \\ &- \sum_{\beta n} \left(h_{i\eta,\beta n} + \sum_{\alpha m,\gamma p} \langle a_{\alpha m}^+ a_{\gamma p} \rangle \left[V_{\alpha m i\eta,\beta n\gamma p} - V_{\alpha m i\eta,\gamma p\beta n} \right] \right) \langle N | a_{j\mu}^+ a_{\beta n} | 0 \rangle \\ &+ \sum_{\alpha m,\beta n,\gamma p} \langle a_{\gamma p}^+ a_{i\eta} \rangle \left[V_{\gamma p\alpha m,\beta n j\mu} - V_{\alpha m\gamma p,\beta n j\mu} \right] \\ &- \langle a_{j\mu}^+ a_{\gamma p} \rangle \left[V_{\alpha m i\eta,\gamma p\beta n} - V_{\alpha m i\eta,\beta n\gamma p} \right] \rangle \langle N | a_{\alpha m}^+ a_{\beta n} | 0 \rangle \end{aligned} \tag{4}$$

where ω_N is the excitation energy. We can immediately simplify equation (4) because the first two pairs of Coulomb interaction terms, multiplying $\langle N | a_{\alpha m}^+ a_{i\eta} | 0 \rangle$ and $\langle N | a_{j\mu}^+ a_{\beta n} | 0 \rangle$, are really one-electron terms. Writing the first set of terms in full

† Atomic units are used with $e = \hbar = m = 1$.

$$\sum_{\beta n,\gamma p}\langle a^{+}_{\beta n}a_{\gamma p}\rangle\,[V_{\alpha m\beta n,\gamma p\mu i}-V_{\beta n\alpha m,\gamma p\mu i}]$$

$$=\sum_{\beta n,\gamma p}\langle a^{+}_{\beta n}a_{\gamma p}\rangle\left[\int d\boldsymbol{x}\int d\boldsymbol{x}'\;\varphi^{*}_{\alpha m}(\boldsymbol{x})\,\varphi^{*}_{\beta n}(\boldsymbol{x}')\,v(\boldsymbol{r}-\boldsymbol{r}')\,\varphi_{\gamma p}(\boldsymbol{x}')\,\varphi_{\mu i}(\boldsymbol{x})\right.$$

$$\left.-\int d\boldsymbol{x}\int d\boldsymbol{x}'\;\varphi^{*}_{\beta n}(\boldsymbol{x})\,\varphi^{*}_{\alpha m}(\boldsymbol{x}')\,v(\boldsymbol{r}-\boldsymbol{r}')\,\varphi_{\gamma p}(\boldsymbol{x}')\,\varphi_{\mu i}(\boldsymbol{x})\right] \tag{5}$$

we see that this is simply the matrix element between orbitals $\varphi_{\alpha m}$, $\varphi_{\mu i}$ of the Hartree and exchange potentials. All the one-electron terms can then be written in tight-binding–LCAO form:

$$h_{\alpha m,\mu i}+\sum_{\beta n,\gamma p}\langle a^{+}_{\beta n}a_{\gamma p}\rangle\,[V_{\alpha m\beta n,\gamma p\mu i}-V_{\beta n\alpha m,\gamma p\mu i}]=\varepsilon_{\mu}\delta_{\mu\alpha}\delta_{\alpha m}+v_{\alpha m,\mu i}, \tag{6}$$

the first term giving the unperturbed energy of orbital μ on atom i, and the second term the hopping integral between orbital μ on i and orbital α on m. Our RPAE equation then becomes

$$[\omega_N-(\varepsilon_{\mu}-\varepsilon_{\nu})]\,\langle N|a^{+}_{\mu i}a_{\nu j}|0\rangle=\sum_{\alpha m}v_{\alpha m,\mu i}\langle N|a^{+}_{\alpha m}a_{\nu j}|0\rangle-\sum_{\beta n}v_{\nu j,\beta n}\langle N|a^{+}_{\mu i}a_{\beta n}|0\rangle$$

$$+\sum_{\alpha m,\beta n,\gamma p}(\langle a^{+}_{\gamma p}a_{\nu j}\rangle\,[V_{\gamma p\alpha m,\beta n\mu i}-V_{\alpha m\gamma p,\beta n\mu i}]$$

$$-\langle a^{+}_{\mu i}a_{\gamma p}\rangle\,[V_{\alpha m\nu j,\gamma p\beta n}-V_{\alpha m\nu j,\beta n\gamma p}])\,\langle N|a^{+}_{\alpha m}a_{\beta n}|0\rangle. \tag{7}$$

With the two atomic indices labelling each matrix element, this corresponds to a very large set of coupled linear equations even for a small atomic cluster, let alone an infinite crystal. However, in a crystal the excitations can be labelled by a Bloch vector $\boldsymbol{\kappa}$ (Ziman 1960) such that:

$$\langle N|a^{+}_{\mu,\boldsymbol{r}_i+\boldsymbol{R}}a_{\nu,\boldsymbol{r}_j+\boldsymbol{R}}|0\rangle=\exp(-i\boldsymbol{\kappa}\cdot\boldsymbol{R})\,\langle N|a^{+}_{\mu,\boldsymbol{r}_i}a_{\nu,\boldsymbol{r}_j}|0\rangle \tag{8}$$

where $\boldsymbol{R}$ is a lattice vector. We now set $\boldsymbol{r}_j=0$, the atom at the origin, in the left-hand side of equation (7) and use equation (8) to give a smaller set of equations with only one varying atomic index:

$$[\omega_N-(\varepsilon_{\mu}-\varepsilon_{\nu})]\,\langle N|a^{+}_{\mu i}a_{\nu 0}|0\rangle$$

$$=\sum_{\alpha m}v_{\alpha m,\mu i}\langle N|a^{+}_{\alpha m}a_{\nu 0}|0\rangle-\sum_{\beta m}v_{\nu m,\beta i}\exp(-i\boldsymbol{\kappa}\cdot[\boldsymbol{r}_i-\boldsymbol{r}_m])\,\langle N|a^{+}_{\mu m}a_{\beta 0}|0\rangle$$

$$+\sum_{\alpha m,\beta n,\gamma p}(\langle a^{+}_{\gamma p}a_{\nu 0}\rangle\,[V_{\gamma p\alpha(m+n),\beta n\mu i}-V_{\alpha(m+n)\gamma p,\beta n\mu i}]$$

$$-\langle a^{+}_{\mu i}a_{\gamma p}\rangle\,[V_{\alpha(m+n)\nu 0,\gamma p\beta n}-V_{\alpha(m+n)\nu 0,\beta n\gamma p}])$$

$$\times\exp(-i\boldsymbol{\kappa}\cdot\boldsymbol{r}_n)\,\langle N|a^{+}_{\alpha m}a_{\beta 0}|0\rangle. \tag{9}$$

By considering the asymptotic behaviour of $\langle N|a^{+}_{\mu i}a_{\nu 0}|0\rangle$ at large r_i we can show that this local orbital representation of RPAE has both extended and localised solutions. The localised nature of the basis orbitals means that a matrix element like $V_{\gamma p\alpha(m+n),\beta n\mu i}$—a direct Coulomb term in equation (9)—is very small except when $m=0$, $p=i$; moreover $\langle a^{+}_{\gamma p}a_{\nu 0}\rangle$ drops off rapidly as p is removed from the origin (§ 3), so this term only couples $\langle N|a^{+}_{\mu i}a_{\nu 0}|0\rangle$ and $\langle N|a^{+}_{\alpha m}a_{\beta 0}|0\rangle$ when $i\approx 0$, $m\approx 0$. Similarly $V_{\alpha(m+n)\gamma p,\beta n\mu i}$ is small except when $m+n\approx i$, $p\approx n$, and as p must be close to the origin we see that this exchange interaction term only couples $\langle N|a^{+}_{\mu i}a_{\nu 0}|0\rangle$ and $\langle N|a^{+}_{\alpha m}a_{\beta 0}|0\rangle$ when m is close to i; the

strength of the coupling drops off as $1/r_i$. Similar considerations apply to the second pair of Coulomb matrix elements in equation (9), so we see that at large i the RPAE equations reduce to

$$[\omega_N - (\varepsilon_\mu - \varepsilon_\nu)]\,\langle N|a^\dagger_{\mu 0}a_{\nu 0}|0\rangle$$
$$= \sum_{\alpha m} v_{\alpha m,\mu 0}\langle N|a^\dagger_{\alpha m}a_{\nu 0}|0\rangle - \sum_{\beta m} v_{\nu m,\beta 0}\exp(-\mathrm{i}\boldsymbol{\kappa}\cdot[\boldsymbol{r}_i - \boldsymbol{r}_m])$$
$$\times \langle N|a^\dagger_{\beta m}a_{\beta 0}|0\rangle \tag{10}$$

which are equations for non-interacting particles. Because of the periodicity of the hopping integrals, equation (10) has extended solutions of the form

$$\langle N|a^\dagger_{\mu 0}a_{\nu 0}|0\rangle = \exp(-\mathrm{i}\boldsymbol{k}\cdot\boldsymbol{r}_i)\,A_\mu(-\boldsymbol{k})\,A_\nu(\boldsymbol{k}-\boldsymbol{\kappa}) \tag{11}$$

where $A_\mu(\boldsymbol{k})$ is the coefficient of orbital φ_μ in a single-particle wavefunction satisfying the single-particle Schrödinger equation with Bloch wavevector $\boldsymbol{k}$, energy $\varepsilon(\boldsymbol{k})$. This is the asymptotic form of the particle–hole excitations (Pines 1963), with energy

$$\omega_N(\boldsymbol{\kappa}) = \varepsilon(\boldsymbol{k}) - \varepsilon(\boldsymbol{k}-\boldsymbol{\kappa}) \tag{12}$$

which are the *extended* solutions of the RPAE equations. The many-body excitations, pulled out of the particle–hole continuum by the Coulomb interaction, correspond to complex $\boldsymbol{k}$ in equation (11):

$$\langle N|a^\dagger_{\mu 0}a_{\nu 0}|0\rangle \sim \exp(-\gamma r_i) \tag{13}$$

and being *localised* can be found by solving equation (9) directly in real space.

Including electron spin explicitly, the excitations can be classified as singlet or triplet states. The matrix element $\langle N|a^\dagger_{\mu\uparrow i}a_{\nu\uparrow 0}|0\rangle$ satisfies

$$[\omega_N - (\varepsilon_\mu - \varepsilon_\nu)]\,\langle N|a^\dagger_{\mu\uparrow i}a_{\nu\uparrow 0}|0\rangle$$
$$= \sum_{\alpha m} v_{\alpha m,\mu 0}\langle N|a^\dagger_{\alpha\uparrow m}a_{\nu\uparrow 0}|0\rangle - \sum_{\beta m} v_{\nu m,\beta 0}\exp(-\mathrm{i}\boldsymbol{\kappa}\cdot[\boldsymbol{r}_i - \boldsymbol{r}_m])\,\langle N|a^\dagger_{\mu\uparrow m}a_{\beta\uparrow 0}|0\rangle$$
$$+ \sum_{\alpha m,\beta n,\gamma p}(\langle a^\dagger_{\gamma\uparrow p}a_{\nu\uparrow 0}\rangle\,[V_{\gamma p\alpha(m+n),\beta n\mu} - V_{\alpha(m+n)\gamma p,\beta n\mu}]$$
$$- \langle a^\dagger_{\mu\uparrow i}a_{\gamma\uparrow p}\rangle\,[V_{\alpha(m+n)i0,\gamma p\beta n} - V_{\alpha(m+n)i0,\beta n\gamma p}])\exp(-\mathrm{i}\boldsymbol{\kappa}\cdot\boldsymbol{r}_n)$$
$$\times \langle N|a^\dagger_{\alpha\uparrow m}a_{\beta\uparrow 0}|0\rangle + \sum_{\alpha m,\beta n,\gamma p}(\langle a^\dagger_{\gamma\uparrow p}a_{\nu\uparrow 0}\rangle\,V_{\gamma p\alpha(m+n),\beta n\mu} - \langle a^\dagger_{\mu\uparrow i}a_{\gamma\uparrow p}\rangle$$
$$\times V_{\alpha(m+n)i0,\gamma p\beta n})\exp(-\mathrm{i}\boldsymbol{\kappa}\cdot\boldsymbol{r}_n)\,\langle N|a^\dagger_{\alpha\downarrow m}a_{\beta\downarrow 0}|0\rangle \tag{14}$$

and is coupled by the direct interaction to $\langle N|a^\dagger_{\alpha\downarrow m}a_{\beta\downarrow 0}|0\rangle$ as well as $\langle N|a^\dagger_{\alpha\uparrow m}a_{\beta\uparrow 0}|0\rangle$. If $|N\rangle$ is a singlet excitation it can be written in the form (Oddershede 1978)

$$|Ns\rangle = (1/\sqrt{2})\sum_{\mu,\nu} O^{Ns}_{\mu\nu}(a^\dagger_{\mu\uparrow}a_{\nu\uparrow} + a^\dagger_{\mu\downarrow}a_{\nu\downarrow})|0\rangle \tag{15}$$

and consequently

$$\langle Ns|a^\dagger_{\alpha\downarrow m}a_{\beta\downarrow 0}|0\rangle = \langle Ns|a^\dagger_{\alpha\uparrow m}a_{\beta\uparrow 0}|0\rangle. \tag{16}$$

The equation for the singlet excitations then becomes:

$$\begin{aligned}
&[\omega_{Ns} - (\varepsilon_\mu - \varepsilon_\nu)]\,\langle Ns|a^+_{\mu\uparrow i}a_{\nu\uparrow 0}|0\rangle \\
&\quad = \sum_{\alpha m} v_{\alpha m,\mu i}\,\langle Ns|a^+_{\alpha\uparrow m}a_{\nu\uparrow 0}|0\rangle \\
&\quad - \sum_{\beta n} v_{\nu m,\beta i}\exp(-\mathrm{i}\boldsymbol{\kappa}\cdot[\boldsymbol{r}_i - \boldsymbol{r}_m])\,\langle Ns|a^+_{\mu\uparrow m}a_{\beta\uparrow 0}|0\rangle \\
&\quad + \sum_{\alpha m,\beta n,\gamma p}(\langle a^+_{\gamma\uparrow p}a_{\nu\uparrow 0}\rangle\,[2V_{\gamma p\alpha(m+n),\beta n\mu i} - V_{\alpha(m+n)\gamma p,\beta n\mu i}] \\
&\quad - \langle a^+_{\mu\uparrow i}a_{\gamma\uparrow p}\rangle\,[2V_{\alpha(m+n)\nu 0,\gamma p\beta n} - V_{\alpha(m+n)\nu 0,\beta n\gamma p}]) \\
&\quad \times \exp(-\mathrm{i}\boldsymbol{\kappa}\cdot\boldsymbol{r}_n)\,\langle Ns|a^+_{\alpha\uparrow m}a_{\beta\uparrow 0}|0\rangle
\end{aligned} \tag{17}$$

with a factor of 2 multiplying the direct Coulomb interaction. On the other hand, the three triplet states have the form (Oddershede 1978):

$$\begin{aligned}
|Nt,+1\rangle &= \sum_{\mu,\nu} O^{Nt}_{\mu\nu}a^+_{\mu\uparrow}a_{\nu\downarrow}|0\rangle \\
|Nt,0\rangle &= (1/\sqrt{2})\sum_{\mu,\nu} O^{Nt}_{\mu\nu}(a^+_{\mu\uparrow}a_{\nu\uparrow} - a^+_{\mu\downarrow}a_{\nu\downarrow})|0\rangle \\
|Nt,-1\rangle &= \sum_{\mu,\nu} O^{Nt}_{\mu\nu}a^+_{\mu\downarrow}a_{\nu\uparrow}|0\rangle.
\end{aligned} \tag{18}$$

Consequently

$$\langle Nt,0|a^+_{\alpha\downarrow m}a_{\beta\downarrow 0}|0\rangle = -\langle Nt,0|a^+_{\alpha\uparrow m}a_{\beta\uparrow 0}|0\rangle \tag{19}$$

and equation (19) gives for the $s_z = 0$ triplet excitation

$$\begin{aligned}
&[\omega_{Nt} - (\varepsilon_\mu - \varepsilon_\nu)]\,\langle Nt,0|a^+_{\mu\uparrow i}a_{\nu\uparrow 0}|0\rangle \\
&\quad = \sum_{\alpha m} v_{\alpha m,\mu i}\langle Nt,0|a^+_{\alpha\uparrow m}a_{\nu\uparrow 0}|0\rangle - \sum_{\beta n} v_{\nu m,\beta i}\exp(-\mathrm{i}\boldsymbol{\kappa}\cdot[\boldsymbol{r}_i - \boldsymbol{r}_m]) \\
&\quad \times \langle Nt,0|a^+_{\mu\uparrow n}a_{\beta\uparrow 0}|0\rangle - \sum_{\alpha m,\beta n,\gamma p}(\langle a^+_{\gamma\uparrow p}a_{\nu\uparrow 0}\rangle\,V_{\alpha(m+n)\gamma p,\beta n\mu i} - \langle a^+_{\mu\uparrow i}a_{\gamma\uparrow p}\rangle \\
&\quad \times V_{\alpha(m+n)\nu 0,\beta n\gamma p})\exp(-\mathrm{i}\boldsymbol{\kappa}\cdot\boldsymbol{r}_n)\,\langle Nt,0|a^+_{\alpha\uparrow m}a_{\beta\uparrow 0}|0\rangle.
\end{aligned} \tag{20}$$

The direct interaction drops out, leaving just the exchange interaction. The matrix elements $\langle Nt,+1|a^+_{\mu\uparrow i}a_{\nu\downarrow 0}|0\rangle$, $\langle Nt,-1|a^+_{\mu\downarrow i}a_{\nu\uparrow 0}|0\rangle$ for the $s_z = \pm 1$ triplet excitations also satisfy equation (20).

The singlet state, whose frequency and matrix elements are given by equation (17), is a charge density wave (Nobile and Tosatti 1980), whereas the triplet states are spin density waves (Anderson 1963).

3. Excitations in an extreme tight-binding insulator

We first apply this RPAE orbital representation to an extreme tight-binding two-band solid (Anderson 1963, Egri 1979) with valence orbitals q_v, energy ε_v, and conduction band orbitals q_c, energy ε_c; in this model we drop the one-electron hopping terms v in

equation (9). The expectation values of the form $\langle a_\mu^+ a_\nu \rangle$ which appear in equation (9) are given by

$$\langle a_\mu^+ a_\nu \rangle = \int \mathrm{d}\boldsymbol{r} \int \mathrm{d}\boldsymbol{r}' \int \mathrm{d}\boldsymbol{r}_2 \ldots \int \mathrm{d}\boldsymbol{r}_n \, \Psi_0(\boldsymbol{r}, \boldsymbol{r}_2 \ldots \boldsymbol{r}_n) \, \varphi_\mu(\boldsymbol{r} - \boldsymbol{r}_i) \, \varphi_\nu(\boldsymbol{r}' - \boldsymbol{r}_j)$$
$$\times \Psi_0(\boldsymbol{r}', \boldsymbol{r}_2 \ldots \boldsymbol{r}_n) \tag{21}$$

where Ψ_0 is the Hartree–Fock ground state. The Hartree–Fock single-particle states, labelled by the Bloch wavevector $\boldsymbol{k}$ and band index l, can be expanded in terms of the basis functions φ_μ:

$$\psi_{\boldsymbol{k},l}(\boldsymbol{r}) = \sum_\mu A_{l,\mu}(\boldsymbol{k}) \, (1/\sqrt{N}) \sum_i \exp(\mathrm{i}\boldsymbol{k} \cdot \boldsymbol{r}_i) \, \varphi_\mu(\boldsymbol{r} - \boldsymbol{r}_i) \tag{22}$$

where N is the number of atoms, and inverting this equation we can write $\varphi_\mu(\boldsymbol{r} - \boldsymbol{r}_i)$ as a Brillouin zone summation (Ziman 1960):

$$\varphi_\mu(\boldsymbol{r} - \boldsymbol{r}_i) = (1/\sqrt{N}) \sum_{\boldsymbol{k} \in \mathrm{BZ}} \sum_l A_{l,\mu}(\boldsymbol{k})^{-1} \, \psi_{\boldsymbol{k},l}(\boldsymbol{r}) \exp(-\mathrm{i}\boldsymbol{k} \cdot \boldsymbol{r}_i). \tag{23}$$

Substituting this into equation (21) we see that the expectation value is given by

$$\langle a_\mu^+ a_\nu \rangle = (1/N) \sum_{\boldsymbol{k} \in \mathrm{BZ}} \sum_l A_{l,\mu}(\boldsymbol{k})^{-1} A_{l,\nu}(-\boldsymbol{k})^{-1} \exp(-\mathrm{i}\boldsymbol{k} \cdot [\boldsymbol{r}_i - \boldsymbol{r}_j]) \, n_{\boldsymbol{k},l} \tag{24}$$

where $n_{\boldsymbol{k},l}$ is the Fermi function, which is unity if $(\boldsymbol{k}, l)$ is occupied in the Hartree–Fock ground state and zero if it is unoccupied. In the two-band model this is extremely simple, as the occupied valence band consists entirely of φ_v orbitals, and the unoccupied conduction band consists entirely of φ_c, so we obtain

$$\langle a_{\mu l}^+ a_{\nu j} \rangle = 0 \qquad \text{if } \mu \text{ or } \nu = \mathrm{c}$$
$$= \delta_{ij} \qquad \text{if } \mu = \nu = \mathrm{v}. \tag{25}$$

Substituting this into equation (17) we obtain the following coupled equations for the singlet excitations:

$$[\omega_N + (\varepsilon_\mathrm{c} - \varepsilon_\mathrm{v})] \langle N | a_{\mathrm{v}i}^+ a_{\mathrm{c}0} | 0 \rangle$$
$$= -\sum_{m,n} \exp(-\mathrm{i}\boldsymbol{\kappa} \cdot \boldsymbol{r}_n) \{(2V_{\mathrm{v}(m+n)\mathrm{c}0,\mathrm{v}i\mathrm{c}n} - V_{\mathrm{v}(m+n)\mathrm{c}0,\mathrm{c}n\mathrm{v}i}) \langle N | a_{\mathrm{v}m}^+ a_{\mathrm{c}0} | 0 \rangle$$
$$+ (2V_{\mathrm{c}(m+n)\mathrm{c}0,\mathrm{v}i\mathrm{v}n} - V_{\mathrm{c}(m+n)\mathrm{c}0,\mathrm{v}n\mathrm{v}i}) \langle N | a_{\mathrm{c}m}^+ a_{\mathrm{v}0} | 0 \rangle\}$$

$$[\omega_N - (\varepsilon_\mathrm{c} - \varepsilon_\mathrm{v})] \langle N | a_{\mathrm{c}i}^+ a_{\mathrm{v}0} | 0 \rangle$$
$$= \sum_{m,n} \exp(-\mathrm{i}\boldsymbol{\kappa} \cdot \boldsymbol{r}_n) \{(2V_{\mathrm{v}0\mathrm{v}(m+n),\mathrm{c}n\mathrm{c}i} - V_{\mathrm{v}(m+n)\mathrm{v}0,\mathrm{c}n\mathrm{c}i}) \langle N | a_{\mathrm{v}m}^+ a_{\mathrm{c}0} | 0 \rangle$$
$$+ (2V_{\mathrm{v}0\mathrm{c}(m+n),\mathrm{v}n\mathrm{c}i} - V_{\mathrm{c}(m+n)\mathrm{v}0,\mathrm{v}n\mathrm{c}i}) \langle N | a_{\mathrm{c}m}^+ a_{\mathrm{v}0} | 0 \rangle\}. \tag{26}$$

But in the extreme tight-binding case there is no orbital overlap between neighbouring atoms, so:

$$V_{\mathrm{v}0\mathrm{v}(m+n),\mathrm{c}n\mathrm{c}i} = 0 \qquad \text{unless } i = 0, m = 0, \text{ etc.} \tag{27}$$

Hence, equations (26) simplify to

$$[\omega_N + (\varepsilon_c - \varepsilon_v)]\,\langle N|a^+_{vi}a_{c0}|0\rangle = V_{vic0,c0vi}\langle N|a^+_{vi}a_{c0}|0\rangle$$
$$- \delta_{i0}\Big(\sum_n 2V_{vnc0,v0cn}\exp(-i\boldsymbol{\kappa}\cdot\boldsymbol{r}_n)\Big)\,\langle N|a^+_{v0}a_{c0}|0\rangle + V_{cic0,v0vi}$$
$$\times\,\langle N|a^+_{ci}a_{v0}|0\rangle - \delta_{i0}\Big(\sum_n 2V_{cnc0,v0vn}\exp(-i\boldsymbol{\kappa}\cdot\boldsymbol{r}_n)\Big)\,\langle N|a^+_{c0}a_{v0}|0\rangle$$

$$[\omega_N - (\varepsilon_c - \varepsilon_v)]\,\langle N|a^+_{ci}a_{v0}|0\rangle = -V_{civ0,c0ci}\langle N|a^+_{v}a_{c0}|0\rangle$$
$$+ \delta_{i0}\Big(\sum_n 2V_{v0vn,cnc0}\exp(-i\boldsymbol{\kappa}\cdot\boldsymbol{r}_n)\Big)\,\langle N|a^+_{v0}a_{c0}|0\rangle - V_{civ0,v0ci}$$
$$\times\,\langle N|a^+_{ci}a_{v0}|0\rangle + \delta_{i0}\Big(\sum_n 2V_{v0cn,vnc0}\exp(-i\boldsymbol{\kappa}\cdot\boldsymbol{r}_n)\Big)\,\langle N|a^+_{c0}a_{v0}|0\rangle. \tag{28}$$

These equations only couple excitations with the same value of i, the separation of the electron and hole. For $i = 0$ the excitation frequency is given by

$$\omega^2_N = \Big[(\varepsilon_c - \varepsilon_v) - V_{v0c0,c0v0} + 2\sum_n V_{vnc0,v0cn}\exp(-i\boldsymbol{\kappa}\cdot\boldsymbol{r}_n)\Big]^2$$
$$- \Big[2\sum_n V_{vnc0,v0cn}\exp(-i\boldsymbol{\kappa}\cdot\boldsymbol{r}_n) - V_{v0c0,v0c0}\Big]^2. \tag{29}$$

This is the Frenkel exciton in which the electron and hole are on the same atom (Anderson 1963, Knox 1963, Gunn and Inkson 1979).

In the first set of terms, the summation over sites n comes from the electron–hole pair on atom 0 de-exciting and simultaneously exciting another electron–hole pair on atom n via the direct dipole–dipole interaction. This summation also includes the term $V_{v0c0,v0c0}$ which corresponds apparently to an unphysical process in which the electron–hole pair de-excites and excites itself (Gunn and Ortuno 1980). In fact this term, together with $-V_{v0c0,c0v0}$, corrects the Hartree–Fock intra-atomic excitation energy $(\varepsilon_c - \varepsilon_v)$. In this extreme tight-binding case the atomic energy levels are given by equation (6):

$$\varepsilon_v = h_{v0,v0} + V_{v0v0,v0v0}$$
$$\varepsilon_c = h_{c0,c0} + 2V_{v0c0,c0v0} - V_{v0c0,v0c0}. \tag{30}$$

ε_v is the one-electron energy corrected by the Hartree interaction with the other electron on the atom, and the Hartree and exchange self-interaction terms cancel; however, ε_c contains non-cancelling self-interactions. The true intra-atom excitation energy is given by

$$(h_{c0,c0} + V_{v0c0,c0v0}) - (h_{v0,v0} + V_{v0v0,v0,v0}) = (\varepsilon_c - \varepsilon_v) - V_{v0c0,c0v0} + V_{v0c0,v0c0}. \tag{31}$$

We see that this corresponds precisely to the correction terms included in the RPAE.

We see that the excitations come in pairs $\pm\omega_N$: this arises from the symmetry between electrons and holes in the RPAE equations (Fetter and Walecka 1971). The symmetry is also responsible for the second set of terms in (29), and as it corresponds to a better ground state containing excitonic zero-point fluctuations, it should give a more accurate exciton frequency than the usual approach (Anderson 1963). Another feature of equation (29) which is more accurate is that both the direct and exchange interactions between electron–hole pairs are included (figure 1), even though it is the direct interaction which dominates the Frenkel exciton.

For $i \neq 0$ we obtain from equation (29):

$$\omega_N^2 = [(\varepsilon_c - \varepsilon_v) - V_{vic0,c0vi}]^2 - V_{vic0,v0ci}^2. \tag{32}$$

The frequency of these excitations does not depend on wavevector $\boldsymbol{\kappa}$ but only on the electron–hole separation r_i. These are charge transfer states (Gunn and Inkson 1979), in which the electron–hole pair have their energy lowered by their electrostatic interaction $V_{vic0,c0vi}$, coming from the exchange terms in the RPAE equations (figure 1). As

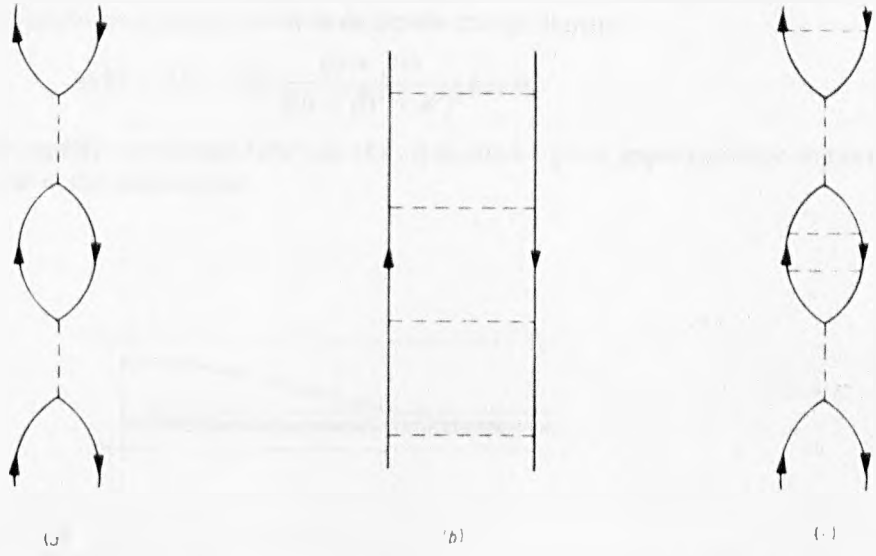

Figure 1. (*a*) Direct interaction and (*b*) exchange interaction between electron–hole pairs, summed (*c*) in the RPAE.

with the Frenkel exciton, the second squared term in equation (32) is a result of the electron–hole symmetry. The charge transfer excitations are dispersionless in this extreme tight-binding limit, because the electron and hole cannot hop or de-excite, being stuck on separate atoms.

We shall now evaluate these expressions for a model insulator with atoms on a simple cubic lattice having hydrogenic valence and conduction band orbitals:

$$\varphi_v = (\alpha^{3/2}/\sqrt{\pi}) \exp(-\alpha r)$$

$$\varphi_c = (\beta^{5/2}/\sqrt{\pi}) z \exp(-\beta r). \tag{33}$$

We only consider excitations with $\boldsymbol{\kappa} = (0, 0, \kappa)$, and for the moment neglect interactions between the dipoles in the z direction and those in the x and y directions. The Coulomb matrix elements in equations (29) and (32) are all straightforward to evaluate:

$$V_{v0c0,c0v0} = \alpha^3\beta^3\left[\frac{1}{\beta^3}\left(\frac{1}{\alpha^2} - \frac{1}{(\alpha+\beta)^2}\right) - \frac{3}{2\beta^2(\alpha+\beta)^3} - \frac{3}{2\beta(\alpha+\beta)^4} - \frac{1}{(\alpha+\beta)^5}\right]$$

$$V_{v0c0,v0c0} = \frac{28\alpha^3\beta^5}{3(\alpha+\beta)^7}$$

$$V_{vic0,c0vi} = \frac{1}{r_i} - \frac{3}{2\beta^2}\frac{(1 - 3\cos^2\theta_i)}{r_i^3}$$

$$V_{\mathrm{vic0,v0ci}} \approx \frac{32^2\alpha^3\beta^5}{(\alpha+\beta)^{10}} \frac{(1-3\cos^2\theta_i)}{r_i^3} \tag{34}$$

and the lattice summation can be carried out by Fourier transform

$$\sum_n V_{\mathrm{vnc0,v0cn}} \exp(-\mathrm{i}\boldsymbol{\kappa}\cdot\boldsymbol{r}_n) = \frac{4\pi}{\Omega}\sum_{\boldsymbol{g}} \frac{|\rho(\boldsymbol{\kappa}+\boldsymbol{g})|^2}{|\boldsymbol{\kappa}+\boldsymbol{g}|^2} \tag{35}$$

where the sum is over reciprocal lattice vectors $\boldsymbol{g}$, Ω is the volume per atom and ρ is the Fourier transform of the electron–hole dipole charge density:

$$\rho(k) = 32\mathrm{i}\sqrt{\alpha^3\beta^5}\,\frac{(\alpha+\beta)k}{[(\alpha+\beta)^2+k^2]^3}\cos\theta_k. \tag{36}$$

As ρ is a rapidly decreasing function of k, it is often a good approximation to take the $\boldsymbol{g}=0$ term in the summation.

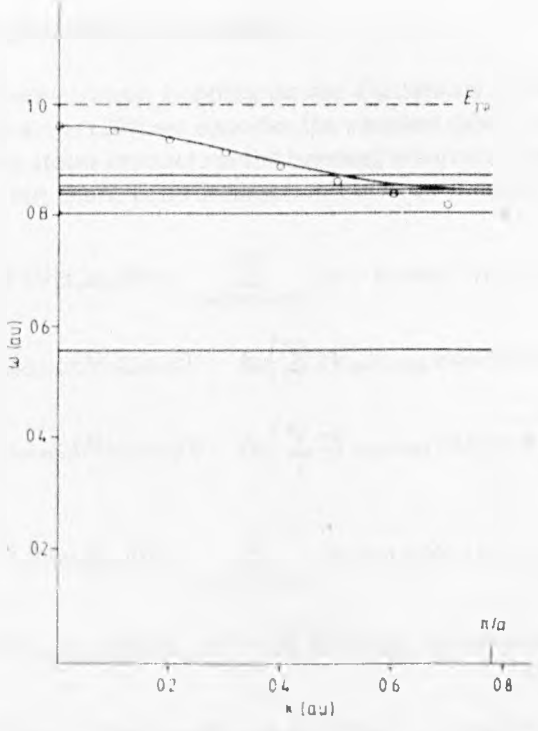

Figure 2. Excitation energies in extreme tight-binding insulator. Lattice parameter $a = 4$ au. Orbital parameters $\alpha = 1$ au, $\beta = 0.5$ au, $(\epsilon_c - \epsilon_v) = E_{\mathrm{gap}} = 1$ au. The Frenkel exciton shows dispersion, and the circles indicate $g = 0$ approximation for ω_N. Dispersionless modes are charge transfer excitations, of which only the lowest are shown.

Figure 2 shows the excitations we obtain for a lattice spacing of $a = 4$ au, with a band gap $(\epsilon_c - \epsilon_v) = 1$ au, and orbital parameters $\alpha = 1$ au, $\beta = 0.5$ au. Taking the $g = 0$ approximation for the dipole summation gives an explicit expression for the dispersion of the Frenkel exciton, which for these parameters is:

$$\omega_N^{\vec{}} = 0.573 + \frac{43.8}{(2.25+\kappa^2)^6}\,(\mathrm{au}). \tag{37}$$

This is in good agreement with the full lattice summation, especially near the centre of the Brillouin zone. With our choice of parameters, the Frenkel exciton always lies under the single-particle excitation energy ($\varepsilon_c - \varepsilon_v$), but at smaller lattice parameter it can have a higher energy—this is because the dipole–dipole interaction, contained in the second term in equation (37), increases rapidly as a decreases.

Up to now we have only considered one p_z orbital; including the other two p orbitals in the conduction band gives a cubic equation in ω_N^2 which has two transverse solutions and one longitudinal (Anderson 1963, Knox 1963). The transverse modes only contain the p orbitals perpendicular to $\boldsymbol{\kappa}$, and the longitudinal mode the orbital parallel to $\boldsymbol{\kappa}$ (the case we have considered); the frequencies of the modes depend only on $|\boldsymbol{\kappa}|$. The charge transfer states polarise in the same way into transverse and longitudinal modes when all three p orbitals are included.

4. Tight-binding insulator with hopping

The effects of one-electron hopping on the excitations in an insulator can be readily included in equations (28): we consider the simplest case in which the valence orbitals on neighbouring atoms interact via the hopping integral v, and the conduction electron orbitals via u, but there is no interaction between bands. The RPAE equations then become

$$[\omega_N + (\varepsilon_c - \varepsilon_v)]\langle N|a_{vi}^\dagger a_{ci}|0\rangle = \sum_{m\,\text{neighbouring}\,i} \{v - u\exp(-i\boldsymbol{\kappa}\cdot[\boldsymbol{r}_i - \boldsymbol{r}_m])\}\langle N|a_{vm}^\dagger a_{ci}|0\rangle$$
$$+ V_{vic0,\,civi}\langle N|a_{vi}^\dagger a_{ci}|0\rangle - \delta_{i0}\Big(\sum_n 2V_{vnc0,\,vicn}\exp(-i\boldsymbol{\kappa}\cdot\boldsymbol{r}_n)\Big)\langle N|a_{vi}^\dagger a_{ci}|0\rangle$$
$$+ V_{cic0,\,vivi}\langle N|a_{ci}^\dagger a_{vi}|0\rangle - \delta_{i0}\Big(\sum_n 2V_{cnc0,\,vivn}\exp(-i\boldsymbol{\kappa}\cdot\boldsymbol{r}_n)\Big)\langle N|a_{ci}^\dagger a_{vi}|0\rangle \qquad (38)$$

and

$$[\omega_N - (\varepsilon_c - \varepsilon_v)]\langle N|a_{ci}^\dagger a_{vi}|0\rangle = \sum_{m\,\text{neighbouring}\,i} \{u - v\exp(-i\boldsymbol{\kappa}\cdot[\boldsymbol{r}_i - \boldsymbol{r}_m])\}\langle N|a_{cm}^\dagger a_{vi}|0\rangle$$
$$- V_{vivi,\,civi}\langle N|a_{vi}^\dagger a_{ci}|0\rangle + \delta_{i0}\Big(\sum_n 2V_{vivn,\,cnc0}\exp(-i\boldsymbol{\kappa}\cdot\boldsymbol{r}_n)\Big)\langle N|a_{vi}^\dagger a_{ci}|0\rangle$$
$$- V_{civi,\,vici}\langle N|a_{ci}^\dagger a_{vi}|0\rangle + \delta_{i0}\Big(\sum_n 2V_{vicn,\,vnc0}\exp(-i\boldsymbol{\kappa}\cdot\boldsymbol{r}_n)\Big)\langle N|a_{ci}^\dagger a_{vi}|0\rangle. \qquad (39)$$

The resulting matrix eigenvalue problem can be solved in the computer.

The results we obtain for excitations in a tight-binding crystal with $(\varepsilon_c - \varepsilon_v) = 1$ au, orbital parameters $\alpha = 1$ au, $\beta = 0.5$ au, lattice spacing $a = 4$ au, and hopping integrals $v = 0.02$ au, $u = -0.02$ au are shown in figure 3. The one-electron excitations (extended solutions of equations (38) and (39)) are now spread out into a band by the one-electron hopping, overlapping the Frenkel exciton. Nevertheless, this still persists as a well defined excitation of the system at small κ, with a frequency quite close to the extreme-tight-binding value shown in figure 2. The structure of the Frenkel exciton is shown in figure 4, which gives the Bethe–Salpeter amplitudes $\langle N|a_{ci}^\dagger a_{vi}|0\rangle$ and $\langle N|a_{vi}^\dagger a_{ci}|0\rangle$ over the crystal lattice at $\kappa = 0.02$ au. As it overlaps with the continuum, the exciton is really a resonance rather than a true localised solution of equations (38) and

(39), but it still has the classic Frenkel exciton structure: essentially an excited electron well localised on the same atom as the hole. The RPAE ground state already contains some excited electrons (Fetter and Walecka 1971), so there is a component of $\langle N|a^{+}_{v\bar{v}}a_{c0}|0\rangle$, but this is very small. With smaller values of hopping parameter, the electron becomes even more localised on the atom with the hole; this is shown by figure 5 giving

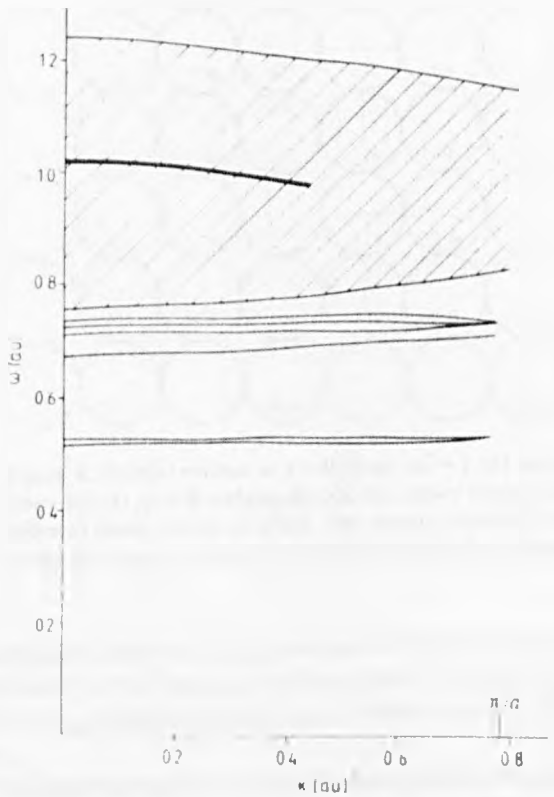

Figure 3. Excitation energies in tight-binding insulator. Lattice parameter $a = 4$ au. Orbital parameters $\alpha = 1$ au, $\beta = 0.5$ au, $(\varepsilon_c - \varepsilon_v) = 1$ au. Hopping parameters $v = 0.02$ au, $u = -0.02$ au. Shaded area indicates one-electron excitation continuum; the heavy line shows the Frenkel exciton. The lowest Wannier excitons are shown, below the continuum edge.

$\langle N|a^{+}_{c\bar{c}}a_{v0}|0\rangle$ for the Frenkel exciton at $\kappa = 0.02$ au with $v = 0.01$ au, $u = -0.01$ au. However, as κ increases the exciton spreads out (figure 6), and becomes less distinct from the particle–hole continuum.

When one-electron hopping is included, the charge-transfer states which we found in § 3 in the extreme tight-binding limit become Wannier excitons (Anderson 1963, Knox 1963). The Wannier excitons, of which figure 3 shows only the lowest, are pushed down in energy compared with the charge transfer states (figure 2) by the broadening of the single-particle states into a band, and become weakly dispersive. Figure 7 shows the Bethe–Salpeter amplitudes of the three lowest modes at small κ, and we see that they consist of excited electrons in distorted s, p and d orbitals around the hole. If the electron–hole interaction term $V_{cv\bar{v}\bar{c}}$ (equation (34)) is approximated by $1/r_{ij}$, we

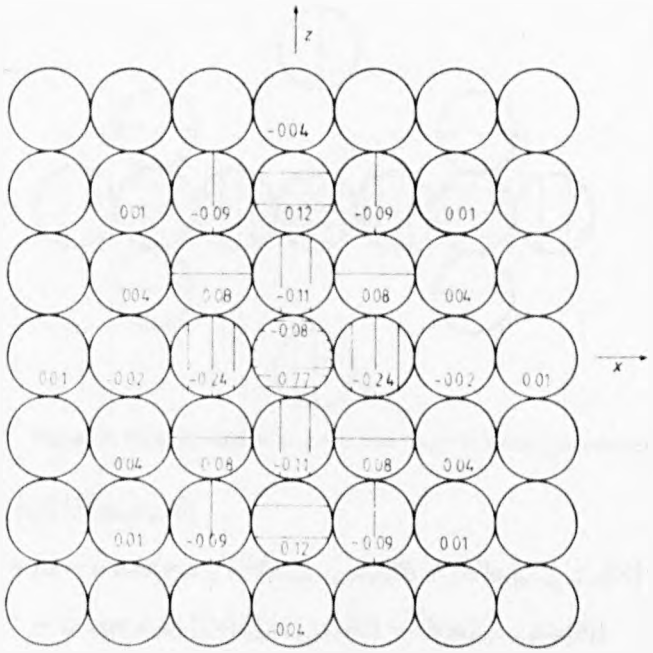

Figure 4. Frenkel exciton at $\kappa = 0.02$ au, $\omega_N = 1.021$ au (parameters as in figure 3). The lower figures give $\mathrm{Re}\langle N|a_{\mathbf{c}}^{\dagger}a_{\mathbf{v}i}|0\rangle$ and the upper figures (where shown) $\mathrm{Re}\langle N|a_{\mathbf{v}i}^{\dagger}a_{\mathbf{c}i}|0\rangle$ for different atoms i in the xz plane. The shading indicates $\mathrm{Re}\langle N|a_{\mathbf{c}}^{\dagger}a_{\mathbf{v}i}|0\rangle$, horizontal shading corresponding to positive values and vertical shading negative values.

obtain the amplitudes shown in figure 8—an s-like orbital (figure 8(a)) (1s though with reduced amplitude at the origin) with excitation energy $\omega_N = 0.617$ au, a 2p orbital (figure 8(b)) with excitation energy $\omega_N = 0.664$ au and a 3d orbital (figure 8(c)) with $\omega_N = 0.700$ au.

We can find approximate analytic solutions for the Wannier excitons by neglecting the $V_{\mathbf{v}i\mathbf{v}0,\mathbf{c}0\mathbf{c}i}\langle N|a_{\mathbf{v}i}^{\dagger}a_{\mathbf{c}0}|0\rangle$ term in equation (39), in which the matrix element is small and in any case is multiplied by the relatively small dipole interaction. For $\boldsymbol{r}_i \neq 0$, and with only nearest-neighbour one-electron hopping, this equation then becomes

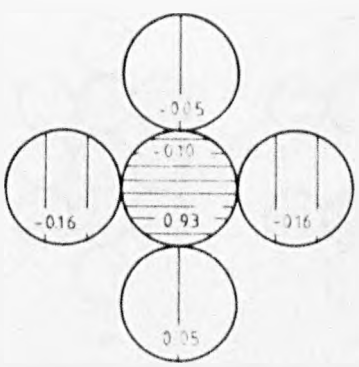

Figure 5. Frenkel exciton at $\kappa = 0.02$ au with $v = 0.01$ au, $u = -0.01$ au, $\omega_N = 0.975$ au.

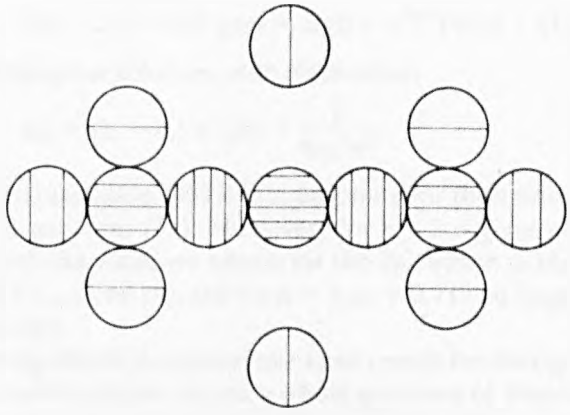

Figure 6. Frenkel exciton at $\kappa = 0.5$ au, $\omega_N = 0.986$ au (parameters as in figure 3).

$$[\omega_N - (\varepsilon_c - \varepsilon_v)]\,\langle N|a^+_{cr_i}a_{v0}|0\rangle$$
$$= [u - v\cos(\kappa_x a)]\,\{\langle N|a^+_{c(r_i+a_x)}a_{v0}|0\rangle + \langle N|a^+_{c(r_i-a_x)}a_{v0}|0\rangle\}$$
$$- iv\sin(\kappa_x a)\,\{\langle N|a^+_{c(r_i+a_x)}a_{v0}|0\rangle - \langle N|a^+_{c(r_i-a_x)}a_{v0}|0\rangle\}$$
$$+ \text{similar terms in the } y, z \text{ directions}$$
$$- V_{cr_iv0,v0cr_i}\langle N|a^+_{cr_i}a_{v0}|0\rangle. \tag{40}$$

If we replace the discrete function $\langle N|a^+_{cr_i}a_{v0}|0\rangle$ by a continuous function of position $\psi(\boldsymbol{r})$, and make a Taylor expansion of this function about $\boldsymbol{r}_i$ this gives:

$$[\omega_N - (\varepsilon_c - \varepsilon_v)]\,\psi(\boldsymbol{r}) = \{[u - v\cos(\kappa_x a)]\,(2 + a^2\partial^2/\partial x^2) - 2iav\sin(\kappa_x a)\,\partial/\partial x$$
$$+ \text{similar terms in the } y, z \text{ directions}\}\,\psi(\boldsymbol{r}) - (1/r)\,\psi(\boldsymbol{r}). \tag{41}$$

We approximate $V_{civ0,v0ci}$ by $1/r_i$ (equation (34)). This is essentially the standard Schrödinger equation for excitons in the Wannier effective mass approximation (Knox 1963). However, in equation (41) the electron–hole interaction, which comes originally from the *exchange* term in the RPAE equations (9), is unscreened: a better approximation is to replace this by $1/\varepsilon r$, where ε is the macroscopic dielectric constant (Hanke and Sham 1975). In our particular case where $u = -v$, equation (41) becomes, in the limit of $\kappa \to 0$:

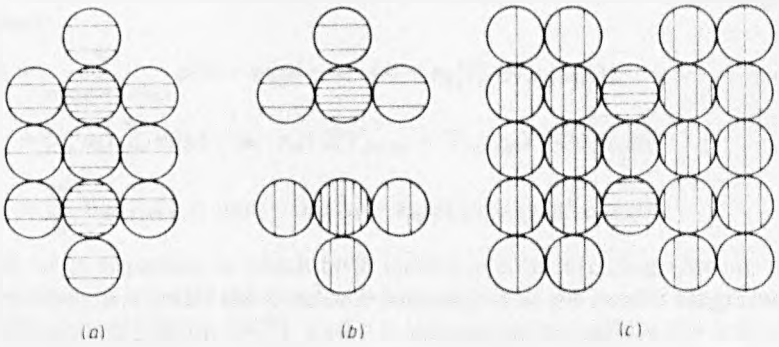

Figure 7. Wannier excitons at $\kappa = 0.02$ au (parameters as in figure 3). (*a*) $\omega_N = 0.520$ au; (*b*) $\omega_N = 0.530$ au, (*c*) $\omega_N = 0.679$ au.

$$[\omega_N - (\varepsilon_c - \varepsilon_v)]\,\psi(\boldsymbol{r}) = 2u(6 + a^2\nabla^2)\,\psi(\boldsymbol{r}) - (1/r)\,\psi(\boldsymbol{r}) \tag{42}$$

which has hydrogenic solutions with eigenvalues

$$\omega_N = (\varepsilon_c - \varepsilon_v) + 12u + \frac{1}{8ua^2n^2}. \tag{43}$$

We can see that equation (43) is inappropriate for the s states because of dropping the $r_i = 0$ term in equation (39). However, for $n = 2$ it gives $\omega_N = 0.662$ au, in excellent agreement with the value we obtain for the 2p exciton in the full calculation when we approximate $V_{cv0,v0c}$ by $1/r_i$, and for $n = 3$ $\omega_n = 0.717$ au, in good agreement with the 3d excitation energy.

The most significant feature of our RPAE results for the tight-binding insulator is that the Frenkel exciton (figure 4) and a whole spectrum of Wannier excitons (figure 7) can coexist at each wavevector (figure 3). To our knowledge this is a new conclusion, as it is usually claimed that the Frenkel exciton is the limit of the Wannier 1s state contracted onto the hole site in the strong-coupling limit (Anderson 1963, Rössler 1976). We suggest that the high-energy collective excitation observed in rare gas solids, usually attributed to a plasmon (Giaquinta *et al* 1976a, b, Gunn and Inkson 1979), is in fact the Frenkel exciton.

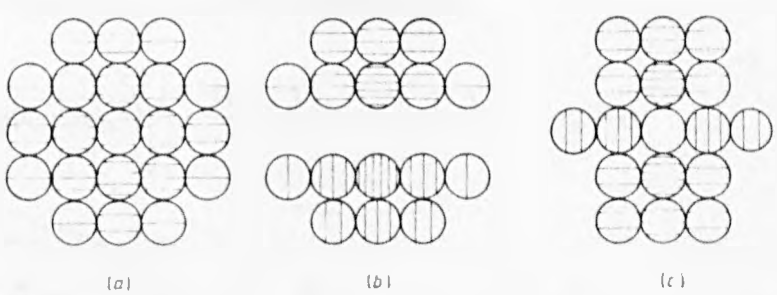

Figure 8. Wannier excitons at $\kappa = 0.02$ au, with parameters as in figure 3 but $V_{cv0,v0c}$ approximated by $1/r_i$. (*a*) $\omega_N = 0.617$ au; (*b*) $\omega_N = 0.664$ au; (*c*) $\omega_N = 0.700$ au.

5. Excitations in a tight-binding metal

Our localised orbital representation can be used to find the excitations in a tight-binding metal: we shall consider s orbital basis functions on a simple cubic lattice, containing one electron per atom. Taking the one-electron hopping integral to be v, and as in § 3 neglecting overlap in the Coulomb matrix elements, equation (17) for the singlet excitations becomes

$$\begin{aligned}\omega_N\langle N|a_i^+a_0|0\rangle = &\sum_{m\,\text{neighbouring}\,i} v(1 - \exp(-\mathrm{i}\boldsymbol{\kappa}\cdot[\boldsymbol{r}_i - \boldsymbol{r}_m]))\,\langle N|a_m^+a_0|0\rangle \\ &+ \langle a_i^+a_0\rangle \sum_m \exp(-\mathrm{i}\boldsymbol{\kappa}\cdot\boldsymbol{r}_m)\,2(V_{im,mi} - V_{m0,0m})\,\langle N|a_0^+a_0|0\rangle \\ &+ \sum_m V_{m0,0m}(1 - \exp(-\mathrm{i}\boldsymbol{\kappa}\cdot[\boldsymbol{r}_i - \boldsymbol{r}_m]))\,\langle a_i^+a_m\rangle\,\langle N|a_n^+a_0|0\rangle.\end{aligned} \tag{44}$$

This is the full RPAE equation in which both ladder and bubble diagrams are summed (figure 1): however, in a metal the Coulomb interaction in the ladder diagrams should be screened (Hanke and Sham 1975), and it is unphysical to include the full exchange term, given by the final summation in equation (44). It is certainly better to drop this term, corresponding to RPA.

From equation (24) the expectation values in equation (44) are given in this single-band model by

$$\langle a_i^+ a_0 \rangle = \frac{1}{N} \sum_{k \text{ inside Fermi surface}} \exp(-i\boldsymbol{k} \cdot \boldsymbol{r}_i). \tag{45}$$

This summation over occupied states must be done numerically, but it is straightforward and need only be done once for the whole excitation spectrum. The various Coulomb matrix elements in equation (44) are easy to evaluate. The sum over sites can be written as a sum over reciprocal lattice vectors:

$$\sum_m \exp(-i\boldsymbol{\kappa} \cdot \boldsymbol{r}_m)\,(V_{im,mi} - V_{m0,0m})$$

$$= \frac{4\pi}{\Omega} (\exp(-i\boldsymbol{\kappa} \cdot \boldsymbol{r}_i) - 1) \sum_{\boldsymbol{g}} \rho(|\boldsymbol{\kappa} + \boldsymbol{g}|)^2 / |\boldsymbol{\kappa} + \boldsymbol{g}|^2 \tag{46}$$

where the Fourier transform of the hydrogenic 1s charge density is given by

$$\rho(k) = \left(\frac{4\alpha^2}{4\alpha^2 + k^2} \right)^2 \tag{47}$$

and the matrix elements in the exchange summation are:

$$V_{00,00} = \tfrac{5}{8}\alpha$$

$$V_{m0,0m} = \frac{1}{r_m} - \exp(-2\alpha r_m) \left(\frac{1}{r_m} + \frac{11\alpha}{8} + \frac{3}{4}\alpha^2 r_m + \frac{1}{6}\alpha^3 r_m^2 \right) \qquad r_m \neq 0. \tag{48}$$

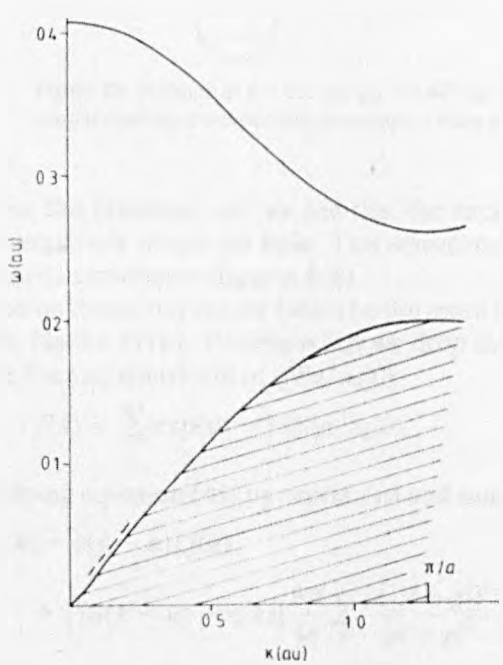

Figure 9. Excitations in tight-binding metal. Lattice parameter $a = 2.5$ au. Orbital parameter $\alpha = 1$ au. Hopping parameter $v = -0.05$ au. Shaded area indicates one-electron excitation continuum; the plasmon appears above the continuum. The broken curve shows the excitation energy when the exchange is included.

The results which we obtain in this way for the excitation spectrum are shown in figure 9 for a metal with lattice spacing = 2.5 au, $\alpha = 1$ au, and hopping parameter $v = -0.05$ au. We see, by omitting the exchange term in equation (44), that there is a well defined plasmon mode above the single-particle excitation spectrum. However if exchange is included, corresponding to RPAE, the plasmon mode is pulled all the way down in energy to just above the single-particle continuum (figure 9). This is obviously unphysical, and it shows the importance of screening or altogether dropping exchange in metals. Figure 10 shows the spatial variation of the Bethe–Salpeter amplitude

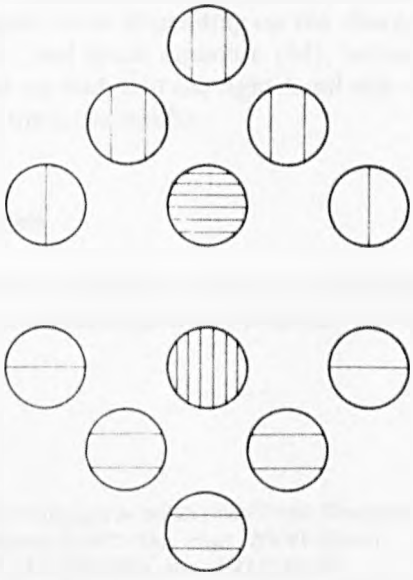

Figure 10. Plasmon at $\kappa = 0.1$ au, $\omega_N = 0.407$ au. The shading indicates $\mathrm{Re}\langle N|a_i^\dagger a_0|0\rangle$, horizontal shading corresponding to positive values and vertical shading to negative values.

$\langle N|a_i^\dagger a_0|0\rangle$ for the plasmon, and we see that the excited electron shows an oscillating probability amplitude about the hole. This wavefunction is completely different from that of excitons in insulators (figures 4–8).

The plasmon frequency can be found by the more usual dielectric function approach (Horie 1959, Hanke 1978). To obtain this we drop the exchange term in equation (44) and take the Fourier transform of $\langle N|a_i^\dagger a_0|0\rangle$:

$$f(\boldsymbol{k}) = \sum_i \exp(\mathrm{i}\boldsymbol{k}\cdot\boldsymbol{r}_i)\,\langle N|a_i^\dagger a_0|0\rangle. \tag{49}$$

Then multiplying equation (44) by $\exp(\mathrm{i}\boldsymbol{k}\cdot\boldsymbol{r}_i)$ and summing over i we obtain

$$\omega_N f(\boldsymbol{k}) = [\varepsilon(\boldsymbol{k}) - \varepsilon(\boldsymbol{k}-\boldsymbol{\kappa})]\,f(\boldsymbol{k}) + \left([n(\boldsymbol{k}-\boldsymbol{\kappa}) - n(\boldsymbol{k})]\,\frac{8\pi}{\Omega}\sum_{\boldsymbol{g}}\frac{\rho(|\boldsymbol{\kappa}+\boldsymbol{g}|)^2}{|\boldsymbol{\kappa}+\boldsymbol{g}|^2}\right)\frac{1}{N}\sum_{\boldsymbol{k}'\,\mathrm{in\,BZ}} f(\boldsymbol{k}') \tag{50}$$

where n is the Fermi function, and we have substituted the tight-binding expression for the energy:

$$\varepsilon(\boldsymbol{k}) = E_0 + v\sum_{m\,\mathrm{neighbours}} \exp(\mathrm{i}\boldsymbol{k}\cdot\boldsymbol{r}_m). \tag{51}$$

From equation (50) we obtain

$$f(\boldsymbol{k}) = \frac{n(\boldsymbol{k}-\boldsymbol{\kappa}) - n(\boldsymbol{k})}{\omega_N - (\varepsilon(\boldsymbol{k}) - \varepsilon(\boldsymbol{k}-\boldsymbol{\kappa}))} \frac{8\pi}{\Omega} \sum_{\boldsymbol{g}} \frac{\rho(|\boldsymbol{\kappa}+\boldsymbol{g}|)^2}{|\boldsymbol{\kappa}+\boldsymbol{g}|^2} \frac{1}{N} \sum_{\boldsymbol{k}' \text{ in BZ}} f(\boldsymbol{k}') \tag{52}$$

so that ω_N satisfies

$$1 = \frac{2}{N} \sum_{\boldsymbol{k} \text{ in BZ}} \frac{n(\boldsymbol{k}-\boldsymbol{\kappa}) - n(\boldsymbol{k})}{\omega_N - (\varepsilon(\boldsymbol{k}) - \varepsilon(\boldsymbol{k}-\boldsymbol{\kappa}))} \frac{4\pi}{\Omega} \sum_{\boldsymbol{g}} \frac{\rho(|\boldsymbol{\kappa}+\boldsymbol{g}|)^2}{|\boldsymbol{\kappa}+\boldsymbol{g}|^2}. \tag{53}$$

The right-hand side of equation (53) has the usual form of a dielectric function, modified by an electrostatic term depending on the charge density. It is less convenient to use than the direct, real space equation (44), because we must scan through a range of energies to find ω_N such that the right-hand side equals 1, but we find numerically that it gives exactly the same results.

Acknowledgments

J Rogan has been supported by an SRC Studentship during the course of this work. We have had useful discussions with Professor T B Grimley, Dr J M F Gunn and Dr K L Sebastian.

References

Anderson P W 1963 *Concepts in Solids* (New York: Benjamin)
Arponen J and Pajanne E 1975 *Ann. Phys., NY* **91** 450–80
Brener N E and Fry J L 1980 *Phys. Rev.* B**22** 2737–43
Brown G E 1972 *Many Body Problems* (Amsterdam: North Holland)
Egri I 1979 *J. Phys. C: Solid State Phys.* **12** 1843–54
Fetter A L and Walecka J D 1971 *Quantum Theory of Many-Particle Systems* (New York: McGraw-Hill)
Giaquinta P V, Parrinello M, Tosatti E and Tosi M P 1976a *J. Phys. C: Solid State Phys.* **9** 2031–48
Giaquinta P V, Tosatti E and Tosi M P 1976b *Solid State Commun.* **19** 123–6
Gunn J M F 1980 *J. Phys. C: Solid State Phys.* **13** 3841–53
Gunn J M F and Inkson J C 1979 *J. Phys. C: Solid State Phys.* **12** 1049–63
Gunn J M F and Ortuno M 1980 *J. Phys. C: Solid State Phys.* **13** 1669–78
Hanke W 1978 *Adv. Phys.* **27** 287–341
Hanke W and Sham L J 1975 *Phys. Rev.* B**12** 4501–11
Hedin L and Lundqvist S 1969 *Solid State Phys.* **23** 1–181
Horie C 1959 *Prog. Theor. Phys.* **21** 113–34
Inglesfield J E and Wikborg E 1974 *Solid State Commun.* **14** 661–4
Knox R S 1963 *Theory of Excitons* (*Solid State Physics Suppl.* 5) (New York: Academic Press)
Nobile A and Tosatti E 1980 *J. Phys. C: Solid State Phys.* **13** 589–610
Oddershede J 1978 *Adv. Quantum Chemistry* **11** 275–352
Pines D 1963 *Elementary Excitations in Solids* (New York: Benjamin)
Rogan J, Inglesfield J E and Grimley T B 1981 to be published
Rössler U 1976 *Rare Gas Solids* vol I, ed M L Klein and J A Venables (London: Academic Press)
Rowe D J 1968 *Rev. Mod. Phys.* **40** 153–66
Schmidt L 1971 *Phys. Lett.* **36**A 87–8
Singwi K S, Tosi M P, Land R H and Sjölander A 1968 *Phys. Rev.* **176** 589–99
Wikborg E and Inglesfield J E 1977 *Phys. Scr.* **15** 37–55
Ziman J M 1960 *Electrons and Phonons* (Oxford: University Press)